UNIVERSITY of CALIFORNIA
Santa Barbara

Fluctuation and Correlation Effects in Electrostatics of Highly-Charged Surfaces

A dissertation submitted in partial satisfaction of the
requirements for the degree of

Doctor of Philosophy

in

Physics

by

Andy Wing-Chi Lau

Committee in charge:

Professor Philip A. Pincus, Chair
Professor Jim S. Langer
Professor Cyrus Safinya

October 2000

The dissertation of Andy Wing-Chi Lau is approved:

Chair

October 2000

Fluctuation and Correlation Effects in Electrostatics of Highly-Charged Surfaces

Copyright 2000

by

Andy Wing-Chi Lau

To my family, of course.

Acknowledgements

This thesis would be absolutely impossible without the helping hand of many individuals. I would like to thank them here. They include Fyl Pincus, my adviser, who never ceases to amaze me with his physical insights; Dov Levine, from whom I have learned many things through our wonderful collaboration; Claus Jeppesen, Becky Menes, Helmut Schiessel, and particularly, Mario Tamashiro, who are always willing to discuss about science, among other things, with me even when most of my ideas are just plain stupid. I have also benefited from the discussion with Jim Langer, Cyrus Safinya, and Jim Allen on various occasions.

To my wonderful, wonderful classmates, friends, and brothers (in the platonic sense, of course), Naser Qureshi and Tobais Eckhause, I deeply thank thee for your great friendship, support, company, and readership throughout these years, and also to Xomalin Peralta and Adriano Batista, classmates and good friends, for your constant kindness. To Julia Chiu, I must thank and am grateful for your immense patience, understanding, and love. Finally, my heartfelt appreciation goes to David Cai, who has always been there to guide, care, and instruct.

Curriculum Vitae

Andy Wing-Chi Lau

Personal

Birthdate	December 15, 1971 Hong Kong

Education

2000	Ph.D. in Physics University of California, Santa Barbara, California
1998	M.A. in Physics University of California, Santa Barbara, California
1994	B.S. in Physics (with Honors) University of California, Davis, California

Awards and Honors

1995	**John Cardy Awards**: For excellent academic performance and evidence of future promise in physics, University of California, Santa Barbara
1994	**Saxon-Patten Prize in Physics**: For achieving an excellent academic record and showing interest and promise in continued work in physics and/or related physical sciences, University of California, Davis
1994	**Department Citation**: For excellence in the major program and outstanding GPA in courses given by the department major program, University of California, Davis

Publications

1. "Fluctuation-Driven Counterion Condensation", A.W.C. Lau and P. Pincus, submitted to Phy. Rev. Lett.
2. "Electrostatic Attraction of Coupled Planar Wigner Crystals: Finite Temperature Effects", A.W.C. Lau, P. Pincus, Dov Levine, and H.A. Fertig, to be published.
3. "Novel Electrostatic Attraction from Plasmon Fluctuations", A.W.C. Lau, Dov Levine, and P. Pincus, Phys. Rev. Lett. **84**, 4116 (2000).
4. "Binding of Oppositely Charged Membranes and Membrane Reorganization", A.W.C. Lau and P. Pincus, Eur. Phys. J. B **10**, 175-180 (1999).
5. "Charge-Fluctuation-Induced Nonanalytic Bending Rigidity", A.W.C. Lau and P. Pincus, Phys. Rev. Lett. **81**, 1338 (1998).
6. "Bunched Fluxons in Coupled Josephson Junctions", Niels Grønbech-Jensen, David Cai, A. R. Bishop, A.W.C. Lau, and Peter S. Lomdahl, Phy. Rev. B **50**, 6352 (1994).
7. "Compressional Oscillation Frequency of an Anharmonic Oscillator – the Spherical Non-neutral Plasma", L. Turner, T. N. Tiouririne, and A.W.C. Lau, J. Math. Phys. **35**, 2349 (1994).
8. "Multipole Traps for Non-neutral Plasmas", T. N. Tiouririne, L. Turner, and A.W.C. Lau, Phys. Rev. Lett. **72**, 1204 (1994).

Abstract

Fluctuation and Correlation Effects in Electrostatics of Highly-Charged Surfaces

by

Andy Wing-Chi Lau

This work explores the statistical mechanics of counterions associated with their oppositely charged surfaces, which is relevant to many systems in soft condensed matter physics: charged colloids, membranes, and polyelectrolytes immersed in solutions containing mobile neutralizing counterions. The mean-field treatment for these systems is the Poisson-Boltzmann (PB) theory, or its linearized version, the Debye-Hückel theory. Among other results, the mean-field theory predicts repulsion between two like-charged plates. However, recent experimental and numerical works suggest that two like-charged objects may attract! After reviewing the main features of PB theory, we describe an approach which takes charge fluctuations explicitly into account to improve the mean-field picture and demonstrate that charge-fluctuations can induce a long-ranged attraction, similar to the van der Waals interaction. We also analyze the effects of charge fluctuations on the bending properties of a charged membrane. Furthermore, we argue that fluctuations may induce a novel condensation phenomenon in an overall neutral system, consisting a single charged plate and its oppositely charged counterions. Finally, we study the interactions between two 2-dimensional Wigner crystals, which may be the ground state of the counterions condensed onto charged surfaces. In particular, we show that at low temperatures, quantum zero-point fluctuations of the plasmon modes (charge-fluctuations) of two mutually coupled 2D Wigner crystals give rise to a novel long-range attractive force.

Contents

1 Introduction **1**

Bibliography **5**

2 The Poisson-Boltzmann Theory **7**
- 2.1 Introduction 7
  - 2.1.1 Relevant Scales and Dimensionless Parameters 9
- 2.2 Derivation of the Poisson-Boltzmann Equation 12
- 2.3 Electrostatics of Charged Surfaces 15
  - 2.3.1 A Single Charged Plate 17
  - 2.3.2 Electrostatic Interaction between Two Charged Plates 19
  - 2.3.3 Manning Condensation 25
- 2.4 Electrostatic Contribution to Bending Rigidity 29
- 2.5 Conclusion 33

Bibliography **35**

3 Effects of Charge Fluctuations **37**
- 3.1 Introduction 37
- 3.2 Debye-Hückel Theory in 2D 38
  - 3.2.1 Charges in a Plane 39
  - 3.2.2 Charges on a Sphere 43
  - 3.2.3 Charges on a Cylinder 44
- 3.3 Renormalization of Bending Rigidity 44
  - 3.3.1 An Undulating “Salty” Membrane 46
- 3.4 Attraction Arising from Charge Fluctuations 48
- 3.5 Conclusion 51

Bibliography **53**

4 Fluctuation-Driven Counterion Condensation **55**
4.1 Introduction 55
4.2 Fluctuation Corrections to Possion-Boltzmann Theory 56
4.3 Counterion Condensation 59
4.4 Conclusion 66

Bibliography **69**

5 The Wigner Crystal Picture **71**
5.1 Introduction 71
5.2 Effective Hamiltonian for Coupled Wigner Crystals 76
5.3 Attractive Force within the Harmonic Approximation 79
5.3.1 Long-Ranged Pressure 79
5.3.2 Short-Ranged Pressure 81
5.3.3 Discussion 82
5.4 Quantum Contribution to the Long-Ranged Attraction 85
5.5 Discussion and Conclusion 88

Bibliography **93**

6 Conclusion **97**

A Membrane Curvature Elasticity **99**

Chapter 1

Introduction

This thesis focuses on the role of the electrostatic interaction in soft condensed matter physics. Soft materials are characterized by their ease of response to external forces and thermal fluctuations[1]. A convenient way to understand this is to consider an elastic modulus for these systems of building blocks of size L:

$$G \sim \frac{k_B T}{L^3}, \tag{1.1}$$

where $k_B T$ is a typical energy scale. Thus, "softness" means that G is small and the building blocks are huge compared to atomic dimensions a: $L \gg a$. Thus, in these systems, quantum effects may often be neglected but thermal fluctuations play an important role. An especially exciting area of current research is the overlap of soft matter physics with biology. Indeed, the fundamental building blocks of life – the plasma membrane, the cytoskeleton, microtubule, DNA, actin molecules – are all soft materials.

To understand the essential properties of any system, we have to study the interactions of its constituents. Of all interactions, electrostatics is arguably the most fundamental for soft systems, and is ubiquitous in biological materials. For example, DNA is a highly negatively charged polymer in solutions with one electronic charge e per 1.7Å, and consequently the rich phase behavior of DNA in solutions is governed by the competition between electrostatic interaction and entropy.

Usually, the charging of a surface can come about by ionization of surface groups. Recall that the energy it takes to break an ionic bond in vacuum is about $100\,k_BT$. However, in aqueous solutions, the dielectric constant $\epsilon \simeq 80$ is sufficiently high that the surface groups are ionized by the thermal fluctuations. For example, some charged membranes made out of polar surfactants carry carboxylic groups COOH. At room temperature, they dissociate protons ($\mathrm{COOH} \rightarrow \mathrm{COO}^- + \mathrm{H}^+$) and leave behind a negatively charged surface which is balanced by oppositely charged mobile *counterions*, (H^+ in this example). In some situations, there may be additional salt present, e.g. NaCl, KCl, and $\mathrm{CaCl_2}$; in practice, even pure water at room temperature is an ionic solution of 10^{-7} M of $\mathrm{H_3O^+}$ and $\mathrm{OH^-}$ ions, which is not always negligible. The physical situation that will be considered in this thesis is the following: Mobile point-like charges (the counterions) in the presence of charged surfaces, in an overall neutral system, interact with each other via the long-ranged Coulomb potential

$$V_{ij}(r) = \frac{e_i e_j}{\epsilon|\mathbf{x}_i - \mathbf{x}_j|}. \tag{1.2}$$

To better appreciate its range, let us try to evaluate the free energy density using the virial expansion for the electrostatic interaction:

$$f = f_0 + \frac{1}{2}B_2\, n^2 + \frac{1}{3!}\, B_3\, n^3 + \cdots. \tag{1.3}$$

We find that the second virial coefficient

$$B_2 = k_BT \int d^3\mathbf{r}\, \left[1 - e^{-\beta V_{ij}(r)}\right] \tag{1.4}$$

diverges for both small and large r. Thus, this naive treatment does not work for electrostatics, and a special treatment has to be employed to deal with electrostatics, namely the Poisson-Boltzmann theory.

In chapter 2, we formulate the standard mean-field approach, *i.e.* the Poisson-Boltzmann (PB) theory. It provides an adequate description for weakly charged membranes and charged polymers. Using the PB theory, we analyze the electrostatic interaction between two charged plates. At higher charge densities, however, the PB theory is no longer valid, because it neglects correlation effects. Indeed, there is experimental[2] and numerical[3] evidence that two highly charged macroions may attract each other in solutions, while the mean-field theory predicts that they should never attract!

In Chapter 3, we present an approach to improve on the mean field picture. Essentially, for a highly charged plate, the counterions become condensed onto the surface[4], forming a quasi-two-dimensional gas interacting with a $1/r$ potential – a "salty" surface. By incorporating the in-plane fluctuations of the "condensed" counterions, we show that this leads to a long-ranged attractive force which scales as d^{-3} for large distances d between two planar surfaces[5]. Using similar ideas, we compute the renormalization of the bending constants of a charge-fluctuating membrane. The result helps to explain the spontaneous formation of vesicles composed of anionic and cationic surfactants, observed in experiments. Furthermore, in Chapter 4, we argue that the mean-field (PB) solution for a single charged plate is unstable against the condensation of counterions driven by fluctuations. Using a "two-fluid" model, in which the counterions are divided into a "free" and a "condensed" fraction, we show a finite fraction of counterions is "condensed" onto the charged plate via a variational approach.

At sufficiently low temperatures, the "condensed" counterions crystallize to form a 2-D hexagonal lattice (a Wigner crystal). The classical force per unit area between two staggered planar Wigner crystals at distance d apart can be computed to give a short-range attraction. These correlation effects have been studied by Rouzina and Bloomfield[6]. However, their treatment does not include fluctuations, which are expected to give rise to yet stronger correlation effects at low temperatures. In Chapter 5, we include the zero-point fluctuations of the counterions to this problem and find a long-ranged attractive interaction. Surprisingly, rather than a force with the usual Casimir-like distance dependence (d^{-4}), this attractive interaction, which owes its existence to the plasmons on two correlated planar Wigner crystals, scales as $d^{-7/2}$ for large separations. Furthermore, we analyze the temperature dependence of this fluctuation-induced force and of the short-ranged force, arising from structural correlations. These results provide insight to the nature of counterion-mediated attractions between like-charged macroions, which are believed to play a major role in DNA condensation.

Bibliography

[1] P.M. Chaikin and T.C. Lubensky, *Principles of Condensed Matter Physics* (Cambridge Univ. Press, NY, 1995); P. Pincus, in *Phase Transitions in Soft Condensed Matter*, edited by E. Riste, D. Sherrington (Plenum Publishing Corporation, 1989).

[2] V.A. Bloomfield, Biopolymers **31**, 1471 (1991); R. Podgornik, D. Rau, and V.A. Parsegian, Biophys. J. **66**, 962 (1994); A.E. Larsen and D.G. Grier, Nature **385**, 230 (1997).

[3] L. Guldbrand, B. Jönsson, H. Wennerström, and P. Linse, J. Chem. Phys. **80**, 2221 (1984); S. Marcelja, Biophys. J. **61**, 1117 (1992); M.J. Stevens and K. Kremer, J. Chem. Phys. **103**, 1669 (1995); N. Grønbech-Jensen, R.J. Mashl, R.F. Bruinsma, and W.M. Gelbart, Phys. Rev. Lett. **78**, 2477 (1997); E. Allahyarov, I. D'Amico, and H. Löwen, Phys. Rev. Lett. **81**, 1334 (1998).

[4] G.S. Manning, J. Chem. Phys. **51**, 924 (1969); S. Alexander, P.M. Chaikin, P. Grant, G.J. Morales, P. Pincus, and D. Hone, J. Chem. Phys. **80**, 5776 (1984).

[5] Phil Attard, Roland Kjellander, and D. John Mitchell, Chem. Phys. Lett. **139**, 219 (1987); B.-Y. Ha and A.J. Liu, Phys. Rev. Lett. **79**, 1289 (1997); P. Pincus and S.A. Safran, Europhys. Lett. **42**, 103 (1998); D.B. Lukatsky and S.A. Safran, Phys. Rev. E **60**, 5848 (1999)

[6] I. Rouzina and V.A. Bloomfield, J. Phys. Chem. **100**, 9977 (1996); B.I. Shklovskii, Phys. Rev. Lett. **82**, 3268 (1999); J. Arenzon, J.F. Stilck, and Y. Levin, Eur. Phys. J. B **12**, 79 (1999).

Chapter 2

The Poisson-Boltzmann Theory

2.1 Introduction

The standard Poisson-Boltzmann equation encapsulates a mean-field approach to the many-body problem of mobile ions in aqueous solutions containing charged surfaces[1, 2]. It may be derived heuristically as follows. Suppose that the charged system generates a local electric field $\mathbf{E}(\mathbf{x}) = -\nabla\varphi(\mathbf{x})$, which causes the mobile ions of species i of charge $Z_i e$ to move, and thus gives rise to a current $\mathbf{J}_e^i$. In a linear response theory, $\mathbf{J}_e^i$ must be proportional to the "external" force

$$\mathbf{J}_e^i = -\frac{Z_i e}{\zeta}\, c_i\, \nabla\varphi, \tag{2.1}$$

where $c_i(\mathbf{x})$ is the mobile ion density and ζ is the friction coefficient; this is just Ohm's law. In addition, the diffusion of the charged particle in the presence of a concentration gradient is described by Fick's law:

$$\mathbf{J}_D^i = -\frac{k_B T}{\zeta}\, \nabla c_i, \tag{2.2}$$

where the diffusion constant $D = k_B T/\zeta$ is the Einstein relation. Thus, the total current of the charged particles of species i is

$$\mathbf{J}_{tot}^i \;\; = \;\; -\frac{1}{\zeta}\left(k_B T\, \nabla c_i + Z_i e c_i\, \nabla\varphi\right)$$

$$= \; -\frac{c_i}{\zeta}\,\nabla\left[k_BT\,\ln(c_i/c_{0i}) + Z_i e\varphi\right]. \tag{2.3}$$

Since the total current must be zero at thermal equilibrium, we have the standard result that the density of charged particles must be Boltzmann weighted:

$$c_i(\mathbf{x}) = c_{0i}\,e^{-\,Z_i e\varphi(\mathbf{x})/k_BT}. \tag{2.4}$$

Note that the constant c_{0i} can be defined through the zero of the potential $\varphi(\mathbf{x})$. Now we need another equation to relate the total charge density in the solutions $\rho(\mathbf{x})$ and the electric potential $\varphi(\mathbf{x})$ self-consistently. This is provided by the Poisson equation:

$$\nabla^2\varphi(\mathbf{x}) = -\frac{4\pi}{\epsilon}\,\rho(\mathbf{x}). \tag{2.5}$$

The total charge density is comprised of the mobile ions and external fixed charges:

$$\rho(\mathbf{x}) = \sum_i Z_i e c_i(\mathbf{x}) + \rho_{ext}(\mathbf{x}). \tag{2.6}$$

Combining Equations (2.5) and (2.4), we obtain a self-consistent equation for the potential φ:

$$\nabla^2\varphi(\mathbf{x}) + \sum_i \frac{4\pi Z_i e c_{0i}}{\epsilon}\,e^{-\,Z_i e\varphi(\mathbf{x})/k_BT} = -\frac{4\pi}{\epsilon}\,\rho_{ext}(\mathbf{x}). \tag{2.7}$$

This is known as the Poisson-Boltzmann (PB) equation. Its solutions describe the electrostatic potential and counterion density in space, where the boundary conditions are determined by the external charges or alternatively, by the charge neutrality condition

$$\int d^3\mathbf{x}\,\rho(\mathbf{x}) = 0. \tag{2.8}$$

We note that the PB equation is a nonlinear equation, and thus it is difficult to solve in general. In fact, exact solutions are known only in special cases, *e.g.* with planar and cylindrical symmetries.

2.1.1 Relevant Scales and Dimensionless Parameters

Before solving the mean-field PB equation for different geometries, we discuss various dimensionless parameters and physical scales in the theory. Multiplying the PB equation by e/k_BT and rescaling the potential $\varphi \rightarrow e\varphi/k_BT$, we obtain

$$\nabla^2\varphi(\mathbf{x}) + \sum_i 4\pi l_B Z_i c_{0i}\, e^{-\,Z_i\varphi(\mathbf{x})} = -4\pi l_B\,[\rho_{ext}(\mathbf{x})/e]. \tag{2.9}$$

The length defined by

$$l_B = \frac{e^2}{\epsilon k_B T} \tag{2.10}$$

is the *Bjerrum length*, at which the electrostatic potential energy of a pair of charges equals their thermal energies. In other words, if two oppositely charged particles with magnitude e are separated by a distance r, they are "bound" if $r < l_B$ and ionized if $r > l_B$ (by thermal fluctuations). In a solution of dielectric constant $\epsilon = 80$ (H_2O) at room temperature, $l_B \simeq 7\,\text{Å}$.

In an electrolyte solution in which there is an equal number of positively and negatively charged particles of valence Z in the absence of any external fixed charges, the PB equation reduces to

$$-\nabla^2\varphi(\mathbf{x}) + 8\pi l_B Z c_s \sinh Z\varphi(\mathbf{x}) = 0, \tag{2.11}$$

where c_s is the bulk ion density. The solution to this equation is trivial: $\varphi(\mathbf{x}) = 0$, since the mean electric field vanishes in an overall neutral system of two uniform and independent charge distributions of opposite sign. To capture correlations, we single out a positive charged particle fixed at $\mathbf{x}'$ and consider the electrostatic potential at $\mathbf{x}$ by linearizing Eq. (2.11)

$$\left[-\nabla^2_{\mathbf{x}} + \kappa_s^2\right] G(\mathbf{x},\mathbf{x}') = 4\pi Z^2 l_B \delta(\mathbf{x}-\mathbf{x}'), \tag{2.12}$$

where $\kappa_s^2 = 8\pi l_B Z^2 c_s$. This is the Debye-Hückel equation. It is important to note that although we have derived Eq. (2.12) from linearizing the PB equation, $G(\mathbf{x},\mathbf{x}')$ should be regarded as a fluctuating potential at point $\mathbf{x}$ generated by the test charge in the presence of fluctuating charges around it. Therefore, $G(\mathbf{x},\mathbf{x}')$ is actually the Green's function which contains information about the correlations of the system. It can also be interpreted as the electrostatic interaction between two Ze test charges located at $\mathbf{x}$ and $\mathbf{x}'$ in the presence of the fluctuating ions in the bulk. (Note that in the limit $c_s \to 0$, $G(\mathbf{x},\mathbf{x}')$ reduces to the usual Coulomb's interaction.) The solution to Eq. (2.12), which decays to zero as $r \to \infty$, is given by the Yukawa potential

$$G(\mathbf{x},\mathbf{x}') = \frac{4\pi Z^2 l_B}{|\mathbf{x}-\mathbf{x}'|}\, e^{-\kappa_s\,|\mathbf{x}-\mathbf{x}'|}, \tag{2.13}$$

with decay length κ_s^{-1}. Hence, this test charge is screened by the induced charges which surround it. The *screening length* κ_s^{-1} associated with this property is

$$\kappa_s^{-1} = \left(8\pi l_B Z^2 c_s\right)^{-\frac{1}{2}}, \tag{2.14}$$

which plays an important role in the classic work of Debye and Hückel[3]. Physically, due to accumulation of oppositely charged particles (an ion cloud) near the test charge, the magnitude of its charge is screened and the potential decays exponentially with distance. For 1 mM of monovalent salt $\kappa_s^{-1} \sim 100\,\text{Å}$.

The modification of the self-energy (correlation energy) of a particle of charge e, when it is brought into an electrolyte solution (assuming monovalent, for simplicity), is given by half the difference between the Yukawa potential and Coulomb potential in the limit of zero separation:

$$\beta V_s = \frac{l_B}{2}\lim_{r\to 0}\left[\frac{e^{-\kappa_s r}}{r} - \frac{1}{r}\right] = -\frac{l_B\kappa_s}{2}. \tag{2.15}$$

Each particle in an electrolyte contributes this correction to the thermodynamic internal energy, and thus the change in the internal energy density is

$$\beta\Delta u = -2c_s\frac{l_B\kappa_s}{2} = -\frac{\kappa_s^3}{8\pi}. \tag{2.16}$$

Using the standard thermodynamic identity

$$\Delta u = \frac{\partial}{\partial\beta}[\beta\Delta f_s] \tag{2.17}$$

with the condition that $\Delta f_s \to 0$ as $T \to \infty$, we obtain the electrostatic contribution to the free energy:

$$\Delta f_s = -\, k_B T \, \frac{\kappa_s^3}{12\pi}. \tag{2.18}$$

This is the well-known result obtained by Debye and Hückel[3, 4]. Note that its dependence on density is $f \sim c_s^{3/2}$, which differs from the c^2 dependence in the usual virial expansion for short-ranged interactions.

Similar to the virial expansion, the Debye-Hückel theory is valid as long as the kinetic energy is much greater than the interaction energy among particles. Defining a dimensionless parameter by the ratio of the potential to kinetic energy:

$$\Gamma \equiv \frac{l_B}{a_0} = l_B \, c_s^{1/3}, \tag{2.19}$$

where $a_0 = c_s^{-1/3}$ is the mean inter-particle separation, we expect that Debye-Hückel theory is valid if $\Gamma \ll 1$. Alternatively, we note that the parameter defined by

$$g = \kappa_s \, l_B \sim \Gamma^{3/2} \tag{2.20}$$

is inversely proportional to the number of particles N_{κ_s} contained within the "Debye" sphere, *i.e.* whose radius equals the screening length:

$$N_{\kappa_s} \sim \kappa_s^{-3} c_s \sim \frac{1}{g}. \tag{2.21}$$

Hence the weak coupling condition $g \ll 1$ is equivalent to the requirement that the number of charges within the screening volume be large, although $\Gamma \ll 1$ indicates that charges must be dilute. In this case, the Debye-Hückel theory captures correlation effects to the leading order and perturbation theory is a controlled approximation.

In the vicinity of a charged surface with charge density σ, a neutralizing counterion (assuming monovalent) in the solution experiences an (unscreened) electrostatic attractive force of magnitude $2\pi l_B (\sigma/e) \, k_B T$. The *Gouy-Chapman length* at which the thermal energy balances the electrostatic energy is given by[5]

$$\lambda = \frac{e}{\pi l_B \sigma}. \tag{2.22}$$

It defines a layer within which most of the counterions are confined. For a moderate charge density of $\sigma/e \sim 1/100$ Å^{-2}, λ is of the order of a few angstroms. To estimate the validity of PB theory for charged surfaces, we note the counterions may be considered as an ideal gas with density $n \sim \sigma/(e\lambda)$. This implies that $\kappa_s^2 \sim nl_B \sim 1/\lambda^2$, and so $g \sim l_B/\lambda$. Thus, we expect that the PB theory is good when $l_B/\lambda \ll 1$. Note that this condition is not satisfied for highly charged surfaces.

2.2 Derivation of the Poisson-Boltzmann Equation

In this section, we derive a functional integral representation of the grand canonical partition function for a system of interacting mobile charges in the presence of an external charged surface. To understand what "mean-field" means, we rigorously derive the Poisson-Boltzmann equation as a saddle-point equation to an exact field theory. For simplicity, we only consider a system of N point-like particles of charge $-Ze$ and a fixed external charge density $\sigma(\mathbf{x}) = en(\mathbf{x})$ at surfaces. The energy for this system is

$$\beta E_N = Z^2 l_B \sum_{j>k}^{N} \frac{1}{\mid \mathbf{x}_j - \mathbf{x}_k \mid} - \sum_{j=1}^{N} \phi(\mathbf{x}_j), \tag{2.23}$$

where $\phi(\mathbf{x}) = Zl_B \int d^3\mathbf{x}' \, \frac{n(\mathbf{x}')}{|\mathbf{x}-\mathbf{x}'|}$ is the "external" field. The partition function for this system is

$$Z_N[\phi] = \frac{1}{N!} \prod_{k=1}^{N} \int \frac{d^3\mathbf{x}_k}{a^3} \, \exp\left(-\beta E_N\right), \tag{2.24}$$

where a is the molecular size of the counterions. To map the partition function Eq. (2.24) into a field theory, we perform the well-known Hubbard-Stratonovich transformation[6], which is just a Gaussian identity for N variables:

$$e^{-\frac{1}{2}\sum_{j,k} y_j \, A^{-1}_{jk} \, y_k} = \frac{\prod_{j=1}^{N} \int_{-\infty}^{\infty} dx_j \, e^{-\frac{1}{2}\sum_{jk} x_j \, A_{jk} \, x_k + i\sum_j x_j \, y_j}}{\prod_{j=1}^{N} \int_{-\infty}^{\infty} dx_j \, e^{-\frac{1}{2}\sum_{jk} x_j \, A_{jk} \, x_k}}. \tag{2.25}$$

First noting that

$$\frac{1}{\mid \mathbf{x}_j - \mathbf{x}_k \mid} = \int \frac{d^3\mathbf{q}}{(2\pi)^3}\, \frac{4\pi}{q^2}\, e^{-i\,\mathbf{q}\cdot(\mathbf{x}_j - \mathbf{x}_k)}, \tag{2.26}$$

the first term in Eq. (2.23) can be written as

$$\begin{aligned} Z^2 l_B \sum_{j>k}^{N} \frac{1}{\mid \mathbf{x}_j - \mathbf{x}_k \mid} &= \sum_{j>k}^{N} \int \frac{d^3\mathbf{q}}{(2\pi)^3}\, \frac{4\pi Z^2 l_B}{q^2}\, e^{-i\,\mathbf{q}\cdot(\mathbf{x}_j - \mathbf{x}_k)} \\ &= \int \frac{d^3\mathbf{q}}{(2\pi)^3}\, \frac{4\pi Z^2 l_B}{q^2} \left[\frac{1}{2} \sum_{jk} e^{-i\,\mathbf{q}\cdot(\mathbf{x}_j - \mathbf{x}_k)} - \frac{N}{2} \right] \\ &= -N V_0 + \frac{1}{2} \int \frac{d^3\mathbf{q}}{(2\pi)^3}\, c(\mathbf{q}) V(q) c(-\mathbf{q}), \end{aligned} \tag{2.27}$$

where $c(\mathbf{q}) = \sum_i^N e^{i\,\mathbf{q}\cdot\mathbf{x}_i}$, $V(q) = \frac{4\pi Z^2 l_B}{q^2}$, and $V_0 = \int \frac{d^3\mathbf{q}}{(2\pi)^3} \frac{4\pi Z^2 l_B}{2q^2}$. Using the Hubbard-Stratonovich transformation Eq. (2.25) to obtain

$$\begin{aligned} e^{-\frac{1}{2}\int \frac{d^3\mathbf{q}}{(2\pi)^3}\, c(\mathbf{q})\, V(q)\, c(-\mathbf{q})} &= \mathcal{N}_0 \prod_{\mathbf{q}} \int d\psi(\mathbf{q}) \left\{ e^{-\frac{1}{2}\int \frac{d^3\mathbf{q}}{(2\pi)^3}\, \psi(\mathbf{q}) V^{-1}(q) \psi(-\mathbf{q})} \right. \\ &\qquad \left. \times\ e^{+i\int \frac{d^3\mathbf{q}}{(2\pi)^3}\, c(\mathbf{q})\, \psi(-\mathbf{q})} \right\}, \end{aligned} \tag{2.28}$$

where $\mathcal{N}_0 = [\det(V^{-1})]^{-1/2}$, and noting that the second term in the exponential is

$$\int \frac{d^3\mathbf{q}}{(2\pi)^3}\, c(\mathbf{q})\, \psi(-\mathbf{q}) = \sum_{j=1}^{N} \int \frac{d^3\mathbf{q}}{(2\pi)^3}\, e^{i\,\mathbf{q}\cdot\mathbf{x}_j}\, \psi(-\mathbf{q}) = \sum_{j=1}^{N} \psi(\mathbf{x}_j), \tag{2.29}$$

the partition function Eq. (2.24) can be cast into

$$\begin{aligned} Z_N[\phi] &= \mathcal{N}_0 \frac{1}{N!} \prod_{j=1}^{N} \int \frac{d^3\mathbf{x}_j}{a^3} \prod_{\mathbf{q}} \int d\psi(\mathbf{q}) \times \\ &\qquad e^{-\frac{1}{2}\int \frac{d^3\mathbf{q}}{(2\pi)^3}\, \psi(\mathbf{q}) V^{-1}(q) \psi(-\mathbf{q}) + i\sum_{k=1}^{N} \psi(\mathbf{x}_k) + \sum_{k=1}^{N} \phi(\mathbf{x}_k) + N V_0} \\ &= \mathcal{N}_0 \frac{1}{N!} \prod_{\mathbf{q}} \int d\psi(\mathbf{q}) \left\{ e^{-\frac{1}{2}\int \frac{d^3\mathbf{q}}{(2\pi)^3}\, \psi(\mathbf{q}) V^{-1}(q) \psi(-\mathbf{q})} \right. \\ &\qquad \left. \times \left[\int \frac{d^3\mathbf{x}}{a^3}\, e^{i\psi(\mathbf{x}) + V_0 + \phi(\mathbf{x})} \right]^N \right\}. \end{aligned} \tag{2.30}$$

In the grand canonical ensemble, a chemical potential μ is introduced:

$$\begin{aligned}\mathcal{Z}_\mu[\phi] &= \sum_{N=0}^{\infty} [e^{\mu}]^N \, Z_N[\phi] \qquad (2.31)\\ &= \mathcal{N}_0 \prod_{\mathbf{q}} \int d\psi(\mathbf{q}) \, e^{-\frac{1}{2}\int \frac{d^3\mathbf{q}}{(2\pi)^3}\,\psi(\mathbf{q})V^{-1}(q)\psi(-\mathbf{q}) + \int \frac{d^3\mathbf{x}}{a^3}\, e^{i\psi(\mathbf{x})+\phi(\mathbf{x})+V_0+\mu}}.\end{aligned}$$

The first term in the exponential can be further simplified by noting that

$$\begin{aligned}\frac{1}{2}\int \frac{d^3\mathbf{q}}{(2\pi)^3}\,\psi(\mathbf{q})V^{-1}(q)\psi(-\mathbf{q}) &= \frac{1}{2}\int \frac{d^3\mathbf{q}}{(2\pi)^3}\,\psi(\mathbf{q})\,\frac{q^2}{4\pi Z^2 l_B}\,\psi(-\mathbf{q})\\ &= \frac{1}{8\pi Z^2 l_B}\int d^3\mathbf{x}\,\psi(\mathbf{x})\,[-\nabla^2]\,\psi(\mathbf{x}). \qquad (2.32)\end{aligned}$$

Therefore, we obtain a functional representation [7] for the grand partition function with the action $\mathcal{S}[\psi,\phi]$:

$$\begin{aligned}\mathcal{Z}_\mu[\phi] &= \mathcal{N}_0 \int \mathcal{D}\psi\, e^{-\mathcal{S}[\psi,\phi]}, \qquad (2.33)\\ \mathcal{S}[\psi,\phi] &= \frac{1}{\ell_B}\int d^3\mathbf{x}\left\{\frac{1}{2}\,\psi(\mathbf{x})\,[-\nabla^2]\,\psi(\mathbf{x}) - \kappa^2 e^{i\psi(\mathbf{x})+\phi(\mathbf{x})}\right\}, \qquad (2.34)\end{aligned}$$

where $\ell_B = 4\pi l_B Z^2$, $\kappa^2 = c_0\ell_B$, and $c_0 = \frac{e^{\mu+V_0}}{a^3}$.

Now, we show that the saddle-point for the action $\mathcal{S}$, *i.e.* $\frac{\delta\mathcal{S}}{\delta\psi(\mathbf{x})} = 0$, corresponds to the mean-field Poisson-Boltzmann equation. Using the Euler-Lagrange equation, we have

$$\nabla^2\psi_0(\mathbf{x}) + i\kappa^2 e^{i\psi_0(\mathbf{x})+\phi(\mathbf{x})} = 0. \qquad (2.35)$$

Defining $\varphi(\mathbf{x}) = -i\psi_0(\mathbf{x}) - \phi(\mathbf{x})$, Eq. (2.35) becomes

$$\begin{aligned}\nabla^2\varphi(\mathbf{x}) + \kappa^2 e^{-\varphi(\mathbf{x})} &= -\nabla^2\phi(\mathbf{x})\\ &= \frac{\ell_B}{Z}\,n(\mathbf{x}). \qquad (2.36)\end{aligned}$$

This is the Poisson-Boltzmann equation, which has been obtained in Sec. 2.1, based on physical arguments. It is also interesting to note that the Poisson equation

$$\nabla^2\langle i\psi(\mathbf{x})\rangle = \ell_B\,\langle c(\mathbf{x})\rangle \qquad (2.37)$$

with the (mean) counterion distribution

$$\langle c(\mathbf{x})\rangle = \frac{1}{Zl_B}\,\frac{\delta \ln \mathcal{Z}_\lambda[\phi]}{\delta\phi(\mathbf{x})} = c_0\,\left\langle e^{i\psi(\mathbf{x})+\phi(\mathbf{x})}\right\rangle, \tag{2.38}$$

follows exactly from the fact that the functional integral of a total derivative must vanish, $\left\langle \frac{\delta \mathcal{S}}{\delta\psi(\mathbf{x})}\right\rangle = 0$:

$$\nabla^2\langle i\psi(\mathbf{x})\rangle = \kappa^2\left\langle e^{i\psi(\mathbf{x})+\phi(\mathbf{x})}\right\rangle. \tag{2.39}$$

2.3 Electrostatics of Charged Surfaces

In this section, we solve the PB equation for planar geometries – systems of charged planes with their neutralizing counterions – to illustrate some physical aspects of the many-body problem of charged particles within a mean-field approach.

Consider an infinite array of parallel uniformly charged planes immersed in an aqueous solution containing only counterions. Due to in-plane translational invariance, the PB equation for these problems is essentially one dimensional and thus the normalized electrostatic potential $\varphi(\mathbf{x})$ and counterion density $c(\mathbf{x})$ depend only on the axis perpendicular to the charged planes – say z. With this in mind, the PB equation can be written as

$$\frac{d^2\varphi(z)}{dz^2} + \kappa^2 e^{-\varphi(z)} = \frac{\ell_B}{Z}\,n(z). \tag{2.40}$$

In the region where the external charge density $n(z)$ is zero, the homogeneous PB equation

$$\frac{d^2\varphi(z)}{dz^2} + \kappa^2 e^{-\varphi(z)} = 0 \tag{2.41}$$

can be solved exactly by the “energy” method. Multiplying both sides by $\frac{d\varphi}{dz}$ and integrating, we obtain a constant of “motion”

$$E = \frac{1}{2}\left(\frac{d\varphi}{dz}\right)^2 - \kappa^2 e^{-\varphi(z)}. \tag{2.42}$$

The solution to the PB equation can now be obtained by solving the following integral

$$z - z' = \pm\int_{\varphi'}^{\varphi}\frac{d\varphi}{\sqrt{2(E+\kappa^2 e^{-\varphi})}}. \tag{2.43}$$

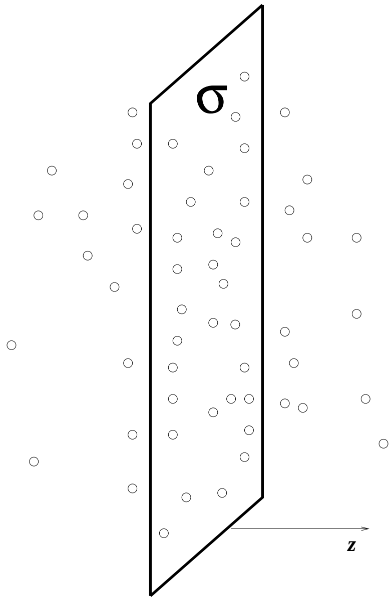

Figure 2.1: A schematic picture of a single charged plane immersed in an aqueous solution containing counterions. The Gouy-Chapman length λ is defined in Eq. (2.50)

It turns out that depending on whether $E > 0$, $E = 0$, or $E < 0$, the solutions given by

$$\varphi(z) = \begin{cases} \ln\left[\frac{\kappa^2}{E}\sinh^2\sqrt{\frac{E}{2}}(z-z')\right] & \text{if } E > 0, \\ \ln\frac{\kappa^2}{2}(z-z') & \text{if } E = 0, \\ \ln\left[\frac{\kappa^2}{|E|}\cos^2\sqrt{\frac{|E|}{2}}(z-z')\right] & \text{if } E < 0. \end{cases} \tag{2.44}$$

correspond to different boundary conditions as imposed by the external charge density $n(z)$. In addition, using Eq. (2.38), the counterions distribute in space according to

$$c(z) = c_0\, e^{-\varphi(z)}, \tag{2.45}$$

at the mean-field level. In the following subsections, we will discuss a few specific physical situations to which these solutions apply.

2.3.1 A Single Charged Plate

For a single charged plane located at $z = 0$, *i.e.* $n(z) = n_0\delta(z) = (\sigma/e)\,\delta(z)$, immersed in an aqueous solution containing only counterions (see Fig. 2.1), the boundary condition is obtained by integrating the PB equation (2.40) over z in the range $-\varepsilon < z < \varepsilon$ and taking the limit $\varepsilon \to 0$:

$$\left.\frac{d\varphi(z)}{dz}\right|_{z=0} = \frac{\sigma\ell_B}{2Ze}. \tag{2.46}$$

Since the counterion density must vanish at infinity, *i.e.* $\rho(z) \to 0$ as $|z| \to \infty$, we must choose the $E = 0$ solution given in Eq. (2.44). When normalized, *i.e.* $\varphi(0) = 0$, the electrostatic potential can be written as

$$\varphi(z) = 2\ln\left(1 + \frac{\kappa|z|}{\sqrt{2}}\right). \tag{2.47}$$

Matching the derivative of this solution at the boundary, Eq. (2.46) leads to

$$\kappa = \frac{\sigma\ell_B}{2\sqrt{2}\,Ze}. \tag{2.48}$$

With this constant determined, the solution to this problem is uniquely specified by σ. Note that due to the screening of the counterions, the potential $\varphi(z)$ is logarithmically divergent as $|z| \to \infty$, in contrast to the linear divergence for a single charged plane without counterions. Furthermore, the counterion distribution

$$c(z) = \frac{c_0}{\left(1 + \frac{\kappa|z|}{\sqrt{2}}\right)^2} = \frac{2}{\ell_B\left(|z| + \lambda\right)^2} \tag{2.49}$$

decays to zero algebraically, instead of the exponential decay naively expected for an ideal gas in an external field. As noted in Sec. 2.1.1, there is a characteristic length given by

$$\lambda \equiv \frac{\sqrt{2}}{\kappa} = \frac{4Ze}{\ell_B\sigma} = \frac{e}{\pi l_B Z\sigma}, \tag{2.50}$$

in the counterion distribution. This Gouy-Chapman length defines a sheath near the charged surface within which most of the counterions are confined. Typically, it is on the order of a few angstroms for a moderate charge density of $\sigma \sim e/100$ Å^{-2} and monovalent counterions. Note that since λ scales inversely with σ and linearly with T, at sufficiently high densities or low temperature, the counterion distribution is essentially 2-dimensional.

The (mean-field) free energy per unit area of this counterion gas may be estimated by noting that they form an ideal gas with a 3D density $c \sim n_0/(Z\lambda)$, which is confined to a slab of thickness λ

$$\beta f_0 \simeq c\,\ln[c\,a^3]\,\lambda = \frac{n_0}{Z}\ln\left(\frac{n_0\,a^3}{Z\lambda}\right). \tag{2.51}$$

To compute the free energy rigorously, we return to the field theory formulation of this problem presented in Sec. 2.2. Let us start with the zero-loop effective action, which is the action $\mathcal{S}[\psi,\phi]$ in Eq. (2.34) evaluated at the saddle point solution $\psi_0(\mathbf{x})$

$$\mathcal{S}_0[\phi] = -\frac{1}{\ell_B}\int d^3\mathbf{x}\left\{\frac{1}{2}\,i\psi_0(\mathbf{x})\,[-\nabla^2]\,i\psi_0(\mathbf{x}) + \kappa^2 e^{i\psi_0(\mathbf{x})+\phi(\mathbf{x})}\right\}, \tag{2.52}$$

where $i\psi_0(\mathbf{x})$ is related to the PB solution by $\varphi(\mathbf{x}) = -i\psi_0(\mathbf{x}) - \phi(\mathbf{x})$. Note that although $\mathcal{S}_0[\phi]$ expressed in terms of $i\psi_0(\mathbf{x})$, $\mathcal{S}_0[\phi]$ is actually independent of $i\psi_0(\mathbf{x})$ because it satisfies the saddle point equation (2.35). In terms of $\varphi(\mathbf{x})$ and the mean field counterion distribution $c(\mathbf{x})$ in Eq. (2.49) for the one plate problem, $\mathcal{S}_0[\phi]$ can be rewritten as

$$\mathcal{S}_0[\phi] = -\frac{1}{2}\int d^3\mathbf{x}\,\phi(\mathbf{x})\,c(\mathbf{x}) - \frac{1}{2}\int d^3\mathbf{x}\,[\,\varphi(\mathbf{x})\,c(\mathbf{x}) + 2c(\mathbf{x})\,]\,. \tag{2.53}$$

Using the Legendre transformation:

$$\Omega_0[c(\mathbf{x})] = \mathcal{S}_0[\phi] + \int d^3\mathbf{x}\,\phi(\mathbf{x})\,c(\mathbf{x}), \tag{2.54}$$

we obtain the Grand potential for the counterions

$$\Omega[c(\mathbf{x})] = \frac{1}{2}\int d^3\mathbf{x}\,\phi(\mathbf{x})\,c(\mathbf{x}) - \frac{1}{2}\int d^3\mathbf{x}\,[\varphi(\mathbf{x})c(\mathbf{x}) + 2c(\mathbf{x})]\,, \tag{2.55}$$

and the Helmholtz free energy is related to the Grand potential $\Omega[c(\mathbf{x})]$ by another Legendre transformation involving the chemical potential:

$$\beta F_0 = \Omega_0[c(\mathbf{x})] + \mu\int d^3\mathbf{x}\,c(\mathbf{x}). \tag{2.56}$$

Using the fact that

$$\int_{-\infty}^{\infty} dz\, \varphi(z) c(z) = \frac{2n_0}{Z}, \tag{2.57}$$

and the chemical potential μ can be solved from its definition

$$\frac{e^{\mu+V_0}}{a^3} = \frac{\kappa^2}{\ell_B} \;\rightarrow\; \mu = -V_0 + \ln\left(\frac{n_0 a^3}{2Z\lambda}\right), \tag{2.58}$$

where V_0 is the (infinite) self-energy, the free energy per unit area is

$$\beta f_0 = -\frac{n_0 V_0}{Z} + \frac{n_0}{Z}\ln\left(\frac{n_0\, a^3}{2Z\lambda}\right) - \frac{2n_0}{Z} + \frac{1}{2}\int dz\, \phi(z)\, c(z). \tag{2.59}$$

Now solving for the external field $\phi(\mathbf{x})$

$$\nabla^2\phi = -\frac{n_0\ell_B}{Z}\,\delta(z) \;\rightarrow\; \phi(z) = U_0 - \frac{n_0\ell_B}{2Z}|z|, \tag{2.60}$$

where U_0 is an arbitrary constant and evaluating

$$\int_{-\infty}^{\infty} dz\, \phi(z)\, \rho_0(z) = \frac{n_0}{Z}\, U_0 \; - \frac{2n_0}{Z}\int_0^{\infty} dx\, \frac{x}{(1+x)^2} = \frac{2n_0}{Z} + \frac{n_0}{Z}\left[U_0 - \int_1^{\infty} dx\, \frac{2}{x}\right],$$

we note that the second term in the parentheses is logarithmic divergent, which can be canceled by the arbitrary constant U_0. Putting these results together, the free energy per unit area is

$$\beta f_0 = -\frac{n_0}{Z}V_0 + \frac{n_0}{Z}\ln\left(\frac{n_0\, a^3}{2Z\lambda}\right) - \frac{n_0}{Z}. \tag{2.61}$$

Apart from the infinite self-energy term, which will be canceled below in Chapter 4, when we consider fluctuation corrections to the PB solution, Eq. (2.61) agrees with Eq. (2.51) above and indeed has the form of the free energy of an ideal gas. Note that λ in the logarithm indicates the effect of mutual interaction of the counterions.

2.3.2 Electrostatic Interaction between Two Charged Plates

In this section, we shall use the PB equation to derive the electrostatic potential, counterion distribution and the pressure between two charged plates as

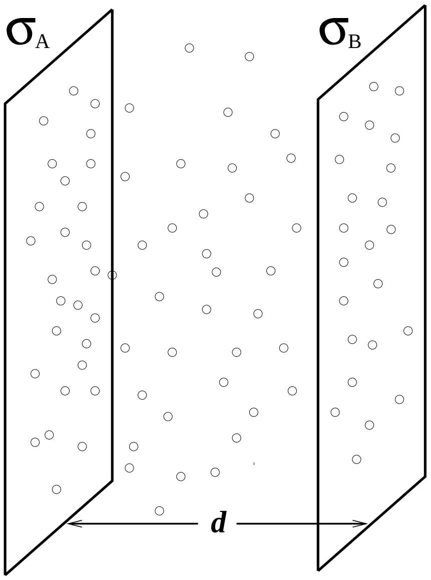

Figure 2.2: A schematic picture of neutralizing counterions confined between two charged plates.

illustrated in Fig. 2.2. We treat both cases of similarly charged and oppositely charged plates[8].

Following Ref. [2], we derive a general expression for the pressure associated with counterions confined between two charged plates. The pressure is defined by the variation of the free energy with respect to the inter-layer distance d:

$$P(d) = -\frac{1}{A_0}\frac{\partial F}{\partial d}, \tag{2.62}$$

where A_0 is the area of the plane and F is the Helmholtz free energy given by

$$\beta F = \int d^3\mathbf{x}\, c(\mathbf{x}) \left[\ln c(\mathbf{x}) a^3 - 1\right] + \frac{1}{2\ell_B}\int d^3\mathbf{x}\, [\nabla\varphi(\mathbf{x})]^2, \tag{2.63}$$

where a is the ionic size of the charges, the first term is the entropy of the counterions, and the second is the electrostatic energy of the system. Defining a normalized electric field

$$\mathcal{E} = -\frac{d\varphi}{dz} \tag{2.64}$$

and using Eq. (2.40), the counterions density $c(z)$ can be rewritten as

$$c(z) = \frac{1}{\ell_B}\frac{d\mathcal{E}}{dz} \tag{2.65}$$

in the region where $n(z) = 0$. Note that the boundary conditions for $\mathcal{E}$ are independent of d. Therefore, rescaling $\xi = z/d$, the free energy can be re-expressed as

$$\beta F/A_0 = \frac{1}{\ell_B}\int_0^1 d\xi \left\{ \frac{d\mathcal{E}}{d\xi}\left[\ln\left(\frac{d\mathcal{E}}{d\xi}\frac{a^3}{\ell_B d}\right) - 1\right] + \frac{\mathcal{E}^2}{2}d \right\}. \tag{2.66}$$

Using Eqs. (2.62) and (2.42), we find

$$P(d) = -\frac{k_BT}{\ell_B}\int_0^1 d\xi \left(\frac{\mathcal{E}^2}{2} - \frac{1}{d}\frac{d\mathcal{E}}{d\xi}\right) = -\frac{k_BT}{\ell_B}E. \tag{2.67}$$

We arrive at a simple result that the pressure is proportional to $-E$; hence, the solutions obtained in Eqs. (2.44) for $E > 0$ and $E < 0$ describe, respectively, two plates attracting and repelling each other. We may have anticipated this result since E in Eq. (2.42),

$$E = \frac{1}{2}\left(\frac{d\varphi}{dz}\right)^2 - \kappa^2 e^{-\varphi(z)},$$

can be interpreted physically as the difference of the electrostatic stress and the thermal pressure of the counterions ($\sim c(z)\,k_BT$), and hence the resulting pressure between two plates.

The boundary conditions for two charged planes with surface charge densities σ_A at $z = 0$ and σ_B at $z = d$ as shown in Fig. 2.2 are

$$\left.\frac{d\varphi(z)}{dz}\right|_{z=0} = \frac{\sigma_A\ell_B}{Ze} \qquad \text{and} \qquad \left.\frac{d\varphi(z)}{dz}\right|_{z=d} = -\frac{\sigma_B\ell_B}{Ze}. \tag{2.68}$$

First, we consider the case $E \geq 0$; using Eq. (2.44) and the boundary conditions, we obtain

$$\sqrt{\frac{E}{2}}\coth\sqrt{\frac{E}{2}}\,z' = -\frac{\sigma_A\,\ell_B}{2Ze}, \tag{2.69}$$

$$\sqrt{\frac{E}{2}}\coth\sqrt{\frac{E}{2}}\,(d - z') = -\frac{\sigma_B\,\ell_B}{2Ze}. \tag{2.70}$$

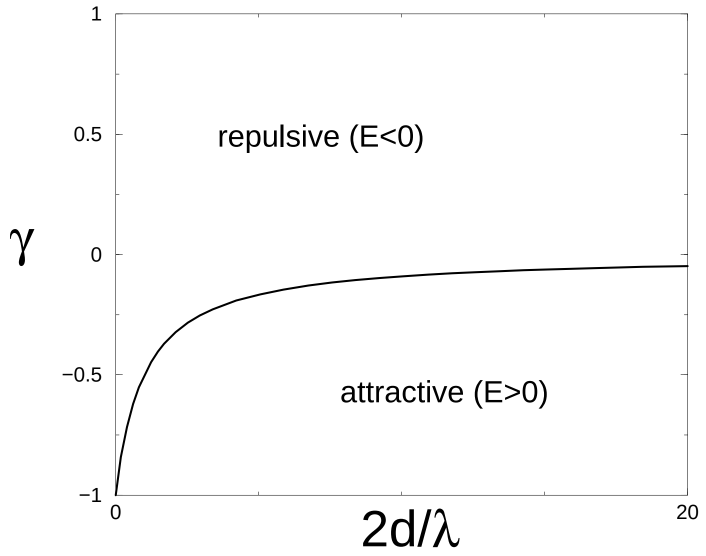

Figure 2.3: The phase diagram of two charged plates. The solid line represents d^* in Eq. (2.73). $\gamma = \sigma_B/\sigma_A$.

Using a standard identity to expand the left-hand side of the latter equation, we find that E satisfies a transcendental equation:

$$E = -\frac{1}{2}\sigma_A\,\sigma_B\left(\frac{\ell_B}{Ze}\right)^2 - \frac{\ell_B(\sigma_A+\sigma_B)}{Ze}\sqrt{\frac{E}{2}}\coth\sqrt{\frac{E}{2}}d. \tag{2.71}$$

Similarly, for $E < 0$ we find

$$|E| = \frac{1}{2}\sigma_A\,\sigma_B\left(\frac{\ell_B}{Ze}\right)^2 + \frac{\ell_B(\sigma_A+\sigma_B)}{Ze}\sqrt{\frac{|E|}{2}}\cot\sqrt{\frac{|E|}{2}}d. \tag{2.72}$$

Interestingly, the $E = 0$ solution, in which the pressure between plates is zero, can be achieved at the equilibrium distance d^* as determined by the $E \to 0$ limit of Eq. (2.71):

$$d^* = -\frac{2Ze}{\ell_B}\left(\frac{1}{\sigma_A}+\frac{1}{\sigma_B}\right). \tag{2.73}$$

The phase diagram depicted in Fig. 2.3 summarizes the physical picture of the PB theory for the two plates problem. For large separations, $d > d^*$, the counterions is dilute and the electrostatic attraction dominates[1]. On the other hand, when the separation is small $d < d^*$, the counterions are dense and thermal pressure dominates. When $d = d^*$, electrostatic and thermal pressure balance out, leaving zero net pressure.

It is clear from Eq. (2.73) or from Fig. 2.3 that zero pressure can be achieved only when $\sigma_B/\sigma_A < 0$, *i.e.* two plates are oppositely charged. As a corollary of this observation, PB theory predicts that two similarly charged plates never attract! This conclusion is general and has been proven within PB theory rather rigorously for other geometries as well[9]. To obtain quantitatively the repulsive pressure between similarly charged plates, we restrict ourselves to the case of $\sigma_A = \sigma_B = \sigma$. In this limit, Eq. (2.72) simplifies to

$$\sqrt{\frac{|E|}{2}}\frac{d}{2}\tan\sqrt{\frac{|E|}{2}}\frac{d}{2} = \frac{d}{\lambda}. \tag{2.74}$$

Let us first consider the large distance limit, $d \gg \lambda$, and note that $\sqrt{\frac{|E|}{2}}\frac{d}{2}$ approaches to a limiting value of $\frac{\pi}{2}$ or $E = -\frac{2\pi^2}{d^2}$. Using Eq. (2.67), we obtain $P(d) = \frac{\pi}{2Z^2}\frac{k_BT}{l_Bd^2}$. In the opposite short distance limit, $d \ll \lambda$, we expand the tangent to obtain $E = -8/(\lambda d)$; Hence, $P(d) = \frac{2}{\pi Z^2}\frac{k_BT}{l_B\lambda d}$. Therefore, we obtain the following regimes for the mean-field repulsion between two similarly charged plates:

$$P(d) \sim \begin{cases} k_BT/l_Bd^2, & \text{for } d \gg \lambda, \\ k_BT/(l_B\lambda\, d), & \text{for } d \ll \lambda. \end{cases} \tag{2.75}$$

In Fig. 2.4, we plot the pressure as a function of d by solving Eq. (2.74) numerically. To understand the results from PB theory physically, we first note that the pressure is independent of the electrostatic field in between the two charged surfaces, as a consequence of the fact that there would be no electric field in this region if there

---

[1] Note that in this regime, the two plates are oppositely charged since $\sigma_B/\sigma_A < 0$ in order to satisfy Eq. (2.71).

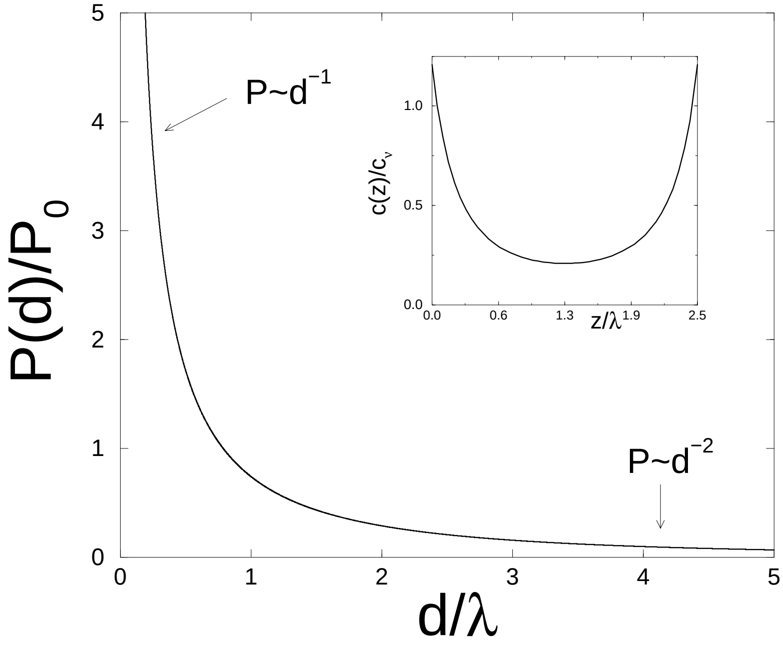

Figure 2.4: The mean-field repulsive pressure as a function of d; $P_0 \equiv \frac{2\sigma k_B T}{Ze\lambda}$. Inset: a plot of the counterion distribution for $d/\lambda = 2.5$, where $c_\nu \equiv 2\sigma/(Ze\lambda)$.

were no counterions between them – the field emanating from one surface is canceled exactly by the other. The spatial non-uniformity in the counterion distribution (see the inset in Fig. 2.4) stems from their mutual repulsion and their entropy of mixing. Furthermore, the surface charge density σ only determines the total number of counterions in the gap by charge neutrality. Thus, the pressure is simply the ideal gas pressure of the counterions. Indeed, since the symmetry of the problem dictates that the electric field must be zero at the mid-plane, the pressure is proportional to the counterion density at $z = d/2$:

$$P(d) = k_B T \, c(d/2). \tag{2.76}$$

This observation helps to understand physically the distance dependence of the mean-field pressure in Eq. (2.75). For small distance $d \ll \lambda$, the counterions distribute uniformly in the gap; thus, $c(d/2) \sim \sigma/(Zed)$, implying $P(d) \sim d^{-1}$. For large distance $d \gg \lambda$, the counterion concentration at midplane can be viewed as a single plate density with z replaced by d in Eq. (2.49): $c(d/2) \sim \sigma\lambda/(Zed^2)$, implying $P(d) \sim d^{-2}$. Finally, we remark that since $P \sim 1/Z$, the mean-field repulsions for higher valence Z are reduced in magnitude, due to the collective behavior of the counterions.

2.3.3 Manning Condensation

In this section, we solve the PB equation with cylindrical symmetry. As it turns out, this symmetry gives rise to an interesting phenomenon, namely, Manning condensation. It is associated with the counterion distribution of a highly charged rigid polyelectrolyte[10]. Intuitively, it can be essentially understood as follows. Consider an infinite charged rod with a radius R and counterions distributed outside the rod, $r > R$ (r is the radial distance), which is depicted in Fig. 2.5. The electrostatic potential arising from the charged rod with a linear charge density of $1/b$ is

$$\phi(r) = \frac{2l_B}{b} \ln(r/R), \tag{2.77}$$

and the counterion density can be estimated by using the Boltzmann distribution:

$$n(r) \sim e^{-\phi(r)}. \tag{2.78}$$

Now, consider the number of counterions contained in a cylindrical shell of radius R_0:

$$\mathcal{Q}(R_0) = 2\pi \int_R^{R_0} r dr\, n(r) \sim \int_R^{R_0} dr r^{1-2\xi_m} \sim r^{2\,(1-\xi_m)}\Big|_R^{R_0}, \tag{2.79}$$

where we have defined $\xi_m \equiv l_B/b$, the Manning parameter. There are two distinct asymptotic behaviors of $\mathcal{Q}(R_0)$ in the limit $R_0 \to \infty$. If $\xi_m < 1$, $\mathcal{Q}(R_0)$ grows with R_0 and counterions escape to infinity. On the other hand, if $\xi_m > 1$, $\mathcal{Q}(R_0)$ is independent of R_0 in the limit $R_0 \to \infty$, and therefore, counterions are bound. This phenomenon is called Manning condensation.

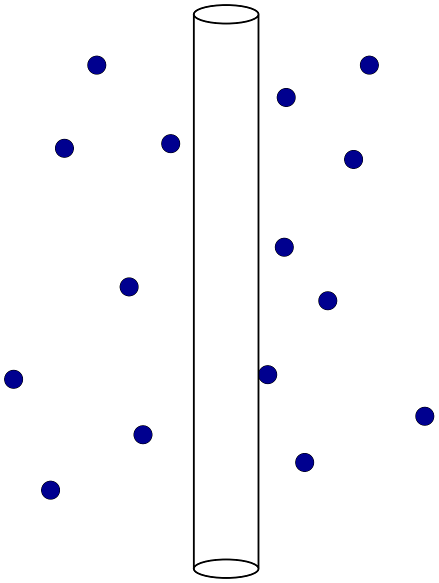

Figure 2.5: A schematic picture of a single infinite charged rod with a surface charged density σ immersed in an aqueous solution containing counterions. Its radius is R

To obtain the behavior of the electrostatic potential and counterion density, we need to solve PB equation in cylindrical coordinates,

$$\frac{d^2\varphi(r)}{dr^2} + \frac{1}{r}\frac{d\varphi(r)}{dr} + \kappa^2 e^{-\varphi(r)} = \frac{\ell_B \sigma}{Ze}\,\delta(r-R). \tag{2.80}$$

This equation belongs to a general class of solvable partial differential equations known as Liouville's equation. In connection to the present problem, its solution was first obtained by Fuoss et al.[11]. Making a change of variable

$$x = R\ln(r/R), \tag{2.81}$$

for $r > R$, Eq. (2.80) can be written as

$$\frac{d^2\varphi(x)}{dx^2} + \kappa^2 e^{-\varphi(x)+2x/R} = 0. \tag{2.82}$$

It can be seen that the shifted potential $\tilde{\varphi}(x) = \varphi(x) - 2x/R$ satisfies the planar PB equation in Eq. (2.40), but with a slightly different boundary condition

$$\left.\frac{d\tilde{\varphi}(x)}{dx}\right|_{x=0} = \frac{\ell_B \sigma}{Ze} - \frac{2}{R}. \tag{2.83}$$

Since the counterion density must vanishes at $r \to \infty$, we choose the $E = 0$ solution, just as in the case of a single charged plane:

$$\tilde{\varphi}(x) = 2 \ln \left(1 + \frac{\kappa\, x}{\sqrt{2}} \right). \tag{2.84}$$

Matching the boundary condition yields

$$\kappa = \frac{1}{\sqrt{2}} \left(\frac{\ell_B \sigma}{Ze} - \frac{2}{R} \right), \tag{2.85}$$

which is, however, fundamentally different from the planar case. If the charge density σ is sufficiently low, in other words

$$\frac{\ell_B R \sigma}{Ze} < 2, \tag{2.86}$$

so that $\kappa < 0$, the solution (2.84) clearly makes no sense.

In this case, we have to make a new assumption that $\kappa = 0$ in the cylindrical PB equation (2.80), as if there were no counterions, to obtain the bare logarithmic potential

$$\varphi(r) = 2\, \xi_m \ln(r/R), \tag{2.87}$$

where we have defined the Manning parameter

$$\xi_m \equiv \frac{\ell_B R \sigma}{2Ze} = \frac{Z l_B}{b} \tag{2.88}$$

and b is the average distance between charges (or inverse of the linear charge density). Therefore, the full solution for the charged rod problem is

$$\varphi(r) = \begin{cases} 2\, \xi_m \ln(r/R), & \text{for } \xi_m \leq 1, \\ 2 \ln(r/R) + 2 \ln \{1 + (\xi_m - 1) \ln(r/R)\} & \text{for } \xi_m > 1. \end{cases} \tag{2.89}$$

We note that when $\xi_m > 1$, the electrostatic potential for $r \gg R$ behaves like

$$\varphi(r) \sim 2 \ln(r/R), \tag{2.90}$$

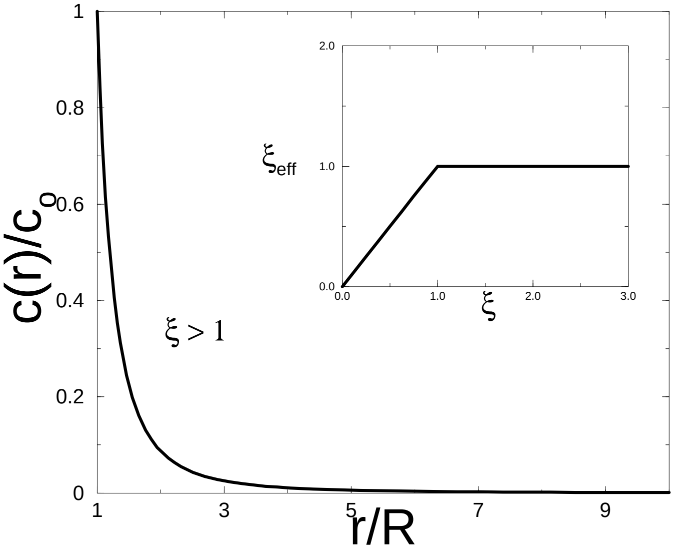

Figure 2.6: Counterion distribution for a single charged rod. Inset: Effective Manning parameter ξ_{eff}.

which is essentially independent of the charge density. Thus, in this case, some of the counterions are loosely "bound" to the rod, partially neutralizing its charge, so that the effective distance between charges b^* is of the order of the Bjerrum length l_B, independent of the bare value of b. Defining the effective Manning parameter by

$$\xi_{\text{eff}} = \begin{cases} \xi_m & \text{for } \xi_m \leq 1; \\ 1 & \text{for } \xi_m > 1, \end{cases} \tag{2.91}$$

as plotted in the inset of Fig. 2.6, the large distance behavior of the electrostatic potential can be conveniently expressed by

$$\varphi(r) \sim 2\,\xi_{\text{eff}} \ln(r/R). \tag{2.92}$$

Finally, The counterion distribution for $\xi_m > 1$ can be obtained by applying Eq.

(2.45). This result is

$$c(r) = \frac{2}{\ell_B \, r^2} \, \frac{(\xi_m - 1)^2}{[1 + (\xi_m - 1)\ln(r/R)]^2}, \tag{2.93}$$

as shown in Fig. 2.6 for $\xi_m = 2$. We note that $c(r)$ is independent of ξ_m for large r. In contrast, for $\xi_m < 1$ all the counterions are at infinity since $c_0 = 0$, as assumed earlier.

2.4 Electrostatic Contribution to Bending Rigidity

As a final application of PB theory, we shall briefly discuss the electrostatic contribution to the elastic constants of a stack of charged membranes[12]. This situation arises from charged surfactants dissolved in water. Under suitable conditions they form lamellar phases, consisting of a stack of alternating amphiphilic bilayers and water regions[1, 2]. The curvature elasticity of these flexible membranes are well described by the Helfrich free energy[13]

$$f_{cur} = \frac{\kappa_b}{2} \, (H \, - \, H_0)^2 + \kappa_G \, K,$$

where H and K are the mean and Gaussian curvature, respectively, κ_b is the bending modulus, κ_G is the Gaussian bending modulus, and H_0 is the spontaneous curvature. As summarized in the Appendix, the electrostatic contribution to the bending moduli κ_b and κ_G can be identified by expanding the electrostatic free energy up to the second order in curvatures H and K and comparing with the Helfrich free energy of the same geometry. In order to calculate the changes in the free energy of these charged layers, the PB equation for curved geometry must be solved for a unit cell of the repeating array of membranes. Thus, we consider counterions confined in between two concentric charged cylindrical shells of radius R_a and $R_b (> R_a)$, as shown in Fig. 2.7. Note that by restricting to the cylindrical geometry, we can only obtain the bending rigidity κ_b, since the solution to the PB equation for spherical geometries is needed to extract κ_G, which is not analytically known. The PB equation

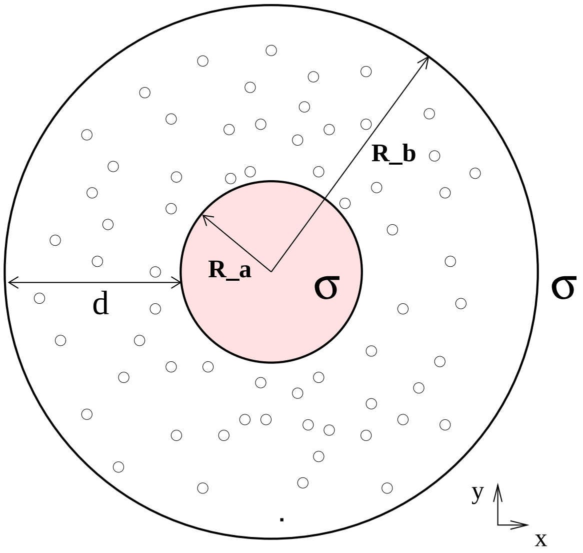

Figure 2.7: Two concentric charged cylindrical shells with counterions in between. This geometry is used to determine the bending rigidity κ_b.

in cylindrical geometry reads

$$\frac{d^2\varphi(r)}{dr^2}+\frac{1}{r}\,\frac{d\varphi(r)}{dr}+\kappa^2 e^{-\varphi(r)}=\frac{\ell_B\sigma}{Ze}\,\left\{\,\delta(r-R_a)+\delta(r-R_b)\,\right\}. \tag{2.94}$$

Using the same transformation as in Sec. 2.3.3:

$$\begin{cases} x = R\ln(r/R); \\ \tilde{\varphi}(x)=\varphi(x)-2x/R, \end{cases} \tag{2.95}$$

the transformed potential $\tilde{\varphi}(x)$ satisfies the planar PB equation Eq. (2.41) with the boundary conditions

$$\left.\frac{d\tilde{\varphi}(x)}{dx}\right|_{x=x_a} = \left(1-\frac{d}{2R}\right)\frac{\ell_B\sigma}{Ze}-\frac{2}{R}; \tag{2.96}$$

$$\left.\frac{d\tilde{\varphi}(x)}{dx}\right|_{x=x_b} = -\left(1+\frac{d}{2R}\right)\frac{\ell_B\sigma}{Ze}-\frac{2}{R}, \tag{2.97}$$

where $R = (R_a + R_b)/2$ and $d = R_b - R_a$. From the general solution obtained in Eq. (2.44), we must choose the $E < 0$ solution

$$\tilde{\varphi}(x) = \ln\left[\cos^2\sqrt{\frac{|E|}{2}}(x - x')\right], \tag{2.98}$$

from which the constant $|E|$ can easily be obtained using the boundary conditions:

$$\frac{|E|}{2} = \left(\frac{\ell_B\sigma}{2Ze}\right)^2 - \frac{1}{R^2}\left(1 + \frac{\ell_B\sigma d}{4Ze}\right)^2 + \frac{\ell_B\sigma}{Ze}\sqrt{\frac{|E|}{2}}\cot\left[\sqrt{\frac{|E|}{2}}\,2R\tanh^{-1}(d/2R)\right]. \tag{2.99}$$

We can now use Eq. (2.63)

$$\beta F = \int d^3\mathbf{x}\, c(\mathbf{x})\left[\ln c(\mathbf{x})a^3 - 1\right] + \frac{1}{2\ell_B}\int d^3\mathbf{x}\,[\nabla\varphi(\mathbf{x})]^2$$

to calculate the free energy per unit area:

$$\begin{aligned}\beta f_{el} &= \frac{2\sigma}{Ze}\left[\ln(|E|\,a^3/\ell_B) - 2\right] + \frac{2R}{\ell_B}\left(|E| + \frac{2}{R^2}\right)\tanh^{-1}(d/2R)\\ &- \frac{\sigma}{Ze}[\varphi(R_b) + \varphi(R_a)] - \frac{2}{\ell_B R}\left(1 + \frac{\ell_B\sigma d}{4Ze}\right)[\varphi(R_b) - \varphi(R_a)].\end{aligned} \tag{2.100}$$

To deduce κ_{el}, the electrostatic contribution to the bending rigidity, we expand the electrostatic free energy in powers of the inverse of the mean radius R up to second order, while keeping d fixed. Substituting the expansion

$$\frac{|E|}{2} = e_0 + \frac{e_1}{R} + \frac{e_2}{R^2} + \cdots \tag{2.101}$$

into Eq. (2.99) and expanding it in powers of $1/R$, we obtain the following coefficients up to second order in $1/R$ by equating terms of the same order:

$$e_0 = a_0^2 + 2a_0\sqrt{e_0}\cot\sqrt{e_0}d; \tag{2.102}$$

$$e_1 = 0; \tag{2.103}$$

$$e_2 = -2e_0\,\frac{2a_0a_1^2 + d^3(a_0^2 + e_0)^2/12}{(a_0^2 + e_0)[2a_0 + d\,(a_0^2 + e_0)]}, \tag{2.104}$$

where $a_0 \equiv \ell_B\sigma/(2Ze) = 2/\lambda$, $a_1 \equiv 1+\ell_B\sigma d/(4Ze) = 1+d/\lambda$, and $\lambda = 4Ze/(\ell_B\sigma)$ is the Gouy-Chapman length. We note that e_0 satisfies the same planar transcendental equation in Eq. (2.74) and the first correction to $|E|$ is of the order of $1/R^2$. Furthermore, the potential at the charged surfaces at R_a and R_b, $\varphi(R_i)$ can be written as

$$\varphi(R_{a/b}) = -\ln\left[1+\frac{(a_0 \mp a_1/R)^2}{E/2}\right] + 2\,\ln\left(1 \mp \frac{d}{2R}\right). \tag{2.105}$$

The free energy Eq. (2.100) can be systematically expanded

$$f_{el} = f_0 + \frac{f_1}{R} + \frac{f_2}{R^2} + \cdots, \tag{2.106}$$

with

$$\begin{aligned}
\beta f_0 &= \frac{2\sigma}{Ze}\left\{\ln[2a^3(4+e_0\lambda^2)/(\ell_B\lambda^2)] - 2\right\} + \frac{2e_0 d}{\ell_B}; && (2.107)\\
\beta f_1 &= 0\,; && (2.108)\\
\beta f_2 &= \frac{1}{\ell_B}\left[\frac{4a_0e_2}{e_0} + \frac{e_0d^3}{6} + 2\,d\,(1+e_2) - 2\,a_1\left(2d - \frac{4a_0a_1}{e_0+a_0^2}\right)\right.\\
&\qquad \left. -\,2\,a_0\left(-\frac{d^2}{2} + \frac{2\,a_1^2\,(a_0^2-e_0)}{(a_0^2+e_0)^2} + \frac{2\,a_0^2e_2}{e_0(e_0+a_0^2)}\right)\right]. && (2.109)
\end{aligned}$$

The first term f_0 is the electrostatic free energy for two interacting charged plates. The term of order $1/R$ vanishes, due to a cancellation of the contributions from the two charged surfaces. The bending modulus is then given simply by $\kappa_{el} = 2f_2$ and after some algebra, the final result reads[14]

$$\kappa_{el} = 4\,k_BT\frac{d}{\ell_B}\left[\frac{\frac{d}{\lambda}\left(1+\frac{2d}{\lambda}-\frac{e_0d^2}{4}\right)}{(\frac{d}{\lambda})^2+\frac{e_0d^2}{4}} - \left(\frac{e_0d^2}{12}+1\right)\right]. \tag{2.110}$$

We first note that this contribution is positive; hence electrostatics make a charged membrane harder to bend. Although Eq. (2.110) is valid for all densities, the most interesting case is the strong coupling limit in which $d \gg \lambda$, $e_0d^2 \approx \pi^2$, and κ_{el} is given by

$$\kappa_{el} \simeq \frac{k_BT}{Z^2}\frac{d}{l_B}\left(\frac{1}{\pi} - \frac{\pi}{12}\right). \tag{2.111}$$

The bending rigidity in this case is proportional to k_BT with an additional factor of l_B^{-1}, which indicates the role of entropy in determining the spatial distribution of the counterions; if $T \to 0$, there would be no resulting contribution to the bending energy, since all the counterions collapse onto the charged surfaces.

2.5 Conclusion

In this chapter, we have studied the mean-field Poisson-Boltzmann theory to understand the interaction of charged surfaces. An interesting aspect is that the counterions may or may not be confined near the charged surface, depending on geometry of the problem. For a charged plane, counterions are always confined, while for an infinite charged rod, condensation depends on the linear charged density. Moreover, PB theory always predicts repulsion between like-charged objects, which may not be the case for highly charged surfaces as recent experiments suggest. This may be attributed to the fact the PB theory neglects correlations among counterions. Indeed, for highly charged surfaces, we have $\lambda \ll l_B$ which, as we have argued, signals the breakdown of PB theory. In this limit, fluctuations and correlations about the mean field potential become so large that the solution to the PB equation no longer provides a reasonable approximation. The next two chapters describe how to go beyond PB theory by incorporating fluctuations.

Bibliography

[1] J.N. Israelachvili, *Intermolecular and Surface Forces* (Academic Press Inc., San Diego, 1992).

[2] S.A. Safran, *Statistical Thermodynamics of Surfaces, Interfaces, and membranes* (Addison-Wesley Publishing Com., Reading, 1994).

[3] P.W. Debye and E. Hückel, Z. Phys., **24** 185 (1923).

[4] L.D. Landau and E.M. Lifshitz, *Statistical Physics*, 3rd Edition, revised and enlarged by E.M. Lifshitz and L.P. Pitaevskii (Pergamon, New York, 1980), §78.

[5] G. Gouy, Ann. Phys. **7**, 129 (1917); D.L. Chapman, Philos. Mag. **25**, 475 (1913); E. Verwey and J.Th.G. Overbeek, *The Theory of the Stability of Lyophobic Colloids* (Elsevier, Amsterdam and New York, 1948).

[6] J. Hubbard, Phys. Rev. Lett. **3**, 77 (1959); R. L. Stratonovitch, Dokl. Akad. Nauk USSR **115**, 1907 (1957).

[7] R.R. Netz and H. Orland, Eur. Phys. J. E **1**, 203 (2000).

[8] A.W.C. Lau and P. Pincus, Eur. Phys. J. B. **10**, 175 (1999).

[9] J.C. Neu, Phys. Rev. Lett. **82**, 1072 (1999); J.E. Sader and D.Y. Chan, J. Colloid Interface Sci. **213**, 268 (1999).

[10] G.S. Manning, J. Chem. Phys. **51**, 924 (1969).

[11] R.M. Fuoss, A. Katachalsky, and S. Lifson, Proc. Natl. Acad. Sci. USA **37**, 275 (1997).

[12] D. Andelman, in *Handbook of Biological Physics,* edited by R. Libowsky, E. Sackman (Elsevier Science Publishers, Amsterdam, 1995), and references therein.

[13] W. Helfrich, Z. Naturforsch. **28C**, 693 (1973).

[14] P.G. Higgs and J.-F. Joanny, J. Physique (France) **51**, 2307; A. Fogden, J. Daicic, D.J. Mitchell, and B.W. Ninham, Physica A **234**, 167 (1996).

Chapter 3

Effects of Charge Fluctuations

3.1 Introduction

As we saw in the last chapter, PB theory provides a mean-field description for charged systems. Among other things, it predicts that for a single charged surface, the counterions are essentially confined to a thin layer defined by the Gouy-Chapman length λ. Note that λ scales inversely with surface charge density σ. At sufficiently high charge densities, $\lambda \ll L$, where L is some characteristic length scale of the plate, the "condensed" counterions can be considered as a quasi-two-dimensional ideal gas (see Fig. 3.1). On physical grounds, we expect that at sufficiently low temperature the fluctuations of these condensed counterions about a uniform density give rise to new phenomena. Indeed, simulations [1] show that the effective force between two like-charged rods and planar surfaces actually becomes attractive at short distances. These surprising results shed new light on the understanding of the electrostatic adhesion between cells [2] and the puzzling problem of DNA condensation [3]. In this chapter, we model the condensed counterions and charges on the charged surfaces effectively as a 2D Coulomb gas interacting with a r^{-1} potential and examine the effect of their in-plane fluctuations.

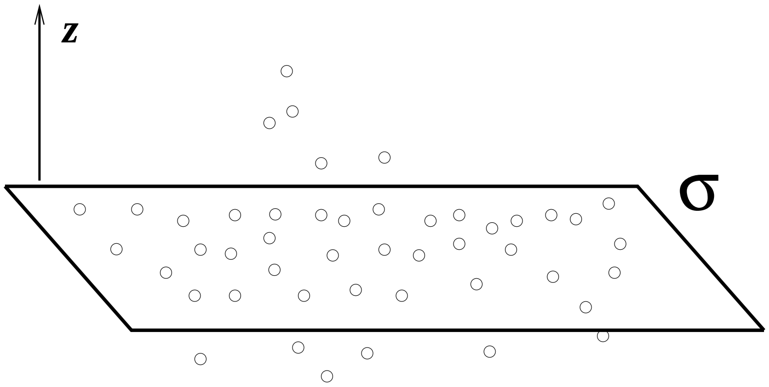

Figure 3.1: For highly charged surfaces, counterions are mostly confined within a layer so thin that they might be considered "condensed". Charge-fluctuations of these counterions can be described by the 2D Debye-Hückel theory.

3.2 Debye-Hückel Theory in 2D

Consider an equal mixture of oppositely charged point-like particles with number density n_0 confined to move on a 2D surface. This "salty" surface model resembles a mixed charged lipid membrane or a highly charged plane whose counterions are restricted to a nearby layer so thin that their fluctuations may be considered as two-dimensional. The effective Hamiltonian for the system is the sum of the entropy of the charges and the electrostatic interaction energy among them:

$$\begin{aligned}\beta\mathcal{H}_{el} &= \sum_{i=\pm}\int d^2\mathbf{r}\; n_i(\mathbf{r})\left\{\ln[n_i(\mathbf{r})\,a^2]-1\right\}+\frac{l_B}{2}\sum_{i=\pm}\int d^2\mathbf{r}\int d^2\mathbf{r}'\,\frac{n_i(\mathbf{r})n_i(\mathbf{r}')}{|\mathbf{r}-\mathbf{r}'|}\\ &- l_B\int d^2\mathbf{r}\int d^2\mathbf{r}'\frac{n_+(\mathbf{r})n_-(\mathbf{r}')}{|\mathbf{r}-\mathbf{r}'|},\end{aligned} \tag{3.1}$$

where $\mathbf{r}$ is the in-plane position vector, a is the molecular size of the charges, $l_B \equiv \frac{e^2}{\epsilon k_B T}$ is the Bjerrum length, ϵ is the dielectric constant, $\beta^{-1} \equiv k_B T$, k_B is the Boltzmann constant, T is the temperature, and $n_i(\mathbf{r})$ is the coarse-grained two-dimensional density of the charges of species i. The domain of the integral in Eq. (3.1) spans the entire surface. In order to calculate the change in the free energy due to fluctuations, we assume that $n_i(\mathbf{r}) = n_0 + \delta n_i(\mathbf{r})$ and expand the electrostatic free energy to second order in δn_i[4]:

$$\beta\delta\mathcal{H}_{el} = \frac{1}{2}\int d^2\mathbf{r}\, d^2\mathbf{r}' \left[\frac{l_B}{|\mathbf{r} - \mathbf{r}'|} + \frac{\delta(\mathbf{r} - \mathbf{r}')}{2n_0}\right] \delta\sigma(\mathbf{r})\, \delta\sigma(\mathbf{r}'), \tag{3.2}$$

where $\delta\sigma = \delta n_+ - \delta n_-$. The first term in the bracket is the Coulomb interaction of the charges. The second term comes from the second variation of the ideal gas entropy of the charges. The change in the free energy is obtained by summing all fluctuations weighted by the Boltzmann factor:

$$\Delta F = -\, k_B T \,\ln\left\{\int \mathcal{D}\sigma(\mathbf{r})\, \exp\left[-\beta\delta\mathcal{H}_{el}\right]\right\}. \tag{3.3}$$

It should be mentioned that Eq. (3.3) contains a divergent self-energy term which has to be subtracted out. This means that we have to discard the first two terms in the expansion for $l_B \rightarrow 0$, as can be seen easily by considering the zero-temperature limit. As $T \rightarrow 0$, the free energy is reduced to the electrostatic energy which is first order in l_B. Since the self-energy is just a constant independent of temperature, it must be linear in l_B. In the following, we use this formalism to study effects of charge fluctuations.

3.2.1 Charges in a Plane

For the case of charges confined to a plane $\delta\mathcal{H}_{el}$ in Eq. (3.2) can be diagonalized by Fourier transform and is quadratic in $\delta\sigma$. Performing the Gaussian integrals in Eq. (3.3) and subtracting out the self-energy term, we obtain the free energy per unit area due to fluctuations [4, 5]

$$\Delta f_{2d} = \frac{k_B T}{2}\int \frac{d^2\mathbf{q}}{(2\pi)^2}\left\{\ln\left[1 + \frac{1}{q\lambda_D}\right] - \frac{1}{q\lambda_D}\right\}, \tag{3.4}$$

where $1/\lambda_D = 4\pi n_0 l_B$, which scales like the Gouy-Chapman length, is a length scale analogous to the Debye screening length in 3-D. Note that Eq. (3.4) is ultravioletly divergent because of the infinite energy associated with the collapse of opposite charges. Thus a microscopic cut-off is necessary. In Ref.[6], the author shows by partial summation of the Mayer series that the resulting free energy is convergent and indeed equivalent to a microscopic cut-off. Eq. (3.4) can be evaluated to yield the electrostatic correction to the the free energy per unit area[7]:

$$\Delta f_{2d} = -\frac{k_B T}{8\pi\lambda_D^2}\ln(\lambda_D/a) + \cdots. \tag{3.5}$$

Note that this correction contains a logarithmic term, in contrast to the DH theory in 3-D, where the change in the free energy per unit volume obtained in Eq. (2.18) is

$$\Delta f_s \sim -\, k_B T\, \lambda_s^{-3} + \cdots,$$

where $\lambda_s \equiv \kappa_s^{-1}$ is the 3D screening length.

It is interesting to consider the charge correlation function $\langle\, \delta\sigma(\mathbf{q})\, \delta\sigma(\,\mathbf{k})\,\rangle$, which can be deduced from $\delta\mathcal{H}_{el}$ in Eq. (3.2) with the help of the equipartition theorem:

$$\langle\, \delta\sigma(\mathbf{q})\, \delta\sigma(\mathbf{k})\,\rangle = (2\pi)^2\delta(\mathbf{q}+\mathbf{k})\,\frac{2n_0\, q\lambda_D}{1+q\lambda_D}. \tag{3.6}$$

In real space, $\langle\, \delta\sigma(\mathbf{0})\, \delta\sigma(\mathbf{r})\,\rangle$ can be interpreted as the 2-D charge distribution given that a point-charge is located at the origin. Fourier transforming Eq. (3.6), we have

$$\langle\, \delta\sigma(\mathbf{0})\, \delta\sigma(\mathbf{r})\,\rangle = 2n_0\delta(\mathbf{r}) - \frac{\tau_0(r/\lambda_D)}{4\pi^2 l_B \lambda_D^2 r}, \tag{3.7}$$

where the function $\tau_0(x)$ defined by

$$\tau_0(x) = \int_0^\infty dy\, \frac{y\, J_0(y)}{x+y}, \tag{3.8}$$

where $J_0(x)$ is the Bessel function, has the following asymptotics

$$\tau_0(x) = \begin{cases} 1 + x\,(\ln\frac{x}{2} + C) - x^2 + O(x^3), & \text{for } x \ll 1, \\ \frac{1}{x^2} - \frac{9}{x^4} + O(x^{-6}), & \text{for } x \gg 1, \end{cases} \tag{3.9}$$

where C is the Euler's constant. The charge distribution decays algebraically for large distances away from the test charge, in contrast with the DH in 3D, where screening charges decay exponentially with distance from the test charge. Thus, physically, the second term in Eq. (3.7) represents a cloud of induced charges, whose charge distribution consists of a multipolar expansion. This point will become clear when we consider the 2D Debye-Hückel equation.

Closely related to the charge correlation function is the Green's function $G_{2d}(\mathbf{x}, \mathbf{x}')$ of the 2-D Debye-Hückel equation

$$\left[-\nabla^2_{\mathbf{x}} + \frac{2}{\lambda_D}\,\delta(z)\right] G_{2d}(\mathbf{x}, \mathbf{x}') = 4\pi l_B \delta(\mathbf{x} - \mathbf{x}'). \tag{3.10}$$

This equation may be derived from the same argument leading to Eq. (2.12), and the second term in the bracket takes into account of the fact that charges are confined on a plane. We note that due to in-plane translation invariance, the Green's function $G_{2d}(\mathbf{x}, \mathbf{x}')$ can be Fourier transformed in the directions parallel to the plane:

$$\left[-\frac{d^2}{dz^2} + q^2 + \frac{2}{\lambda_D}\,\delta(z)\right] G_{2d}(z, z'; q) = 4\pi l_B \delta(z - z'), \tag{3.11}$$

where $q^2 = q_x^2 + q_y^2$. A physically transparent way to solve this equation is to split $G_{2d}(z, z'; q)$ into two parts:

$$G_{2d}(z, z'; q) = G_0(z - z'; q) + \mathcal{G}_{2d}(z, z'; q), \tag{3.12}$$

where

$$G_0(z - z'; q) = \frac{2\pi l_B}{q}\, e^{-q|z-z'|} \tag{3.13}$$

is the potential for a point charge, which satisfies

$$\left[-\frac{d^2}{dz^2} + q^2\right] G_0(z - z'; q) = 4\pi l_B \delta(z - z'). \tag{3.14}$$

Substituting the decomposition into Eq. (3.10) and rearranging, we obtain

$$G_{2d}(z, z'; q) = G_0(z - z'; q) - \frac{1}{2\pi l_B \lambda_D} \int_{-\infty}^{\infty} dz''\, G_{2d}(z, z''; q)\, \delta(z'')\, G_0(z' - z''; q), \tag{3.15}$$

which can be solved algebraically for $G_{2d}(z,0;q)$:

$$G_{2d}(z,0;q) = \frac{2\pi l_B \lambda_D \, G_0(z;q)}{2\pi l_B \lambda_D + G_0(0;q)} = \frac{2\pi l_B \lambda_D}{1+q\lambda_D} \, e^{-q|z|}. \tag{3.16}$$

Physically, $G_{2d}(z,0;q)$ is the electrostatic potential at a distance z above or below the plane due to a point charge located at origin. The in-plane potential is the Fourier transform of $G_{2d}(z,0;q)$ at $z=0$,

$$G_{2d}(\mathbf{r},\mathbf{0}) = \int \frac{d^2\mathbf{q}}{(2\pi)^2} \, e^{-i\mathbf{q}\cdot\mathbf{r}} \, G_{2d}(0,0;q) = \frac{l_B}{r} \tau_0(r/\lambda_D), \tag{3.17}$$

where in the last line, we have made use of the function defined in Eq. (3.8). From this result, we see that the screening is weak in 2D: the potential decays algebraically as $\sim r^{-3}$ to the lowest order, similar to that of a dipolar field where λ_D plays the role of the dipole moment. Using Eq. (3.10) and Poisson's equation Eq. (2.5), we can calculate the probability of finding a charged particle at $\mathbf{x}$ given that a test charge is fixed at the origin:

$$g(\mathbf{x},\mathbf{0}) = -\frac{1}{4\pi l_B} \nabla^2 G_{2d}(\mathbf{x},\mathbf{0}) = \delta(\mathbf{x}) - \frac{2}{\lambda_D} \, \delta(z) \, G_{2d}(\mathbf{x},\mathbf{0}). \tag{3.18}$$

In Fourier space, $g(z,0;q)$ can be easily shown to be

$$g(z,0;q) = \delta(z) - \frac{\delta(z)}{1+q\lambda_D} = \delta(z) \, \frac{q\lambda_D}{1+q\lambda_D}, \tag{3.19}$$

which is indeed proportional to the charge correlation function $\langle \, \delta\sigma(\mathbf{q}) \, \delta\sigma(-\mathbf{q}) \, \rangle$, as it should be. Finally, $G_{2d}(z,0;q)$ can be substituted back into Eq. (3.15) to obtain the full Green's function

$$G_{2d}(z,z';q) = \frac{2\pi l_B}{q} \left\{ e^{-q|z-z'|} - \frac{e^{-q\,(\,|z|+|z'|\,)}}{1+q\lambda_D} \right\}. \tag{3.20}$$

The physical meaning of the Green's function

$$G_{2d}(\mathbf{x},\mathbf{x}') = \int \frac{d^2\mathbf{q}}{(2\pi)^2} \, e^{-i\mathbf{q}\cdot(\mathbf{r}-\mathbf{r}')} \, G_{2d}(z,z';q), \tag{3.21}$$

is identical to the Coulomb potential – the electrostatic interaction between two unit charges located at $\mathbf{x}$ and $\mathbf{x}'$ in the presence of a “salty” surface. In particular, the self-energy of a charged particle on the plane is related to the Green’s function by

$$\beta V_s = \frac{1}{2} \int \frac{d^2\mathbf{q}}{(2\pi)^2}\, \mathcal{G}_{2d}(0,0;q), \tag{3.22}$$

from which the correlation energy for the “salty” surface follows:

$$\beta E_c = \frac{2n_0}{2} \int \frac{d^2\mathbf{q}}{(2\pi)^2}\, \mathcal{G}_{2d}(0,0;q) = -\frac{1}{2} \int \frac{d^2\mathbf{q}}{(2\pi)^2}\, \frac{1}{q\lambda_D(1+q\lambda_D)}. \tag{3.23}$$

Alternatively, this result can be derived from Eq. (3.4) using a standard thermodynamic identity

$$E_c = \frac{\partial}{\partial \beta}[\beta f_{2d}]; \tag{3.24}$$

therefore, the two formulations – charge-fluctuations and the DH equation – are completely equivalent, as it should be. In the next two subsections, we compute the fluctuation free energy for charges confined on the surface a sphere and a cylinder, respectively.

3.2.2 Charges on a Sphere

For the case of charges confined on a sphere of radius R, after following a similar procedure leading to Eq. (3.4), we obtain the free energy

$$f_{sp} = \frac{k_BT}{8\pi R^2} \sum_{l=0}^{\infty} (\,2l+1\,) \left\{ \ln\left[1 + \frac{R/\lambda_D}{2l+1}\right] - \frac{R/\lambda_D}{2l+1} \right\}. \tag{3.25}$$

It is easy to show that by setting $k = l/R$ and taking the limit $R \to \infty$, we recover the planar result. Equivalently we may write Eq. (3.4) as

$$f_{2d} = \frac{k_BT}{8\pi R^2} \int_{-1/2}^{\infty} dl\, (\,2l+1\,) \left\{ \ln\left[1 + \frac{R/\lambda_D}{2l+1}\right] - \frac{R/\lambda_D}{2l+1} \right\}. \tag{3.26}$$

The difference $f_{sp} - f_{2d}$, can be evaluated as an asymptotic expansion in $1/R$ using the Euler-MacLaurin summation formula [8]

$$\sum_{l=0}^{N} f(l) = \int_0^N dx\, f(x) + \frac{1}{2}\,[f(0) + f(N)] + \frac{1}{12}\,[f'(0) + f'(N)] + \cdots, \tag{3.27}$$

with $f(l) = (2l+1)\ln(2l+1+R/\lambda_D)$. The result is:

$$f_{sp} - f_{2d} = -\frac{11\,k_BT}{96\pi R^2}\,\ln(\,R/\lambda_D\,) + \cdots . \tag{3.28}$$

In deriving the result above, we have regularized the integral in Eq. (3.26) and the sum in Eq. (3.25) by an ultraviolet cut-off Λ. However, the leading term in Eq. (3.28) is cut-off independent and those higher order cut-off dependent terms tend to zero as $\Lambda \to \infty$.

3.2.3 Charges on a Cylinder

For the case of a cylinder, we obtain the free energy:

$$f_{cyl} = \frac{k_BT}{4\pi R}\sum_{m\geq 0}\int_0^\infty dq\,\frac{2}{\pi}\left\{\ln\left[1+\frac{R}{\lambda_D}\,I_m(qR)K_m(qR)\right] - \frac{R}{\lambda_D}\,I_m(qR)K_m(qR)\right\}, \tag{3.29}$$

where I_m and K_m are modified Bessel functions of order m. The evaluation of the integrals here is relatively difficult. However, we argue that $f_{cyl} - f_{2d}$ has the following asymptotic expansion:

$$f_{cyl} - f_{2d} = -\frac{k_BT}{48\pi R^2}\,\ln(\,R/\lambda_D\,) + \cdots , \tag{3.30}$$

for $R \to \infty$. First, we note that the only relevant contributions to the q-integral in Eq. (3.29) are sharply peaked at $q \approx 0$ with width $\Delta\,q \approx m/R$. Hence, the Bessel functions can be approximated by $I_m(qR)K_m(qR) \sim 1/2m$, yielding

$$f_{cyl} = \frac{k_BT}{4\pi R^2}\sum_{m\geq 0} m\left[\ln\left(1+\frac{R/\lambda_D}{2m}\right) - \frac{R/\lambda_D}{2m}\right] + O(1/R^3). \tag{3.31}$$

Equation (3.30) can now be obtained by using the Euler-MacLaurin summation formula with $f(m) = m\ln(2m + R/\lambda_D)$.

3.3 Renormalization of Bending Rigidity

The problem of the electrostatic contribution to the bending constants of charged membranes within the PB mean field approach has been briefly discussed in Section 2.4. The electrostatic renormalization of the bending rigidity turns out to be positive; hence electrostatics augments the rigidity of a charged membrane. Here we go beyond these PB approaches by assuming that the surface charge density n_0 of the membrane is sufficiently high that the condensed counterions are confined to a layer of thickness $\lambda \ll L$, where λ is the Gouy-Chapman length and L is the linear size of the charged membrane.

As mentioned in Section 2.4, the electrostatic contribution to the bending moduli κ_b and κ_G can be identified by expanding the electrostatic free energy up to second order in curvatures H and K and comparing with the Helfrich free energy

$$f = \frac{\kappa_b}{2}\,(H \,-\, H_0)^2 + \kappa_G\,K$$

of the same geometry. Using the results from previous section, the renormalization of the bending constants can be deduced from Eqs. (3.28) and (3.30) to yield[9]

$$\begin{aligned} \Delta\kappa_b &= -\frac{k_B T}{24\pi}\,\ln(R/\lambda_D), && (3.32) \\ \Delta\kappa_G &= -\frac{k_B T}{12\,\pi}\,\ln(R/\lambda_D). && (3.33) \end{aligned}$$

We thus find that the contribution to the membrane elastic constants due to charge fluctuations is non-analytic. This kind of non-analyticity in the bending constants exists in the literature in other situations, for example in a system consisting of a membrane and rod-like cosurfactants[10]. In the present case, this non-analyticity can be considered a signature of 2-D charged systems. Recall that the free energy contains a logarithmic term as in Eq. (3.5). Therefore, it is not surprising to find logarithmic corrections to the bending constants. Typically, for $R/\lambda_D \sim 10^4 - 10^6$ the factor $\ln(R/\lambda_D)$ is of order 10 and thus $\Delta\kappa$ and $\Delta\kappa_G$ are of the order of $k_B\,T$.

Secondly, we remark that both $\Delta\kappa_b$ and $\Delta\kappa_G$ are negative, in contrast to the mean-field PB contributions, where the renormalization of the bending moduli are always positive and the Gaussian moduli may be negative in some cases. In a system in which $R/\lambda_D \gg 1$, $\Delta\kappa_b$ is large compared to the mean-field contribution and the membrane becomes more flexible. Therefore, charge fluctuations induce bending of a charged membrane. The negative contribution of $\Delta\kappa_G$ from charge fluctuations has interesting experimental consequences since strongly negative values of κ_G favor the formation of many disconnected pieces with no rims, like spherical vesicles. Therefore, when the surface charge density is made sufficiently large, the membrane might spontaneously form vesicles, due to fluctuations of condensed counterions. Experiments [11] on charged surfactant systems support this conclusion.

The results presented in this section are particularly relevant to recent experiments [12] where the authors find the formation of vesicles by mixing anionic and cationic surfactants. In the regions of the phase diagram where vesicles form spontaneously, the composition of each vesicle in oppositely charged species is almost equimolar [13]. Two aspects of their experiment can be qualitatively accounted for by the present model. They find, in equilibrium, large vesicles with $R \sim 1000\,$Åand substantial size polydispersity. Indeed, the vesicle free energy per unit area given by

$$f_{ves} = \kappa_b^0/R^2 - \frac{11\,k_B\,T}{96\pi R^2}\,\ln(\,R/\lambda_D\,), \tag{3.34}$$

where κ_b^0 is the bare value of the bending rigidity, including possibly the mean field contribution due to the small excess charges on the vesicle, has an equilibrium value $R^* \sim \lambda_D \exp(\kappa_b^0/k_BT)$, which can be large even for a moderate value of κ_b^0 of the order of 5–7 k_BT. Furthermore, the second derivative of the free energy $f''(R^*) \sim e^{-\kappa_b^0/k_BT}$ is exponentially small. Hence the variance or fluctuations in R, $\langle(\Delta R)^2\rangle \sim 1/f''(R^*)$ is large, implying size polydispersity.

3.3.1 An Undulating "Salty" Membrane

In this subsection, we evaluate the charge fluctuation contribution to the bending rigidity from a different geometry, namely an undulating 2D membrane embedded in 3D space. In the Monge gauge (see Appendix), the shape of the membrane is described by a height field $h(\mathbf{r})$. Confined on the membrane are equal numbers of positive and negative mobile charges, interacting via the Coulomb's law. In the continuum limit, the Hamiltonian for an undulating "salty" membrane is

$$\begin{aligned}\beta\mathcal{H} &= \frac{1}{2}\int d^2\mathbf{r}\left[r_0(\nabla h)^2+\kappa_b(\nabla^2 h)^2\right] \qquad (3.35)\\ &+ \frac{1}{2}\int d^2\mathbf{r}\,d^2\mathbf{r}'\left[\frac{\delta^2(\mathbf{r}-\mathbf{r}')}{2\,n_0}+\frac{l_B}{\sqrt{(\mathbf{r}-\mathbf{r}')^2+[\,h(\mathbf{r})-h(\mathbf{r}')\,]^2}}\right]\delta\sigma(\mathbf{r})\,\delta\sigma(\mathbf{r}'),\end{aligned}$$

where r_0 is the surface tension of the membrane. The first term is the Helfrich free energy and the second term is the charge-fluctuation free energy Eq.(3.2), modified by the out-of-plane displacement $h(\mathbf{r})$ of the membrane. Now, we rewrite the electrostatic contribution $\beta\mathcal{H}_{el}$ as

$$\begin{aligned}\beta\mathcal{H}_{el} &= \frac{1}{2}\int d^2\mathbf{r}\,d^2\mathbf{r}'\left[\frac{l_B}{|\mathbf{r}-\mathbf{r}'|}+\frac{\delta^2(\mathbf{r}-\mathbf{r}')}{2\,n_0}\right]\delta\sigma(\mathbf{r})\,\delta\sigma(\mathbf{r}')\\ &- 4\,l_B\int d^2\mathbf{r}\,d^2\mathbf{r}'\int_0^\infty\frac{d\alpha}{2\pi}\,K_0(\alpha\,r)\sin^2\left(\frac{\alpha\,\Delta h}{2}\right)\delta\sigma(\mathbf{r})\,\delta\sigma(\mathbf{r}'), \qquad (3.36)\end{aligned}$$

where $K_0(x)$ is the modified Bessel function, $\mathbf{r}=\mathbf{r}-\mathbf{r}'$, and $\Delta h\equiv h(\mathbf{r})-h(\mathbf{r}')$; we treat the last term as a perturbation:

$$\beta\mathcal{H}_I=-\,4\,l_B\int d^2\mathbf{r}\,d^2\mathbf{r}'\int_0^\infty\frac{d\alpha}{2\pi}\,K_0(\alpha\,r)\sin^2\left(\frac{\alpha\,\Delta h}{2}\right)\delta\sigma(\mathbf{r})\,\delta\sigma(\mathbf{r}'), \qquad (3.37)$$

and expand $\mathcal{H}_I$ in the cumulant expansion:

$$\beta\delta\mathcal{H}[h(\mathbf{r})]=\beta\langle\mathcal{H}_I\rangle-\frac{1}{2}\,\beta^2\left[\langle\mathcal{H}_I^2\rangle-\langle\mathcal{H}_I\rangle^2\right]+\cdots, \qquad (3.38)$$

where the average is only taken with respect to charge fluctuations $\delta\sigma(\mathbf{r})$. To calculate the renormalization of bending rigidity, we make use of a gradient expansion of $\Delta h=h(\mathbf{R}+\mathbf{r}/2)-h(\mathbf{R}-\mathbf{r}/2)$:

$$\Delta h=\sum_i r_i\partial_i h+\frac{2}{2^3\,3!}\sum_{ijk}r_ir_jr_k\partial_i\partial_j\partial_k h+\cdots, \qquad (3.39)$$

where $\mathbf{R}=(\mathbf{r}+\mathbf{r}')\,/2$. To second order in Δh, $\mathcal{H}_I$ is given by

$$\langle\beta\mathcal{H}_I\rangle=-\,l_B\int d^2\mathbf{r}\,d^2\mathbf{r}'\int_0^\infty\frac{d\alpha}{2\pi}\,K_0(\alpha\,r)\,\alpha^2\,(\Delta h)^2\,\langle\delta\sigma(\mathbf{r})\,\delta\sigma(\mathbf{r}')\rangle. \qquad (3.40)$$

Expanding out $(\Delta h)^2$:

$$(\Delta h)^2 = \sum_{ij} r_i r_j \partial_i h \partial_j h + \frac{4}{2^3\,3!} \sum_{ijkl} r_i r_j r_k r_l \partial_i h \partial_j \partial_k \partial_l h + O(r^6), \tag{3.41}$$

shifting the spatial integrals in Eq. (3.40) from $\int d^2\mathbf{r}\, d^2\mathbf{r}' \to \int d^2\mathbf{R}\, d^2\mathbf{r}$, and evaluating the angular integrals of the form:

$$\begin{aligned} \int d^2\mathbf{r}\, r_i r_j\, \mathcal{I}(r) &= \pi \int dr\, r^3\, \mathcal{I}(r)\, \delta_{ij}; & (3.42) \\ \int d^2\mathbf{r}\, r_i r_j r_k r_l\, \mathcal{I}(r) &= \frac{\pi}{4} \int dr\, r^5\, \mathcal{I}(r)\, [\delta_{ij}\delta_{kl} + \delta_{ik}\delta_{jl} + \delta_{il}\delta_{jk}], & (3.43) \end{aligned}$$

where $\mathcal{I}(r)$ is defined by

$$\mathcal{I}(r) = \frac{l_B}{2\pi} \int_0^\infty d\alpha\, \alpha^2\, K_0(\alpha\, r)\, \langle \delta\sigma(\mathbf{r})\, \delta\sigma(\mathbf{r}') \rangle, \tag{3.44}$$

we finally obtain

$$\langle \beta \mathcal{H}_I \rangle = -\pi \int d^2\mathbf{R}\, (\nabla h)^2 \cdot \int dr\, r^3\, \mathcal{I}(r) + \frac{\pi}{16} \int d^2\mathbf{R}\, (\nabla^2 h)^2 \cdot \int dr\, r^5\, \mathcal{I}(r) + \cdots \tag{3.45}$$

Clearly, the second term renormalizes the bending rigidity:

$$\beta \Delta\kappa_b = \frac{\pi}{8} \int dr\, r^5\, \mathcal{I}(r). \tag{3.46}$$

Now, using the asymptotics of the correlation function $\langle \delta\sigma(\mathbf{0})\, \delta\sigma(\mathbf{r}) \rangle$ calculated in Eq. (3.8), we have

$$\Delta\kappa_b = -\frac{k_B T}{128\pi} \int_1^{L/\lambda_D} dx\, x\, \tau_0(x) = -\frac{k_B T}{128\pi} \ln(L/\lambda_D) + O(L^{-2}), \tag{3.47}$$

which agrees with the logarithmic correction to the bending rigidity obtained previously, but the overall numerical prefactor is quite different, a factor of 5-10 smaller.

3.4 Attraction Arising from Charge Fluctuations

As mentioned in the Introduction to this chapter, experiments and simulations suggest that there could be attraction between highly like-charged surfaces.

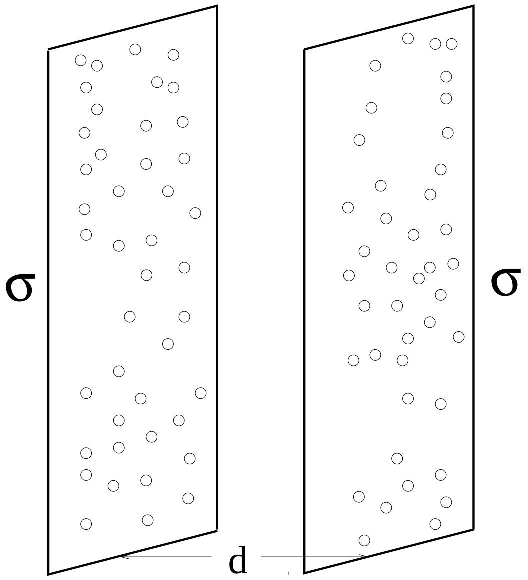

Figure 3.2: Density fluctuations of "condensed" counterions lead to an attractive force between two plates.

This attraction cannot be accounted for by PB theory, since it only predicts repulsion. To go beyond mean-field theory, we consider the in-plane fluctuations of the "condensed" counterions, shown in Fig. 3.2, and show that attraction between two plates is possible.

The effective Hamiltonian for this system is

$$\mathcal{H} = \sum_{i=A,B} \mathcal{H}^i_{el} + \mathcal{H}_{int}, \tag{3.48}$$

where $\mathcal{H}^i_{el}$ is the intralayer electrostatic energy as in Eq. (3.2):

$$\beta\mathcal{H}^i_{el} = \frac{1}{2}\int d^2\mathbf{r}\, d^2\mathbf{r}' \left[\frac{l_B}{|\,\mathbf{r}\,-\,\mathbf{r}'\,|} + \frac{\delta^2(\mathbf{r}\,-\,\mathbf{r}')}{2\,n_0}\right] \delta\sigma_i(\mathbf{r})\,\delta\sigma_i(\mathbf{r}'), \tag{3.49}$$

and $\mathcal{H}_{int}$ is the interlayer electrostatic interaction:

$$\beta\mathcal{H}_{int} = \frac{l_B}{2}\int d^2\mathbf{r}\, d^2\mathbf{r}'\, \frac{\delta\sigma_A(\mathbf{r})\,\delta\sigma_B(\mathbf{r}')}{\sqrt{(\mathbf{r}\,-\,\mathbf{r}')^2 + d^2}}. \tag{3.50}$$

A convenient way of calculating the pressure is to use the expression

$$\Pi(d) = -\frac{1}{A_0}\left\langle \frac{\partial \mathcal{H}_{int}}{\partial d} \right\rangle_{\mathcal{H}}. \tag{3.51}$$

Using the Fourier transform of Eq. (3.50), the pressure can be expressed in terms of the interlayer density correlation function $\langle\, \delta\sigma_A(\mathbf{q})\, \delta\sigma_B(-\,\mathbf{q})\, \rangle$ as

$$\beta\Pi(d) = \frac{2\pi l_B}{A_0} \int \frac{d^2\mathbf{q}}{(2\pi)^2}\, e^{-qd}\, \langle\, \delta\sigma_A(\mathbf{q})\, \delta\sigma_B(-\,\mathbf{q})\, \rangle. \tag{3.52}$$

To calculate the correlation function, we note that $\mathcal{H}$ can be diagonalized by introducing $\delta\sigma_\pm(\mathbf{r}) = \frac{1}{\sqrt{2}}\,\{\delta\sigma_A(\mathbf{r}) \pm \delta\sigma_B(\mathbf{r})\}$; in Fourier space, we have

$$\beta\mathcal{H} = \frac{1}{2}\sum_{\pm}\int \frac{d^2\mathbf{q}}{(2\pi)^2}\left[\frac{1}{2n_0} + \frac{2\pi l_B}{q}\left(1 \pm e^{-qd}\right)\right]\, \delta\sigma_\pm(\mathbf{q})\, \delta\sigma_\pm(-\mathbf{q}). \tag{3.53}$$

Using the equipartition theorem, it follows that

$$\frac{1}{A_0}\,\langle\, \delta\sigma_\pm(\mathbf{q})\, \delta\sigma_\pm(-\,\mathbf{q})\, \rangle = \frac{q}{2\pi l_B}\,\frac{2}{(1 + q\lambda_D) \pm e^{-qd}}, \tag{3.54}$$

and thus

$$\begin{aligned} \frac{1}{A_0}\langle\, \delta\sigma_A(\mathbf{q})\, \delta\sigma_B(-\,\mathbf{q})\, \rangle &= \frac{1}{2A_0}\,\{\, \langle\, \delta\sigma_+(\mathbf{q})\, \delta\sigma_+(-\,\mathbf{q})\, \rangle - \langle\, \delta\sigma_-(\mathbf{q})\, \delta\sigma_-(-\,\mathbf{q})\, \rangle\, \} \\ &= -\frac{q}{2\pi l_B}\,\frac{e^{-qd}}{(1 + q\lambda_D)^2 - e^{-2qd}}. \end{aligned} \tag{3.55}$$

Substituting this result into Eq. (3.52), we obtain the pressure[4]

$$\Pi(d) = -\,k_B T \int_0^\infty \frac{dq}{2\pi}\,\frac{q^2}{e^{2qd}\,(1 + q\lambda_D)^2 - 1}. \tag{3.56}$$

Thus, charge-fluctuations indeed give rise to an attraction between charged planes.

To evaluate the integral, we consider two limiting cases: $(i)\, d \gg \lambda_D$ and $(ii)\, d \ll \lambda_D$. In the large distance limit, $d \gg \lambda_D$, the integral may be expanded in powers of $q\lambda_D$ in the denominator, and the leading term is independent of λ_D and scales like d^{-3}. For small distances, we expand $1/(q\lambda_D)$ to obtain $\Pi \sim d^{-1}$. Therefore, we have the following regimes:

$$\Pi(d) = \begin{cases} -\frac{\zeta(3)}{8\pi}\,\frac{k_B T}{d^3}, & \text{for } d \gg \lambda_D, \\ -\frac{k_B T}{4\pi\lambda_D^2 d}, & \text{for } d \ll \lambda_D. \end{cases} \tag{3.57}$$

Note that this attraction is long-ranged and the prefactor $\frac{\zeta(3)}{8\pi} \approx 0.048$ is universal for this interaction, induced by the long wavelength fluctuations. Furthermore, this charge-fluctuation-induced force is similar to the van der Waals interaction, and indeed formally identical to the Casimir force between two partially transmitting mirrors at high temperature. Also, we note that $\Pi(d) \to 0$ as $T \to 0$, as it should be since charge fluctuations are entirely controlled by thermal energy.

It is interesting to compare the magnitude of this attraction to the mean-field PB repulsion. For large distances, the mean-field repulsion which scales as $P \sim d^{-2}$ always dominates the fluctuation-induced attraction. Note that this conclusion is independent of the charge density of the surfaces. In the opposite limit, $d \ll \lambda$, the attraction can overcome the mean-field repulsion provided that $l_B/\lambda > 8Z^{-2}$, which is the case for sufficiently low temperature or high valence. It is important to note that the charge-fluctuation picture as described by the Debye-Hückel theory may break down at such temperature. Nevertheless, this picture provides some insight into the correlation effects for charged surfaces beyond PB theory.

3.5 Conclusion

In this chapter, we have formulated the "salty" surface model to describe the fluctuations of the "condensed" counterions near a highly charged plate. We argue that their fluctuations neglected in PB theory are well captured by the 2D Debye-Hückel theory. First, we learn that charge-fluctuations may reduce the bending constants of a "salty" membrane to the extent that they may spontaneously form large vesicles. More interestingly, we have shown that the charge fluctuations are correlated between two "salty" planes in such a way that there is a long-ranged attractive force, scaled as d^{-3}, for large distances d. This attractive force may explain the attractions observed in experiments and simulations.

Bibliography

[1] N. Grønbech-Jensen, R.J. Mashl, R.F. Bruinsma, and W.M. Gelbart, Phys. Rev. Lett. **78**, 2477 (1997); L. Guldbrand, B. Jönsson, H. Wennerström, and P. Linse, J. Chem. Phys. **80**, 2221 (1984); S. Engström, H. Wennerström, O.G. Mouritsen, and H.C. Fogedby, Chemica Scripta **25**, 92 (1985).

[2] S. Marcelja, Biophys. J. **61**, 1117 (1992).

[3] V.A. Bloomfield, Biopolymers **31**, 1471 (1991); B.-Y. Ha and A.J. Liu, Phys. Rev. Lett. **79**, 1289 (1997).

[4] P. Pincus and S.A. Safran, Europhys. Lett. **42**, 103 (1998).

[5] Phil Attard, Roland Kjellander, and D. John Mitchell, J. Chem. Phys. **89**, 1664 (1988) and Chem. Phys. Lett., **139**, 219 (1987); Phil Attard, D. John Mitchell, and Barry W. Ninham, J. Chem. Phys. **88**, 4987 (1988).

[6] H. Totsuji, J. Phys. Soc. Japan **40**, 857 (1976).

[7] E.S. Velazquez and L. Blum, Physica A **244**, 453 (1997).

[8] G. Arfken, *Mathematical Methods for Physicists* (Academic Press Inc., San Diego, 1996).

[9] A.W.C. Lau and P. Pincus, Phys. Rev. Lett. **81**, 1338 (1998).

[10] J.B. Fournier, Phys. Rev. Lett. **76**, 4436 (1996); K. Yaman, P. Pincus, and C.M. Marques, Phys. Rev. Lett. **78**, 4514 (1997).

[11] See J. Oberdisse and G. Porte, Phys. Rev. E **56**, 1965 (1997), and references therein.

[12] E.W. Kaler, A.K. Murthy, B.E. Rodriguez, J.A.N. Zasadzinski, Science **245**, 1371 (1989); E.W. Kaler, K.L. Herrington, A.K. Murthy, and J.A.N. Zasadzinski, J. Phys. Chem. **96**, 6698 (1992).

[13] J.A.N. Zasadzinski (private communication). Note also that equimolar mixtures of anionic and cationic surfactants precipitate from solution. This is due to the residual Van der Waals attractions between surfactants; thus this situation cannot be investigated by the present theory.

Chapter 4

Fluctuation-Driven Counterion Condensation

4.1 Introduction

In this chapter, we continue to illustrate the importance of fluctuations by presenting a novel condensation phenomenon in an overall neutral system, consisting a single charged plate and its oppositely charged counterions. We saw in Chapter 2, that at the mean-field level, the counterion distribution as described by PB theory is valid only for sufficiently high temperature, where fluctuation and correlation effects are negligible. Here, we propose a "two-fluid" model for the low temperature regime, in which the counterions are divided into a "free" and a "condensed" part. Using a variational approach, we show that for sufficiently low temperatures, a finite fraction of counterions is "condensed" onto the charged plate.

4.2 Fluctuation Corrections to Possion-Boltzmann Theory

In this section, we discuss fluctuation corrections to the mean-field PB free energy. This will establish the technical tools we need to tackle the interesting problem of counterion condensation. First, we expand the action $\mathcal{S}[\phi,\psi]$ in Eq. (2.34) about the saddle point ψ_0, which satisfies Eq. (2.35), in the second order in $\Delta\psi(\mathbf{x}) = \psi(\mathbf{x}) - \psi_0(\mathbf{x})$:

$$\begin{aligned}\mathcal{S}[\phi,\psi] &= \mathcal{S}[\phi,\psi_0] + \int d^3\mathbf{x}\ \left.\frac{\delta\mathcal{H}}{\delta\psi(\mathbf{x})}\right|_{\psi=\psi_0} \Delta\psi(\mathbf{x}) \\ &+ \frac{1}{2}\int d^3\mathbf{x}\int d^3\mathbf{y}\ \left.\frac{\delta^2\mathcal{H}}{\delta\psi(\mathbf{x})\,\delta\psi(\mathbf{y})}\right|_{\psi=\psi_0} \Delta\psi(\mathbf{x})\,\Delta\psi(\mathbf{y}) + \cdots. \qquad (4.1)\end{aligned}$$

Defining the operator

$$\begin{aligned}K(\mathbf{x},\mathbf{y}) &= \left.\frac{\delta^2\mathcal{H}}{\delta\psi(\mathbf{x})\,\delta\psi(\mathbf{y})}\right|_{\psi=\psi_0} \\ &= \frac{1}{\ell_B}\left[-\nabla^2_{\mathbf{x}} + \kappa^2 e^{i\psi_0(\mathbf{x})+\phi(\mathbf{x})}\right]\delta(\mathbf{x}-\mathbf{y}), \qquad (4.2)\end{aligned}$$

and performing the Gaussian integrals in the function integral, we obtain a formal expression for the change in the free energy due to fluctuations of the counterions:

$$\beta\Delta F = \frac{1}{2}\ln\det\hat{\mathbf{K}} - \frac{1}{2}\ln\det\left[-\frac{\nabla^2}{\ell_B}\right], \qquad (4.3)$$

where the second term comes from the normalization constant $\mathcal{N}_0$ in Eq. (2.34). To evaluate $\beta\Delta F$ explicitly for the case of a single charged plate, we first differentiate it with respect to ℓ_B by making use of the identity $\delta\ln\det\hat{\mathbf{X}} = \mathrm{Tr}\,\hat{\mathbf{X}}^{-1}\,\delta\,\hat{\mathbf{X}}$ to obtain

$$\frac{\partial\beta\Delta F}{\partial\ell_B} = -\frac{2}{\ell_B}\frac{\partial\lambda}{\partial\ell_B}\int d^3\mathbf{x}\,\frac{G_{pb}(\mathbf{x},\mathbf{x})}{(|z|+\lambda)^3}, \qquad (4.4)$$

where we use the fact that

$$i\psi_0(\mathbf{x}) + \phi(\mathbf{x}) = -\varphi(z) = -\,2\ln\left(1+\frac{\kappa|z|}{\sqrt{2}}\right) \qquad (4.5)$$

for the saddle point solution for a single charged plate, and $G_{pb}(\mathbf{x}, \mathbf{x}')$ is the Green's function defined by

$$\int d^3\mathbf{y}\, K(\mathbf{x}, \mathbf{y})\, G_{pb}(\mathbf{y}, \mathbf{x}') = \delta(\mathbf{x} - \mathbf{x}'), \tag{4.6}$$

i.e. $G_{pb}(\mathbf{x}, \mathbf{x}')$ is the inverse of $\hat{\mathbf{K}}$. Using the definition of $K(\mathbf{x}, \mathbf{y})$ above, we find that $G_{pb}(\mathbf{x}, \mathbf{x}')$ satisfies the following differential equation

$$\left[-\nabla^2_{\mathbf{x}} + \frac{2}{(|z| + \lambda)^2} \right] G_{pb}(\mathbf{x}, \mathbf{x}') = \ell_B\, \delta(\mathbf{x} - \mathbf{x}'), \tag{4.7}$$

where λ is the Gouy-Chapman length. Since the second term in the bracket only depends on z, we Fourier transform $G_{pb}(\mathbf{x}, \mathbf{x}')$ to obtain

$$\left[-\frac{d^2}{dz^2} + q^2 + \frac{2}{(|z| + \lambda)^2} \right] G_{pb}(z, z'; q) = \ell_B\, \delta(z - z'), \tag{4.8}$$

where $q^2 = q_x^2 + q_y^2$, and λ is the Gouy-Chapman length.

Clearly, to obtain fluctuation energy in Eq. (4.4) explicitly, we must solve for $G_{pb}(z, z; q)$. First, consider the homogeneous equation of Eq.(4.8)

$$\left[-\frac{d^2}{dz^2} + q^2 + \frac{2}{(|z| + \lambda)^2} \right] h(z; q) = 0. \tag{4.9}$$

For $|z| > 0$, this equation can be reduced to the Wittaker's equation, which has two linearly independent solutions:

$$h_+(z; q) = e^{-q\,|z|} \left[1 + \frac{1}{q\,(|z| + \lambda)} \right], \tag{4.10}$$

$$h_-(z; q) = e^{q\,|z|} \left[1 - \frac{1}{q\,(|z| + \lambda)} \right]. \tag{4.11}$$

To solve for the Green's function, we need only to consider the case $z' > 0$ since $G(z, z') = G(-z, -z')$ by symmetry. We split space into 3 regions:

$$G_>(z, z'; q) = A(z')\, h_+(z; q), \qquad \text{for } z > z', \tag{4.12}$$

$$G_<(z, z'; q) = B(z')\, h_+(z; q) + C(z')\, h_-(z; q), \qquad \text{for } 0 \le z < z', \tag{4.13}$$

$$G_-(z, z'; q) = D(z')\, h_+(z; q), \qquad \text{for } z < 0, \tag{4.14}$$

and impose the following boundary conditions:

$$\begin{aligned}
&1) && G_<(0,z';q) = G_-(0,z';q), && (4.15)\\
&2) && \left.\frac{dG_<(z,z';q)}{dz}\right|_{z=0} = \left.\frac{dG_-(z,z';q)}{dz}\right|_{z=0}, && (4.16)\\
&3) && G_<(z',z';q) = G_>(z',z';q), && (4.17)\\
&4) && \left.\frac{dG_<(z,z';q)}{dz}\right|_{z=z'} - \left.\frac{dG_>(z,z';q)}{dz}\right|_{z=z'} = \ell_B, && (4.18)
\end{aligned}$$

to determine the coefficients $A(z')$, $B(z')$, $C(z')$, and $D(z')$. After some algebra, the Green's function follows, and $G_{pb}(z,z;q)$ is given by

$$\begin{aligned}
G_{pb}(z,z;q) &= \frac{\ell_B}{2q}\left\{1 - \frac{1}{q^2\,(|z|+\lambda)^2}\right.\\
&\left.+\frac{e^{-2q|z|}}{(1+q\lambda)[1+q\lambda+(q\lambda)^2]}\left[1+\frac{1}{q\,(|z|+\lambda)}\right]^2\right\}. \qquad (4.19)
\end{aligned}$$

Note that the first term is just the usual Coulomb self-energy, which upon substituting into Eq. (4.4) exactly cancels the self-energy in the mean-field free energy Eq. (2.61). Subtracting out this self-energy, i.e. replacing $G_{pb}(\mathbf{x},\mathbf{x})$ by $\mathcal{G}_{pb}(\mathbf{x},\mathbf{x}) = G_{pb}(\mathbf{x},\mathbf{x}) - G_0(\mathbf{x},\mathbf{x})$ in Eq. (4.4), and using the following integrals

$$\begin{aligned}
\int_0^\infty dz \frac{1}{(z+\lambda)^5} &= \frac{1}{4\lambda^4}\\
\int_0^\infty dz \frac{e^{-2qz}}{(z+\lambda)^3}\left[1+\frac{1}{q(z+\lambda)}\right]^2 &= q^2\,\frac{1+2q\lambda}{4(q\lambda)^4},
\end{aligned}$$

Eq. (4.4) can be evaluated to be

$$\frac{1}{A_0}\frac{\partial\beta\Delta F}{\partial\ell_B} = \frac{1}{2}\frac{\partial\lambda}{\partial\ell_B}\int\frac{d^2\mathbf{q}}{(2\pi)^2}\,\frac{q}{(q\lambda)^2}\,\frac{2+q\lambda}{(1+q\lambda)\,[1+q\lambda+(q\lambda)^2]} = \frac{1}{4\pi\lambda^3}\,\frac{\pi}{\sqrt{3}}\,\frac{\partial\lambda}{\partial\ell_B}. \qquad (4.20)$$

This can be integrated back to obtain the fluctuation correction to the mean-field free energy for a single charged plate:

$$\Delta f = -\frac{k_B T}{8\sqrt{3}\lambda^2}. \qquad (4.21)$$

Note that fluctuations lower the mean-field free energy. The result in Eq. (4.21) may be understood physically as follows. According to PB theory, the counterions are confined to a slab of thickness λ, and thus may be considered as an ideal gas with a 3D concentration of $c \sim n_0/\lambda$. This implies that the inverse of the 3D "screening" length is $\kappa_s \sim \sqrt{c\, l_B} \sim 1/\lambda$. Using the 3D Debye-Hückel free energy (per unit volume) $\beta\Delta f_s \sim -\kappa_s^3$, the correction to the mean-field PB free energy (per unit area) scales like $\beta\Delta f \sim -\lambda \cdot \lambda^{-3} \sim -\lambda^{-2}$, as obtained above. Note also that Eq. (4.21) is not logarithmic divergent in contrast to the 2D Debye-Hückel theory. Combining with the mean-field free energy, the total free energy for the one plate system is

$$\beta f = \frac{n_0}{Z} \ln\left(\frac{n_0\, a^3}{2Z\lambda}\right) - \frac{n_0}{Z} - \frac{1}{8\sqrt{3}\lambda^2}. \tag{4.22}$$

4.3 Counterion Condensation

Recall that for a single plate of charge density $\sigma(\mathbf{x}) = en_0\delta(z)$ immersed in an aqueous solution of dielectric constant ϵ, containing point-like counterions of charge $-Ze$ on both sides of the plate, PB theory predicts that the counterion distribution in Eq. (2.49)

$$c(z) = \frac{1}{2\pi Z^2 l_B\left(|z| + \lambda\right)^2},$$

decays to zero algebraically with a characteristic length $\lambda \equiv 1/(\pi l_B Z n_0)$. This Gouy-Chapman length λ defines a sheath near the charged surface within which most of the counterions are confined. Typically, it is on the order of few angstroms for a moderate charge density of $n_0 \sim 1/100$ Å^{-2}. Note that since λ scales inversely with n_0 and linearly with T, at sufficiently high density or low temperature, the counterion distribution is essentially two-dimensional:

$$\lim_{T\to 0} \int_{-\zeta}^{\zeta} c(z)\, dz = \lim_{T\to 0}\, 2 \cdot \frac{n_0}{2Z} \cdot \frac{\zeta}{\lambda + \zeta} = \frac{n_0}{Z}, \tag{4.23}$$

where ζ is an arbitrarily small but fixed positive value of z, *i.e.* the counterion concentration $c(z)$ reduces to a surface density coating the charged plane with a density of n_0/Z as $T \rightarrow 0$. Therefore, according to PB theory, all of the counterions collapse onto the charged plane at zero temperature.

However, at low temperatures $Z^2 l_B \gg \lambda$, the fluctuation corrections become so large that the solution to the PB equation no longer provides a reasonable approximation[1, 2]. Therefore, we might expect a quantitative deviation from the conclusion above. Indeed, as pointed out by Netz *et al.*[1], when the temperature is sufficiently low, a perturbative expansion about the PB solution breaks down, as indicated by an unphysical (negative) counterion density in the one-loop approximation. This suggests that a simple perturbation theory may not capture the additional binding, which may lead to condensation of the counterions. To capture this, we propose here a "two-fluid" model in which the counterions are divided into a "free" and a condensate fraction. The "free" counterions have the usual 3D spatial distribution, while the "condensed" counterions are confined to move only on the charged plane. By minimizing the total free energy, which includes fluctuations of the whole system, we show that a finite fraction of the counterions is "condensed" onto the charged surface if $g \equiv l_B/\lambda$ exceeds some critical value $g \geq g_c$ (see Fig. 4.2). We emphasize that our approach, in which fluctuation and correlation effects play a crucial role, differs from the more familiar theory of counterion condensation, *e.g.* Manning condensation, which considers only the competition between electrostatics and entropy in a mean field framework.

In our picture, the 2D density of "condensed" counterions has a spatially dependent fluctuation about a uniform mean: $n_c(\mathbf{r}) = n_c + \delta n_c(\mathbf{r})$[3]. Thus, the presence of the condensate modifies the electrostatics of the "free" counterions in two ways. First, the condensate partially neutralizes the charged plane, effectively reducing its surface charge density from en_0 to $en_R = e(n_0 - Zn_c)$. Second, their fluctuations renormalize the electrostatic interaction of the system; thus, instead of the usual Coulomb potential, the "free" counterions and the charged plane interact via the interaction $G_{2d}(\mathbf{x}, \mathbf{x}')$, which is the inverse (the Green's function) of the 2D

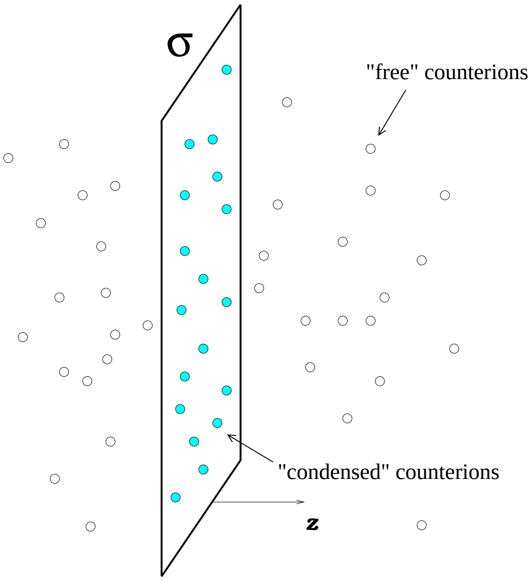

Figure 4.1: A schematic picture of the system considered.

Debye-Hückel operator in Eq. (3.10)

$$\left[-\nabla^2_{\mathbf{x}} + \frac{2}{\lambda_D}\,\delta(z)\right] G_{2d}(\mathbf{x},\mathbf{x}') = \ell_B \delta(\mathbf{x}-\mathbf{x}'), \tag{4.24}$$

where $\ell_B = 4\pi l_B Z^2$, $\lambda_D = 2/(\ell_B n_c)$ is the Debye screening length in 2-D, and the second term in the bracket takes into account of the fluctuating "condensate". Hence, in the limit $n_c \to 0$ or $\lambda_D \to \infty$, $G_{2d}(\mathbf{x},\mathbf{x}')$ reduces to the usual Coulomb interaction $G_0(\mathbf{x},\mathbf{x}') = \ell_B/|\mathbf{x}-\mathbf{x}'|$.

In order to obtain the condensate density n_c consistently, the "order" parameter $\tau \equiv Zn_c/n_0$ must minimize the free energy per unit area of the system: $f(\tau) = f_{2d}(\tau) + f_{3d}(\tau)$. The free energy for the "condensed" counterions $f_{2d}(n_c)$ is given by Eq. (3.4)

$$\beta f_{2d}(n_c) = n_c \left\{ \ln[n_c\, a^2] - 1 \right\} + \frac{1}{2}\int \frac{d^2\mathbf{q}}{(2\pi)^2} \left\{ \ln\left[1 + \frac{1}{q\lambda_D}\right] - \frac{1}{q\lambda_D} \right\}, \tag{4.25}$$

where $\beta^{-1} = k_B T$ and a is the molecular size of the counterions. The first term in Eq. (4.25) is their entropy and the second term arises from the 2D charge-fluctuation of the "condensed" counterions, which lowers the 2D ideal gas entropy (see Eq. (3.4)). The task now is to determine $f_{3d}(\tau)$.

As argued above, the electrostatic energy of the "free" counterions, in the presence of the fluctuating "condensate" on the the charged plane, is

$$\beta E_N = -NV_0 + \int d^3\mathbf{x} \int d^3\mathbf{x}' \, \rho(\mathbf{x}) G_{2d}(\mathbf{x},\mathbf{x}') \rho(\mathbf{x}') - \int d^3\mathbf{x}\, \phi(\mathbf{x})\, \rho(\mathbf{x}), \tag{4.26}$$

where $V_0 = \frac{\ell_B}{2} \int \frac{d^3\mathbf{q}}{(2\pi)^3}\, q^{-2}$ is the self-energy of the free counterions, $\rho(\mathbf{x}) = \sum_{i=1}^{N} \delta(\mathbf{x} - \mathbf{x}_i)$ is their number density, $G_{2d}(\mathbf{x},\mathbf{x}')$ is the interaction among them taking into account the fluctuating "condensate", and $\phi(\mathbf{x}) \equiv \int d^3\mathbf{x}'\, Z^{-1}\, G_{2d}(\mathbf{x},\mathbf{x}')\, n_R(\mathbf{x}')$ is the external field arising from the charged plate. After a Hubbard-Stratonovich transformation similar to what is done in Sec. 2.2, the grand canonical partition function for the "free" counterions, characterized by the interaction energy in Eq. (4.26), can be mapped into a functional integral representation: $\mathcal{Z}_\mu[\phi] = \mathcal{N}_0 \int \mathcal{D}\psi\, e^{-\mathcal{S}[\psi,\phi]}$ with an action

$$\mathcal{S}[\psi,\phi] = \frac{1}{\ell_B} \int d^3\mathbf{x} \left\{ \frac{1}{2}\, \psi(\mathbf{x})[\, -\nabla^2\,]\psi(\mathbf{x}) + \frac{1}{\lambda_D}\, \delta(z)\, [\psi(\mathbf{x})]^2 - \kappa^2 e^{i\psi(\mathbf{x}) + \phi(\mathbf{x})} \right\}, \tag{4.27}$$

where $\psi(\mathbf{x})$ is the fluctuating field, $\ell_B = 4\pi l_B Z^2$, $\kappa^2 = e^{\mu + V_0} \ell_B / a^3$, μ is the chemical potential, and $\mathcal{N}_0$ is the normalization factor. The minimum of the action $\frac{\delta \mathcal{S}}{\delta \psi(\mathbf{x})}\Big|_{\psi=\psi_0} = 0$, defines the saddle-point equation for $\psi_0(\mathbf{x})$, which reads

$$\nabla^2 \varphi(\mathbf{x}) + \kappa^2 e^{-\varphi(\mathbf{x})} = \frac{\ell_B n_R}{Z}\, \delta(z) + \frac{2}{\lambda_D}\, \delta(z)\, \varphi(\mathbf{x}) \tag{4.28}$$

in terms of the mean-field potential $\varphi(\mathbf{x}) = -i\psi_0(\mathbf{x}) - \phi(\mathbf{x})$. It has the solution $\varphi(\mathbf{x}) = 2 \ln\left(1 + \frac{\kappa |z|}{\sqrt{2}}\right)$, which satisfies the boundary conditions: *i)* $\varphi(0) = 0$ and *ii)* $\frac{d\varphi}{dz}\Big|_{z=0} = \frac{n_R \ell_B}{2Z}$, with $\kappa = n_R\, \ell_B / (2\sqrt{2} Z)$. Thus, at the mean-field level, the distribution of the "free" counterions $\rho_0(\mathbf{x}) = \kappa^2\, e^{-\varphi(\mathbf{x})} / \ell_B = 2/[\, \ell_B(|z| + \lambda_R)^2\,]$ has the standard form as in Eq. (2.49) with a renormalized Gouy-Chapman length $\lambda_R \equiv \sqrt{2}/\kappa = 4Z/(\ell_B n_R)$, in terms of the "reduced" surface charge density n_R.

To obtain the mean-field free energy of the "free" counterions $F_0(n_R)$, we note that it is related to the Gibbs potential $\Gamma_0[\phi] \equiv \mathcal{S}[\psi_0, \phi]$ by two Legendre transformations: $F_0(n_R) = \Gamma_0[\phi] + \int d^3\mathbf{x}\, \phi(\mathbf{x})\, \rho_0(\mathbf{x}) + \mu \int d^3\mathbf{x}\, \rho_0(\mathbf{x})$. Solving for the chemical potential μ from its definition: $\mu = -V_0 + \ln\left(\frac{n_R a^3}{2Z\lambda_R}\right)$ and using the mean-field solution $\varphi(\mathbf{x})$, we find

$$\beta F_0(n_R)/A_0 = -\frac{n_R}{Z}\, V_0 + \frac{n_R}{Z} \ln\left(\frac{n_R\, a^3}{2Z\lambda_R}\right) - \frac{n_R}{Z} \tag{4.29}$$

where A_0 is the area of the charged plane. Apart from the infinite self-energy term V_0 to be canceled below, $F_0(n_R)$ has the form of an ideal gas entropy with a 3D concentration of a gas confined to a slab of thickness λ_R. To capture correlation effects, we must also include fluctuations of the "free" counterions, thereby treating the "free" and "condensed" counterions on the same level. Expanding the action $\mathcal{S}[\psi, \phi]$ about the saddle-point $\psi_0(\mathbf{x})$ to second order in $\Delta\psi(\mathbf{x}) = \psi(\mathbf{x}) - \psi_0(\mathbf{x})$ and performing the Gaussian integrals in the functional integral, we obtain a formal expression for the change in the free energy due to fluctuations of the "free" counterions: $\beta\Delta F_{3d} = \frac{1}{2} \ln\det \hat{\mathbf{K}}_{3d} - \frac{1}{2} \ln\det \hat{\mathbf{K}}_{2d}$, where the differential operator $\hat{\mathbf{K}}_{3d}(\mathbf{x}, \mathbf{y}) \equiv \left[-\nabla^2_{\mathbf{x}} + \frac{2}{\lambda_D}\, \delta(z) + \frac{2}{(|z|+\lambda_R)^2}\right] \delta(\mathbf{x} - \mathbf{y})$ comes from the second variation of the action $\mathcal{S}[\psi, \phi]$ and $\hat{\mathbf{K}}_{2d}(\mathbf{x}, \mathbf{y}) \equiv \left[-\nabla^2_{\mathbf{x}} + \frac{2}{\lambda_D}\, \delta(z)\right] \delta(\mathbf{x} - \mathbf{y})$ is the 2D Debye-Hückel operator, coming from the normalization factor $\mathcal{N}_0$.

To evaluate $\beta\Delta F_{3d}$ explicitly, we first differentiate it with respect to ℓ_B by making use of the identity $\delta \ln\det \hat{\mathbf{X}} = \mathrm{Tr}\, \hat{\mathbf{X}}^{-1}\, \delta\, \hat{\mathbf{X}}$ to obtain

$$\begin{aligned} \frac{\partial \beta\Delta F_{3d}}{\partial \ell_B} &= -\frac{2}{\ell_B} \frac{\partial \lambda_R}{\partial \ell_B} \int d^3\mathbf{x}\, \frac{G_{3d}(\mathbf{x}, \mathbf{x})}{(|z| + \lambda_R)^3} \\ &\quad - \frac{1}{\ell_B} \frac{\partial \lambda_D}{\partial \ell_B} \int d^3\mathbf{x}\, \frac{\delta(z)}{\lambda_D^2}\, \left[G_{3d}(\mathbf{x}, \mathbf{x}) - G_{2d}(\mathbf{x}, \mathbf{x})\right], \end{aligned} \tag{4.30}$$

where

$$G_{2d}(\mathbf{x}, \mathbf{x}) = \int \frac{d^2\mathbf{q}}{(2\pi)^2} \frac{\ell_B}{2q} \left[1 - \frac{e^{-2q|z|}}{1 + q\lambda_D}\right] \tag{4.31}$$

is the diagonal part of the 2D Green's function and $G_{3d}(\mathbf{x}, \mathbf{x}')$ is the Green's function for the 3D "free" counterions. It satisfies

$$\left[-\nabla^2_{\mathbf{x}} + \frac{2}{\lambda_D}\, \delta(z) + \frac{2}{(|z| + \lambda_R)^2}\right] G_{3d}(\mathbf{x}, \mathbf{x}') = \ell_B\, \delta(\mathbf{x} - \mathbf{x}'), \tag{4.32}$$

which can be solved in a similar fashion in Sec. 4.2 to yield an expression for $G_{3d}(\mathbf{x},\mathbf{x})$:

$$\begin{aligned} G_{3d}(\mathbf{x},\mathbf{x}) &= \int \frac{d^2\mathbf{q}}{(2\pi)^2}\,\frac{\ell_B}{2q}\left\{ 1 - \frac{1}{q^2(|z|+\lambda_R)^2} + \frac{e^{-2q|z|}\left[1+\frac{1}{q\,(|z|+\lambda_R)}\right]^2}{(1+q\lambda_R)[1+q\lambda_R+(q\lambda_R)^2]} \right. \\ & \left. - \frac{\gamma\,(q\lambda_R)^3\,e^{-2q|z|}\left[1+\frac{1}{q\,(|z|+\lambda_R)}\right]^2}{[1+q\lambda_R+(q\lambda_R)^2]\,[(1+q\lambda_R)(1+\gamma)+(q\lambda_R)^2]} \right\}, \qquad (4.33) \end{aligned}$$

where $\gamma \equiv \lambda_R/\lambda_D = 2\,\tau/(1-\tau)$. Note that the first term in $G_{3d}(\mathbf{x},\mathbf{x})$ is just the Coulomb self-energy $G_0(\mathbf{0}) = \int \frac{d^2\mathbf{q}}{(2\pi)^2}\,\frac{\ell_B}{2q}$ which, upon substituting into Eq. (4.30), exactly cancels the self-energy term in the mean-field free energy Eq. (4.29). Inserting Eq. (4.33) with the self-energy term subtracted and the expression for $G_{2d}(\mathbf{x},\mathbf{x})$ into Eq. (4.30), we obtain $\frac{1}{A_0}\frac{\partial\beta\Delta F_{3d}}{\partial\ell_B} = \frac{\mathcal{I}_1(\gamma)}{4\pi\lambda_R^3}\frac{\partial\lambda_R}{\partial\ell_B} + \frac{\mathcal{I}_2(\gamma)/\gamma}{4\pi\lambda_D^3}\frac{\partial\lambda_D}{\partial\ell_B} + (\text{self-energy})$, where the functions $\mathcal{I}_{1,2}(\gamma)$ are given by

$$\begin{aligned} \mathcal{I}_1(\gamma) &= \frac{1}{2}\ln(1+\gamma) + 3\left|\sqrt{\frac{1+\gamma}{3-\gamma}}\,\tan^{-1}\sqrt{\frac{3-\gamma}{1+\gamma}}\right|, \\ \mathcal{I}_2(\gamma) &= \frac{\gamma}{2}\ln\frac{\gamma^2}{1+\gamma} + (2-\gamma)\left|\sqrt{\frac{1+\gamma}{3-\gamma}}\,\tan^{-1}\sqrt{\frac{3-\gamma}{1+\gamma}}\right|. \end{aligned}$$

Because $\mathcal{I}_{1,2}(\gamma)$ are independent of ℓ_B, we can integrate Eq. (4.30) back to obtain $\beta\Delta F_{3d}$; thus, the total free energy per unit area for the "free" counterions is

$$\beta f_{3d}(\tau) = \frac{n_R}{Z}\ln\left(\frac{n_R\,a^3}{2Z\lambda_R}\right) - \frac{n_R}{Z} - \frac{\mathcal{I}_1(\gamma)}{8\pi\lambda_R^2} - \frac{\mathcal{I}_2(\gamma)}{8\pi\lambda_D\lambda_R}. \qquad (4.34)$$

Incidentally, in the limit $n_c \to 0$ (or $\lambda_R \to \lambda$), $\mathcal{I}_1(0) = \frac{\pi}{\sqrt{3}}$. Eq. (4.34) reduces to the fluctuation correction to the mean-field PB free energy: $\Delta f_{pb} = -\,k_BT/(8\sqrt{3}\,\lambda^2)$, obtained in the previous section. Note that Eq. (4.34) also contains additional couplings among the fluctuations of the "condensed" and "free" counterions.

The result of the minimization of the total free energy $f(\tau) = f_{2d}(\tau) + f_{3d}(\tau)$ with respect to the order parameter τ is summarized by its behavior as a function of the bare coupling constant $g = l_B/\lambda$, as shown in Fig. 4.2 (at a fixed temperature

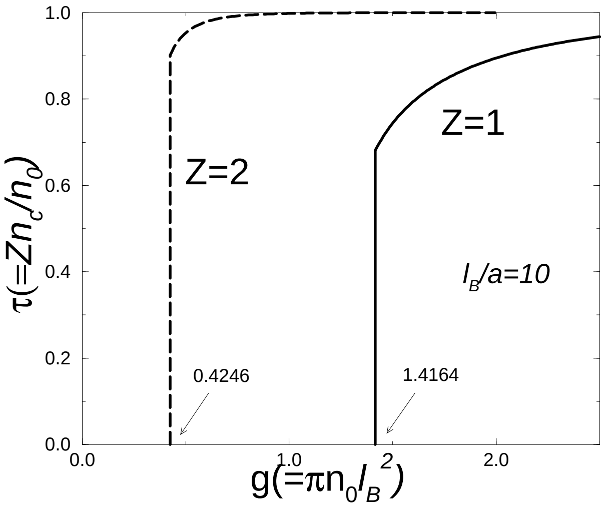

Figure 4.2: The fraction of "condensed" counterions $\tau \equiv Zn_c/n_0$ as a function of $g \equiv l_B/\lambda$. It is obtained through the minimization of the total free energy for $l_B/a = 10$, where $a \sim 1\,\text{Å}$ is the size of the counterions. At low surface charge $g \ll 1$, there is no "condensate" and the counterion distribution is described by PB theory. However, at high surface charge, correlation effects leads to a finite fraction of condensate.

$l_B = 10\,\text{Å}$) [4]. At weak coupling $g \ll 1$ (low surface charge density), where fluctuation corrections are negligibly small, the counterions prefer to be "free", i.e. $n_c \to 0$, in order to gain entropy. This is because $f_{3d}(n_R)$ in Eq. (4.34) is lower than the 2D ideal gas entropy by a term $\sim \ln(\,\lambda_R/a\,)$ which is large when $\lambda_R/a \gg 1$. This is not surprising since PB theory is a weak-coupling theory which becomes exact in the limit $T \to \infty$. However, for higher surface charge density, where correlation effects become more important, the order parameter τ (the fraction of counterions "condensed") makes a finite jump at $g_c \approx 1.42$ for monovalent counterions ($Z = 1$). Thus, the system appears to exhibit a first order phase transition[5]. The physical mechanism leading to this counterion "condensation" is the additional binding arising from 2D charge-fluctuations, which dominate the system at lower temperatures.

For divalent counterions ($Z = 2$), the correlation effects are even more pronounced (as expected): the jump occurs at $g_c \approx 0.42$ with a magnitude ≈ 0.9. Thus, in this case the charged plate is almost neutralized by the "condensed" counterions. For $l_B = 10\,\text{Å}$, the "bare" surface charge density at the condensation threshold is one unit charge per $\Sigma_c \sim 2\,\text{nm}^2$ for monovalent counterions and $\Sigma_c \sim 15\,\text{nm}^2$ for divalent counterions. Furthermore, we find that Σ_c decreases with increasing temperature, *e.g.*, at room temperature $l_B \approx 7\,\text{Å}$, $\Sigma_c \sim 1\,\text{nm}^2$, $7\,\text{nm}^2$ for $Z = 1$ and $Z = 2$, respectively. These estimates suggest that our results are within the reach of experiments on charged membranes.

4.4 Conclusion

In summary, using a "two-fluid" model and a variational approach, we have demonstrated that correlation and fluctuation effects may lead to a "condensation" transition of the counterions onto their oppositely charged plate. This results, which may be tested experimentally, provide new insights into the counterion distribution for highly charged macroions. In particular, this condensation picture may be crucial to understanding the attraction between two similarly charged plates, separated by a distance d. Recall that the total pressure of this system is comprised of the mean-field repulsion and the correlated fluctuation attraction. The repulsion comes solely from the ideal gas entropy and it is proportional to the concentration at the mid-plane: $\Pi_0(d) = k_B T \rho_0(d/2) = 8 k_B T/(\ell_B \lambda_R d)$ for $d < \lambda_R$. The fluctuation-induced attraction is $\Pi(d) = -\,\alpha\, k_B T/d^3$ for $d > \lambda_D$, where $\alpha \approx 0.048$. Clearly, when a large fraction of the counterions is "condensed", the mean-field repulsion is greatly reduced. Therefore, the attraction arising from correlated fluctuations of the "condensed" counterions can overcome the mean-field repulsion. This is achieved if $d^2 < \alpha\, \ell_B \lambda_R/8$ and $d > \lambda_D$. Using the estimates in the last paragraph above, these conditions are met only for divalent counterions at $g = g_c$ (corresponding to one unit charge per $\Sigma_c \sim 7\,\text{nm}^2$ at room temperature). This is in accord with the simulation performed by Guldbrand *et al.*[6], where the attraction is observed only for divalent counterions for surface charge densities greater than one unit charge per $\Sigma \sim 2\,\mathrm{nm}^2$. However, our estimates should be supplemented by a more precise calculation for the system of two charged plates.

Bibliography

[1] R. Netz and H. Orland, Eur. Phys. J. E **1**, 203 (2000); André G. Moreira and Roland R. Netz, preprint.

[2] V.I. Perel and B.I. Shklovskii, Physica A **274**, 446 (1999); B.I. Shklovskii, Phys. Rev. E **60**, 5802 (1999).

[3] A similar formulation of this problem is treated heuristically by Shklovskii in Ref. [2], where he assumes the "condensed" counterions form a Wigner crystal and considers the "free" counterion distribution according to PB theory. This approach may be valid at low temperature. Here, we shall treat the fluctuations of the "condensed" and "free" counterions on an equal footing, and thus be able to capture the onset of the condensation.

[4] Note that the term containing $\tau \ln \tau$ in $f(\tau)$ gives rise to finite value of τ even in the high temperature regime. The origin of this term is the entropy of the "condensed" counterion in Eq. (4.25). However, this expression for the entropy is not valid when $\tau \ll 1$ because the Stirling approximation breaks down. In this limit, we expect that fluctuations dominate the free energy. Therefore, we have discarded this term when minimizing $f(\tau)$ for small τ.

[5] We remark that the jump in τ may be an artifact of our one-loop approximation. It is conceivable that higher loop corrections may smooth out the finite jump

to a sharply rising curve. Therefore, whether this “condensation” transition is first-order or not remains to be examined more carefully.

[6] L. Guldbrand, B. Jönsson, H. Wennerström, and P. Linse, J. Chem. Phys. **80**, 2221 (1984)

Chapter 5

The Wigner Crystal Picture

5.1 Introduction

Recent interest in understanding the attraction arising from correlations between highly-charged macroions focus on formulating theories that go beyond the PB treatment. For an idealized system of two highly charged planar surfaces, with counterions distributed between them, PB theory as demonstrated in Sec. 2.3.2 always predicts repulsions. To account for the attraction arising from correlations, two distinct approaches have been proposed. The first approach as discussed in Sec. 3.4, based on charge fluctuations, treats the "condensed" counterion fluctuations in the Gaussian approximation. This theory predicts a long-ranged attraction which vanishes as $T \rightarrow 0$[1]. In the other approach based on "structural" correlations first proposed by Rouzina and Bloomfield [2], the attraction comes from the ground state configuration of the "condensed" counterions. Indeed, at low temperature, the "condensed" counterions crystallize on the charged surface to form a 2D Wigner crystal. When brought together, the counterions of two Wigner crystals correlate themselves to minimize the electrostatic energy (see Fig. 5.1). The pressure between

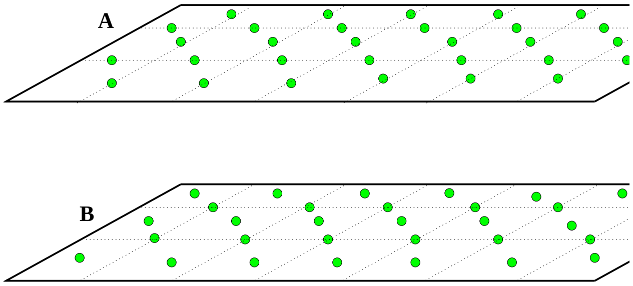

Figure 5.1: A schematic picture of two staggered Wigner crystals formed by the "condensed" counterions at very low temperatures.

them can easily be calculated at zero temperature[2, 4]

$$\Pi_{SR}(d) = -\frac{\partial}{\partial d}\left\{\frac{e^2 n}{\epsilon}\sum_l \frac{1}{\sqrt{|\mathbf{R}_l + \mathbf{c}|^2 + d^2}} - \frac{(en)^2}{\epsilon}\int \frac{d^2\mathbf{r}}{\sqrt{\mathbf{r}^2 + d^2}}\right\} \simeq -\frac{2\pi(en)^2}{\epsilon}\, e^{-G_0 d} \tag{5.1}$$

for large d, where $\mathbf{R}_l$ are the lattice sites, $\mathbf{c}$ is the relative displacement vector between two lattices of the different plane, $G_0 \equiv 4\pi/(\sqrt{3}\,a)$ is the magnitude of the first reciprocal lattice vector, and $a \equiv \left(2/(\sqrt{3}\,n)\right)^{1/2}$ is the lattice constant. Hence, these staggered Wigner crystals attract each other via a short-range force which decays exponentially with the lattice constant as the characteristic length scale. Clearly, this short-ranged force is strongest at zero temperature and thermal fluctuations diminish this attraction.

Although the physical origin of the attraction is clear in each approach, the relationship between them remains somewhat obscure, and this has generated a debate in the literature[5]. Therefore, it is desirable to formulate a unified approach which captures the physics of both mechanisms and addresses some important issues, for example, the temperature dependence of the short-ranged force, computed only at zero-temperature in Eq. (5.1). It is the goal of this chapter to formulate such an approach. Since at low temperature the counterion distribution is essentially two-dimensional, we consider a model system composed of two uniformly charged planes a distance d apart, each having a charge density en. Confined on the surfaces are negative point-like mobile charges of magnitude e. In order to understand correlation effects that are not captured by PB theory, we assume that the charges form a system of interacting Wigner crystals and develop a detailed physical picture of the electrostatic interaction between them at finite temperatures but below their melting temperature[6].

In particular, we compute the electrostatic attraction between the two layers by explicitly taking into account both *correlated fluctuations* and *"structural" correlations*. (By *"structural" correlations*, we mean the residual ground state spatial correlations which remain at finite temperature.) By adopting an elasticity theory, the total force of the system can be decomposed (approximately) into a short-ranged component arising from "structural" correlations and a long-ranged component from correlated fluctuations. They are calculated in Sec. 5.2 within the harmonic approximation using Boltzmann statistics (classical), which is valid below the melting temperature of the Wigner crystals. We show that the short-ranged force persists at finite temperature, and obtain a simple expression – see Eq. (5.24) below – which reduces to the zero-temperature result in Eq. (5.1) above[2, 4]. The interesting effect of thermal fluctuations is to reduce the *range* of this force and thus the effect is not negligible even below the melting temperature of the Wigner crystals. For the long-ranged force, this "elastic" calculation – see Eq. (5.20) below – finds exactly the same result, even including the prefactor, as the Debye-Hückel (Gaussian) approximation[1]. This is to be expected since the long-wavelength density fluctuations, which gives rise to the long-ranged force, are independent of the local Wigner-crystal-like ordering. Thus, an important insight gained here is that what is previously thought of as disparate mechanisms for the attractions – the short-ranged attraction (ground state) for low-temperature and the long-ranged attraction (charge-fluctuation) for high-temperature – are both captured within a single framework.

In addition, at zero temperature there must also be a long-ranged attraction derived from the *quantum* fluctuations of the plasmons[4]. This is the low temperature counterpart of the long-ranged force arising from charge-fluctuation at finite temperature. While this low-temperature result only bears a conceptual interest for macroions, it may have real relevance in the larger context of fluctuation-induced interactions in general, and in semiconductor bilayers in particular[7]. Interestingly, although similar to the Casimir effect, arising from zero-point fluctuations at $T = 0$, the fluctuation-induced force associated with two coupled Wigner crystals is fundamentally different. The Casimir effect pertains to two metal slabs separated by a gap of distance d, outside of which there is no electric field; this force scales d^{-4} at $T = 0$[8]. For the case of coupled Wigner crystals, zero-point fluctuations of the plasmons lead to a characteristically different force, which decays with a novel power-law: $d^{-7/2}$[4]. Hence, this long-ranged attractive force dominates the ground state short-ranged attraction in Eq. (5.1) for large d. Furthermore, it is of fundamental interest to consider finite temperature effects as well. This is done in Sec. 5.4, where we first recall the phonon spectrum of the coupled Wigner crystals, identify the plasmon modes, which characterize the density fluctuations of the system, and compute the attractive force arising from fluctuations using explicitly the Bose-Einstein distribution, which appropriately captures quantum effects at very low temperatures and thermal effects at higher temperatures for phonons in general and for plasmons in this particular case. Our result in the classical regime, which scales d^{-3}, agrees exactly including the prefactor with that based on 2D Debye-Hückel theory and "elasticity" theory in Sec. 5.2. Thus, we have provided an interesting but different perspective on the same problem and explicitly show how the $d^{-7/2}$ force-law at zero temperature crosses over to the d^{-3} law at high temperature via an intermediate d^{-2} regime.

Another point worth mentioning concerns the ordering of 2D solids which exhibit quasi-long-range-order (QLRO)[9]. It is well-known that a true long-range order is impossible for 2D systems with continuous symmetries. For a 2D solid, which is describable by continuum elasticity theory with nonzero long-wavelength elastic constants, the Fourier components of the density function $n(\mathbf{r}) = \sum_{\mathbf{G}} n_{\mathbf{G}}(\mathbf{r})\, e^{i\,\mathbf{G}\cdot\mathbf{r}}$ average out (thermally) to zero for a nonzero reciprocal lattice vector $\mathbf{G}$, *i.e.* $\langle n_{\mathbf{G}}(\mathbf{r})\rangle =$

$\langle e^{i\,\mathbf{G}\cdot\mathbf{u}(\mathbf{r})}\rangle = 0$, where $\mathbf{u}(\mathbf{r})$ are the displacements of the particles from their equilibrium positions; the correlation function decays algebraically to zero: $\langle n_{\mathbf{G}}(\mathbf{r})n^*_{\mathbf{G}}(\mathbf{0})\rangle \sim r^{-\eta_{\mathbf{G}}(T)}$ with $\eta_{\mathbf{G}}(T) = \frac{k_BTG^2(3\mu_s+\lambda_e)}{4\pi\mu_s(2\mu_s+\lambda_e)}$, where μ_s and λ_e are Lamé elastic constants. This slow power-law decay of the correlation function is very different from the exponential decay one would expect in a liquid. Hence the term QLRO. For a single 2D Wigner crystal, QLRO implies that the thermal average of the electrostatic potential at a distance d above the plane is zero at any non-zero temperature, in contrast to a perfectly ordered lattice ($T = 0$) where the electrostatic potential decays exponentially with d. This may lead to the conclusion that at finite temperatures the short-ranged force between two coupled Wigner crystals should likewise be zero. As we show below, this is not the case because the susceptibility, which measures the linear response of a 2D lattice to an external potential, nevertheless diverges at the reciprocal lattice vectors as in 3D solids[10].

However, we should mention that in real biological systems the counterions are best described as a correlated Coulomb fluid, which may be far away from a Wigner crystal. Nevertheless, it is important to understand counterion-mediated attractions between two highly charged surfaces in this Wigner-crystal limit, since it does provide useful *qualitative* insights into the nature of this problem, and moreover, the present formulation may serve as a starting point for a more sophisticated theory which includes melting of coupled Wigner crystals.

This chapter is organized as follows. In Sec. 5.2, we derive an effective Hamiltonian which describes two interacting planar Wigner crystals starting from the zero temperature ground state. The total pressure is then decomposed into a long-ranged and a short-ranged component, which are evaluated in Sec. 5.3.1 and 5.3.2, respectively, and a detailed discussion of our results is presented in Sec. 5.3.3. In Sec. 5.4, we present an argument for a long-ranged attractive force arising from the zero-point fluctuations at zero temperature. In addition, we use the Bose-Einstein distribution to calculate the attractive long-ranged pressure in the quantum regimes.

5.2 Effective Hamiltonian for Coupled Wigner Crystals

We start with the Hamiltonian for two interacting Wigner crystals: $\mathcal{H} = \mathcal{H}_0 + \mathcal{H}_{int}$. Here, $\mathcal{H}_0$ is the elastic Hamiltonian for two isolated Wigner crystals

$$\beta\mathcal{H}_0 = \frac{1}{2}\sum_i \int \frac{d^2\mathbf{q}}{(2\pi)^2}\,\Pi_{\alpha\beta}(\mathbf{q})\; u_\alpha^{(i)}(\mathbf{q})\,u_\beta^{(i)}(-\mathbf{q}), \tag{5.2}$$

where $\beta^{-1} = k_BT$, $\mathbf{u}^{(i)}(\mathbf{q})$ is the Fourier transform of the displacement field of ith layer ($i = A$ or B), $\Pi_{\alpha\beta}(\mathbf{q}) = \left[\frac{2\pi l_B n^2}{q}\,P^L_{\alpha\beta} + \mu_s\,P^T_{\alpha\beta}\right]q^2$ is the dynamical matrix, $\mu_s \approx 0.245\,n^{3/2}\,l_B$ is the shear modulus[11] in units of k_BT, $P^L_{\alpha\beta} = q_\alpha q_\beta/q^2$ and $P^T_{\alpha\beta} = \delta_{\alpha\beta} - q_\alpha q_\beta/q^2$ are longitudinal and transverse projection operator, respectively. $\mathcal{H}_{int}$ is the electrostatic interaction between the two layers:

$$\beta\mathcal{H}_{int} = l_B\int d^2\mathbf{x}\,d^2\mathbf{x}'\,\frac{(\,\rho_A(\mathbf{x}) - n\,)\,(\,\rho_B(\mathbf{x}') - n\,)}{\sqrt{(\mathbf{x}-\mathbf{x}')^2 + d^2}}, \tag{5.3}$$

where $\rho_i(\mathbf{x})$ is the number density of charges in the ith layer. In order to capture the long-wavelength coupling as well as discrete lattice effects which are essential for our discussions on the short-ranged force, we employ a method, similar to that in Ref.[12], which allows us to derive an effective Hamiltonian that is valid in the elastic regime where the displacement fields are slowly varying in space, *i.e.* $\nabla\cdot\mathbf{u}^{(i)}(\mathbf{x}) \ll 1$, but $|\mathbf{u}^A(\mathbf{x}) - \mathbf{u}^B(\mathbf{x})|$ need not be small compared to the lattice constant a.

Let us introduce a slowly varying field for each layer:

$$\phi_\alpha^{(i)}(\mathbf{x}) = x_\alpha - u_\alpha^{(i)}[\vec{\phi}^{(i)}(\mathbf{x})], \tag{5.4}$$

where the displacement field $\mathbf{u}^{(i)}(\mathbf{x})$ is defined in such a way that it has no Fourier components outside of the Brillouin Zone (BZ). Then, the density $\rho_i(\mathbf{x})$ can be written as:

$$\rho_i(\mathbf{x}) = \sum_l \delta^2(\mathbf{R}_l - \vec{\phi}^{(i)}(\mathbf{x}))\;\det[\partial_\alpha\,\phi_\beta^{(i)}(\mathbf{x})], \tag{5.5}$$

where $\mathbf{R}_l$ are the equilibrium positions of the charges, *i.e.* the underlying lattice sites. Using the Fourier expansion of the delta function and solving $\phi_\alpha^{(i)}(\mathbf{x})$ iteratively in terms of the displacement field, we obtain a decomposition of the density for the ith layer into a slowly and a rapidly spatially varying pieces:

$$\rho_i(\mathbf{x}) - n \cong -\, n\,\nabla\cdot\mathbf{u}^{(i)}(\mathbf{x}) + \sum_{\mathbf{G}\neq 0} n\, e^{i\,\mathbf{G}\cdot[\,\mathbf{x}+\mathbf{u}^{(i)}(\mathbf{x})\,]}, \tag{5.6}$$

where $\mathbf{G}$ is a reciprocal lattice vector. Note that we have neglected terms that are products of the slowly and the rapidly varying terms. Physically, the first term represents density fluctuations for wavelengths greater than the lattice constant, and the second term represents the underlying lattice, modified by thermal fluctuations. Using the density decomposition (5.6), $\mathcal{H}_{int}$ may be written as

$$\begin{aligned}\beta\mathcal{H}_{int} &= \int \frac{d^2\mathbf{q}}{(2\pi)^2}\,\frac{2\pi l_B}{q}e^{-qd}\int d^2\mathbf{x}\int d^2\mathbf{x}'\,e^{i\mathbf{q}\cdot(\mathbf{x}-\mathbf{x}')}\Bigg(n\,\nabla\cdot\mathbf{u}^A(\mathbf{x}) \\ &- \sum_{\mathbf{G}\neq 0} n\,e^{i\,\mathbf{G}\cdot[\,\mathbf{x}+\mathbf{u}^A(\mathbf{x})\,]}\Bigg)\Bigg(n\,\nabla\cdot\mathbf{u}^B(\mathbf{x}') - \sum_{\mathbf{G}'\neq 0} n\,e^{i\,\mathbf{G}'\cdot[\,\mathbf{x}'+\mathbf{c}+\mathbf{u}^B(\mathbf{x}')\,]}\Bigg),\end{aligned}$$

where $\mathbf{c}$ is the relative displacement vector between two lattices of the different plane and we have used the fact that $\frac{1}{\sqrt{x^2+d^2}} = \int \frac{d^2\mathbf{q}}{(2\pi)^2}\,e^{i\mathbf{q}\cdot\mathbf{x}}\,\frac{2\pi}{q}\,e^{-qd}$. Again neglecting the products of slowly and rapidly varying terms, which give vanishingly small contributions when integrating over all space, $\mathcal{H}_{int}$ separates into two pieces: a long-wavelength term

$$\beta\mathcal{H}^L_{int} = \int \frac{d^2\mathbf{q}}{(2\pi)^2}\,\frac{2\pi l_B n^2}{q}e^{-qd}\,q_\alpha q_\beta\,u^A_\alpha(\mathbf{q})\,u^B_\beta(-\mathbf{q}), \tag{5.7}$$

and a short-wavelength term

$$\begin{aligned}\beta\mathcal{H}^S_{int} = \;+\; &\sum_{\mathbf{G}\neq 0}\sum_{\mathbf{G}'\neq 0}\int \frac{d^2\mathbf{q}}{(2\pi)^2}\frac{2\pi l_B n^2}{q}e^{-qd} \\ &\times\int d^2\mathbf{x}\int d^2\mathbf{x}'\,e^{i\,\mathbf{q}\cdot(\mathbf{x}-\mathbf{x}')}\;e^{i\,\mathbf{G}\cdot[\,\mathbf{x}+\mathbf{u}^A(\mathbf{x})\,]}\;e^{i\,\mathbf{G}'\cdot[\,\mathbf{x}'+\mathbf{c}+\mathbf{u}^B(\mathbf{x}')\,]}.\end{aligned} \tag{5.8}$$

In order to obtain a tractable analytical treatment, we approximate this expression by splitting the sum over $\mathbf{G}'$ into two parts. The dominant part, with $\mathbf{G}' = -\mathbf{G}$ is

$$\beta\mathcal{H}^S_{int} = -\sum_{\mathbf{G}\neq 0}\int \frac{d^2\mathbf{q}}{(2\pi)^2}\frac{2\pi l_B n^2 e^{-qd}}{q}\int d^2\mathbf{x}\int d^2\mathbf{x}' e^{i\,(\mathbf{q}+\mathbf{G})\cdot(\mathbf{x}-\mathbf{x}')}e^{i\,\mathbf{G}\cdot[\,\mathbf{u}^A(\mathbf{x})\,-\mathbf{u}^B(\mathbf{x}')]}, \tag{5.9}$$

where we have used $e^{i\mathbf{G}\cdot\mathbf{c}} = -1$. The second part (those terms with $\mathbf{G}' \neq -\mathbf{G}$) contains extra phase factors which tend to average to zero in the elastic limit. As a first approximation, we neglect such terms. Finally, Eq. (5.9) can be systematically expanded using a gradient expansion:

$$\beta\mathcal{H}^S_{int} = -\sum_{\mathbf{G}\neq 0} \Delta_{\mathbf{G}}(d) \int d^2\mathbf{x}\, \cos\left\{\mathbf{G}\cdot\left[\mathbf{u}^A(\mathbf{x}) - \mathbf{u}^B(\mathbf{x})\right]\right\} + \mathcal{O}(\partial_\alpha u^{(i)}_\beta \partial_\gamma u^{(j)}_\tau), \quad (5.10)$$

where $\Delta_{\mathbf{G}}(d) = \frac{4\pi l_B n^2}{G} e^{-Gd}$. Putting Equations (5.2), (5.7), and (5.10) together, we obtain an effective Hamiltonian for the coupled planar Wigner crystals:

$$\begin{aligned}\beta\mathcal{H}_e = \beta\mathcal{H}_0 \quad &+ \int \frac{d^2\mathbf{q}}{(2\pi)^2} \frac{2\pi l_B n^2}{q} e^{-qd}\, q_\alpha q_\beta\, u^A_\alpha(\mathbf{q})\, u^B_\beta(-\mathbf{q}) \\ &- \sum_{\mathbf{G}\neq 0} \Delta_{\mathbf{G}}(d) \int d^2\mathbf{x}\, \cos\left\{\mathbf{G}\cdot\left[\mathbf{u}^A(\mathbf{x}) - \mathbf{u}^B(\mathbf{x})\right]\right\}. \qquad (5.11)\end{aligned}$$

The second term in Eq. (5.11) comes from the long-wavelength couplings while the third term reflects the periodicity of the underlying lattice structure. It is convenient to transform the displacement fields into in-phase and out-of-phase displacement fields by $\mathbf{u}^+(\mathbf{x}) = \mathbf{u}^A(\mathbf{x}) + \mathbf{u}^B(\mathbf{x})$ and $\mathbf{u}^-(\mathbf{x}) = \mathbf{u}^A(\mathbf{x}) - \mathbf{u}^B(\mathbf{x})$, respectively, so that the Hamiltonian (5.11) separates into two independent parts: $\mathcal{H}_e = \mathcal{H}_+ + \mathcal{H}_-$ with

$$\beta\mathcal{H}_+ = \frac{1}{2} \int \frac{d^2\mathbf{q}}{(2\pi)^2}\, \Pi^+_{\alpha\beta}(\mathbf{q})\; u^+_\alpha(\mathbf{q})\, u^+_\beta(-\mathbf{q}), \qquad (5.12)$$

and

$$\beta\mathcal{H}_- = \frac{1}{2} \int \frac{d^2\mathbf{q}}{(2\pi)^2}\, \Pi^-_{\alpha\beta}(\mathbf{q})\; u^-_\alpha(\mathbf{q})\, u^-_\beta(-\mathbf{q}) - \sum_{\mathbf{G}\neq 0} \Delta_{\mathbf{G}}(d) \int d^2\mathbf{x}\, \cos[\mathbf{G}\cdot\mathbf{u}^-(\mathbf{x})], \quad (5.13)$$

where $\Pi^\pm_{\alpha\beta}(\mathbf{q}) = \frac{1}{2}\left[\frac{2\pi l_B n^2}{q}(1 \pm e^{-qd})\, P^L_{\alpha\beta} + \mu_s\, P^T_{\alpha\beta}\right] q^2$. Furthermore, at low temperature, where $|\mathbf{u}^-(\mathbf{x})|$ is small compared to the lattice constant a, the cosine term in Eq. (5.13) can be expanded up to second order in $|\mathbf{u}^-(\mathbf{x})|$ to obtain the "mass" terms. Within a harmonic approximation $\mathcal{H}_-$, up to an additive constant, may be written as

$$\beta\mathcal{H}_- \quad \simeq \quad \frac{1}{2} \int \frac{d^2\mathbf{q}}{(2\pi)^2}\, \Pi^-_{\alpha\beta}(\mathbf{q})\; u^-_\alpha(\mathbf{q})\, u^-_\beta(-\mathbf{q})$$

$$+\frac{1}{2}\int\frac{d^2\mathbf{q}}{(2\pi)^2}\left[m_L^2 P^L_{\alpha\beta}+m_T^2\,P^T_{\alpha\beta}\right]u^-_\alpha(\mathbf{q})\,u^-_\beta(-\mathbf{q}), \qquad (5.14)$$

where $m_{L,T}^2 = 4\pi l_B n^2 \sum_{\mathbf{G}\neq 0} G\,e^{-Gd} = 4\pi l_B n^2 \Delta_0(d)$. This approximation is valid below the melting temperature of the Wigner crystals. Note that the mass terms vanish exponentially with d as also found in Ref.[13]. The fact that the transverse m_T and longitudinal "mass" m_L are degenerate is related to the underlying triangular structure of the lattices[13]. These "masses" are associated with the finite energy required to uniformly shear the two Wigner crystals, and thus give rise to a gap in the dispersion relations of the out-of-phase modes. In the next two subsections, we derive expressions for the long-ranged and the short-ranged pressure as given in Eq. (5.15) within the harmonic approximation.

5.3 Attractive Force within the Harmonic Approximation

In this section, we compute the attractive pressure between two planar Wigner crystals within the harmonic approximation at finite temperatures. The density decomposition Eq. (5.6) leading to the effective Hamiltonian allows the total force to be separated into two pieces – an exponentially decaying (short-ranged) force and a long-ranged power-law force:

$$\begin{aligned}\Pi(d) &= -\frac{1}{A_0}\left\langle\frac{\partial\mathcal{H}_{int}}{\partial d}\right\rangle_{\mathcal{H}_e} = -\frac{1}{A_0}\left\langle\frac{\partial\mathcal{H}^S_{int}}{\partial d}\right\rangle_{\mathcal{H}_e} - \frac{1}{A_0}\left\langle\frac{\partial\mathcal{H}^L_{int}}{\partial d}\right\rangle_{\mathcal{H}_e}\\ &= \Pi_{SR}(d)+\Pi_{LR}(d),\end{aligned} \qquad (5.15)$$

where A_0 is the area of the plane.

5.3.1 Long-Ranged Pressure

The long-ranged power-law force comes from the correlated long-wavelength density fluctuations (the plasmon modes). Using Eqs. (5.7) and (5.15), we obtain an expression for the long-ranged force:

$$\beta\Pi_{LR}(d) = \frac{2\pi l_B}{A_0} \int \frac{d^2\mathbf{q}}{(2\pi)^2}\, e^{-qd}\, \langle\, \delta\rho_A(\mathbf{q})\, \delta\rho_B(-\,\mathbf{q})\,\rangle, \tag{5.16}$$

where $\delta\rho_i(\mathbf{x}) \;=\; -\,n\,\nabla\cdot\mathbf{u}^{(i)}(\mathbf{x})$ is the long-wavelength density fluctuation to the lowest order. Making use of the equipartition theorem, the correlation function $\langle\, \delta\rho_A(\mathbf{q})\, \delta\rho_B(-\,\mathbf{q})\,\rangle$ can be evaluated

$$\begin{aligned}\langle\, \delta\rho_A(\mathbf{q})\, \delta\rho_B(-\,\mathbf{q})\,\rangle \;&\equiv\; \mathcal{N}^{-1} \int D\mathbf{u}^{\pm}(\mathbf{q})\, \delta\rho_A(\mathbf{q})\, \delta\rho_B(-\,\mathbf{q})\, e^{-\beta\mathcal{H}_e} \\ &=\; -A_0\, \frac{q^2}{4\pi l_B} \left[\frac{1}{q\,(1-e^{-qd})+4\Delta_0} - \frac{1}{q\,(1+e^{-qd})}\right], \end{aligned}\tag{5.17}$$

where $\mathcal{N} \;\equiv\; \int D\mathbf{u}^{\pm}(\mathbf{q})\, e^{-\beta\mathcal{H}_e}$ is the normalization factor and $\Delta_0 \;\equiv\; \sum_{\mathbf{G}\neq 0} G e^{-Gd}$. Substituting this result into Eq. (5.16), we find

$$\Pi_{LR}(d) = -\,\frac{k_B T}{d^3}\, \alpha(\Delta_0\, d), \tag{5.18}$$

where

$$\alpha(x) \cong \frac{\zeta(3)}{8\pi} + \frac{x}{\pi}\, \left[\, \mathrm{Ci}\,(\, 2\sqrt{x}\,)\, \cos(\, 2\sqrt{x}\,) + \mathrm{Si}\,(\, 2\sqrt{x}\,)\, \sin(\, 2\sqrt{x}\,)\,\right], \tag{5.19}$$

ζ is the Riemann zeta function, and $\mathrm{Ci}(x)$ and $\mathrm{Si}(x)$ are the cosine and sine integral functions, respectively. In the large distance limit, the second term in Eq. (5.19) is exponentially suppressed and can be neglected, yielding $\alpha = \frac{\zeta(3)}{8\pi}$. Therefore, for large d we have

$$\Pi_{LR}(d) = -\,\frac{\zeta(3)}{8\pi}\, \frac{k_B T}{d^{\,3}}. \tag{5.20}$$

This is the well-known result from the Debye-Hückel approximation[1]. Note also that the amplitude $\frac{\zeta(3)}{8\pi} \cong 0.048$ is universal for this interaction, induced by the long wavelength fluctuations[3]. Although the scaling of this charge-fluctuation-induced force coincides with that of the finite temperature van der Waals interaction, they are very different at low temperature. This is explored in Sec. 5.4.

5.3.2 Short-Ranged Pressure

The short-ranged force which decays exponentially owes its existence to the "structural" correlations. It survives even at non-zero temperature, in contrast to the conclusion drawn from a single 2D Wigner crystal, as discussed in the Introduction. However, we expect on physical grounds that the short-ranged force is weakened by thermal fluctuations. To compute explicitly its temperature dependence, we start with the expression for this force derived from Eqs. (5.9) and (5.15):

$$\beta\Pi_{SR}(d) = -\,2\pi l_B n^2 \sum_{\mathbf{G}\neq 0} e^{-\frac{G^2}{2}\langle|\,\mathbf{u}^-(0)|^2\rangle}\, f_{\mathbf{G}}(d), \tag{5.21}$$

where $f_{\mathbf{G}}(d) = \int \frac{d^2\mathbf{q}}{(2\pi)^2}\,\mathcal{S}(\mathbf{q}-\mathbf{G})\,e^{-qd}$, $\mathcal{S}(\mathbf{q}-\mathbf{G}) = \int d^2\mathbf{r}\,e^{i\,(\mathbf{q}-\mathbf{G})\cdot\mathbf{r}}\,e^{-\frac{G^2}{8}\,[\,B^+(\mathbf{r})\,-\,B^-(\mathbf{r})]}$, and $B^{\pm}(\mathbf{r}) = \langle\,[\mathbf{u}^{\pm}(\mathbf{r}) - \mathbf{u}^{\pm}(\mathbf{0})]^2\,\rangle$. Note that Eq. (5.21) is exact, provided all the expectation values are evaluated exactly. For a system of coupled perfect Wigner crystals at zero temperature, $f_{\mathbf{G}}(d) = e^{-Gd}$. At finite temperature, but below the melting temperature T_m, we note that $B^{\pm}(r)$ varies very slowly in space, so that $f_{\mathbf{G}}(d)$ can be approximated by its zero temperature value: $f_{\mathbf{G}}(d) \simeq e^{-Gd}$. Hence, we obtain

$$\beta\Pi_{SR}(d) \cong -\,2\pi l_B n^2 \sum_{\mathbf{G}\neq 0} e^{-Gd}\,\left\langle e^{i\,\mathbf{G}\cdot[\mathbf{u}^A(\mathbf{0})-\mathbf{u}^B(\mathbf{0})]}\right\rangle_{\mathcal{H}_e}. \tag{5.22}$$

The thermal average of the displacement fields in Eq. (5.22) resembles a "Debye-Waller" factor which measures the degree to which the short-ranged force is depressed by thermal fluctuations from its zero temperature maximum value. Because of the cosine term present in Eq. (5.11), this "Debye-Waller" factor is in general not zero, unlike the case of a single 2D Wigner crystal. However, if the system has melted into a Coulomb fluid, this cosine term, which comes from the lattice structure, would have to be modified.

The required expectation value in Eq. (5.22) only involves $\mathcal{H}_-$. Within the harmonic approximation, the mean-square out-of-phase displacement field can be evaluated

$$\langle|\mathbf{u}^-(\mathbf{x})|^2\rangle = \frac{\lambda_D}{2\pi nd}\ln\left[\frac{d}{4\Delta_0(d)a^2}\right] + \frac{1}{2\pi\mu_s}\ln\left[\frac{\mu_s}{8\pi l_B n^2\Delta_0(d)a^2}\right] \simeq \frac{G_0 d}{2\pi}\left[\frac{\lambda_D}{nd} + \frac{1}{\mu_s}\right], \tag{5.23}$$

where $\lambda_D = 1/(2\pi l_B n)$, a is the lattice constant, $\mu_s \approx 0.245\, n^{3/2}\, l_B$ is the shear modulus of an isolated Wigner crystal in units of k_BT, and in the last line, we have approximated $\Delta_0(d)$ by the first nonzero reciprocal lattice vector contribution: $\Delta_0(d) \approx G_0\, e^{-G_0 d}$. Note also that the logarithmic dependence on the "mass" ($= 4\pi n^2 l_B \Delta$) is a characteristic of 2D solids. Inserting Eq. (5.23) into Eq. (5.22), we obtain an expression for the short-ranged pressure at finite temperatures

$$\beta\Pi_{SR}(d) \simeq -\,2\pi l_B n^2\, e^{-(1+\xi/2)\,G_0 d}. \tag{5.24}$$

Here, the parameter ξ defined by

$$\xi = \frac{G_0^2}{2\pi}\left(\frac{\lambda_D}{nd} + \frac{1}{\mu_s}\right), \tag{5.25}$$

characterizes the relative strengths of thermal fluctuations and the electrostatic energy of a Wigner crystal, *i.e.* $\xi \sim \frac{k_BT\,a}{e^2}$. Thus, the sole effect of thermal fluctuations on the short-ranged force is to reduce its *range*: $G_0 \to G_0\left(1 + \frac{\xi}{2}\right)$.

5.3.3 Discussion

In summary, we have shown that the total pressure between two coupled Wigner crystals can be decomposed into a long-ranged Π_{LR} and a short-ranged pressure Π_{SR}. Each force is computed below their melting temperature, where the harmonic approximation is expected to be valid. The result for the total force is

$$\beta\Pi(d) \simeq -\,2\pi l_B n^2\, e^{-(1+\xi/2)\,G_0 d} - \frac{\alpha(\Delta_0 d)}{d^3}, \tag{5.26}$$

where $\xi = \frac{G_0^2}{2\pi}\left[\frac{\lambda_D}{nd} + \frac{1}{\mu_s}\right]$ and $\alpha(\Delta_0 d) = \frac{\zeta(3)}{8\pi}$ for large d. In Fig. 5.2, we have plotted Π_{SR} and Π_{LR} for two values of the coupling constant, $\Gamma \equiv \frac{l_B}{a} = 150$ and 50. Note that $\Gamma \equiv e^2\sqrt{\pi n}/(\epsilon k_BT)$ is the ratio of the average Coulomb energy among charges and their thermal energy. Not surprisingly, they show that Π_{SR} dominates for small d, and Π_{LR} for large d. However, it is interesting to note that even for high values of Γ, Π_{LR} dominates as soon as $d \sim a$.

According to Eq. (5.24), the magnitude of Π_{SR} tends to decrease exponentially with temperature. This strong decrease with increasing temperature is consistent with the Brownian dynamics simulations of Grønbech-Jensen *et al.*[3]. The shortening of its range may be attributed to the generic nature of strong fluctuations in 2D systems, and can also be understood by the following scaling argument. Referring back to $\mathcal{H}_-$ in Eq. (5.13), one can show that the anomalous dimension of the operator $\cos[\mathbf{G}_0 \cdot \mathbf{u}^-(\mathbf{x})]$ is [Length $]^{-\xi}$ and correspondingly the dimension of $\Delta_{\mathbf{G}_0}(d)$ is [Length $]^{\xi-2}$. Since $\Delta_{\mathbf{G}_0}(d)$ is the only relevant length scale in $\mathcal{H}_-$, we must have $\left\langle e^{i\,\mathbf{G}_0\cdot\mathbf{u}^-(\mathbf{0})}\right\rangle \sim \Delta_{\mathbf{G}_0}^{\frac{\xi}{2-\xi}}$[14]. Therefore, the short-ranged pressure scales like

$$\Pi_{SR}(d) \sim -\,\Delta_{\mathbf{G}_0}(d) \times \left\langle e^{i\,\mathbf{G}_0\cdot\mathbf{u}^-(\mathbf{0})}\right\rangle \sim -\,\Delta_{\mathbf{G}_0} \times \Delta_{\mathbf{G}_0}^{\frac{\xi}{2-\xi}} \sim -\,e^{-G_0 d\left(\frac{2}{2-\xi}\right)}. \qquad (5.27)$$

In the low temperature limit ($\xi \ll 1$), we see that the range of Π_{SR} is $G_0\left(1+\frac{\xi}{2}\right)$ as in Eq. (5.24). This scaling argument also suggests that at higher temperatures thermal fluctuations may have interesting nonperturbative effects. At zero temperature $\xi = 0$, so Π_{SR} in Eq. (5.24) reproduces the known result of exponentially decaying attractive force[2, 4]. It should be mentioned that in real biological systems, counterions are likely to be a correlated fluid with short-ranged order. However, as long as $\Gamma \gg 1$ and the lateral characteristic correlation length is much larger than the spacing between the layers, it is possible to have "structural" correlations and our calculation should capture the short-ranged attraction at least qualitatively.

The long-ranged pressure for large d in Eq. (5.20) agrees exactly, including the prefactor, with the Debye-Hückel approximation. This is hardly surprising since the existence of plasmons (average density fluctuations) is independent of local structure, and they are present for solids and fluids alike. Thus, the asymptotic long-ranged power-law force must manifest itself even after QLRO is lost via a 2D

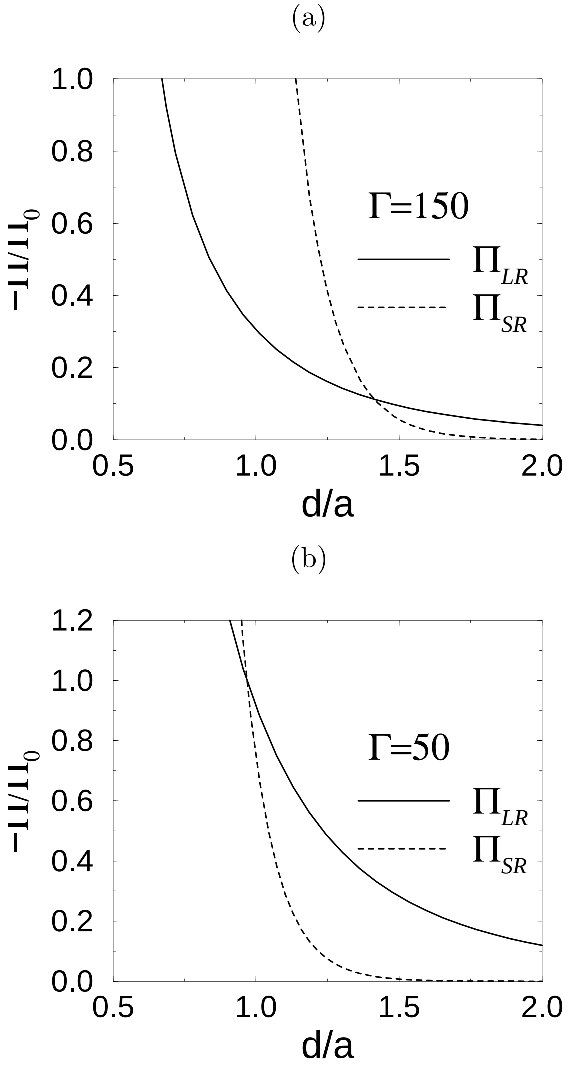

Figure 5.2: Plots of Π_{SR} and Π_{LR} versus d for $\Gamma = 150$ (a) and 50 (b). Observe that the crossover ($\Pi_{LR} \approx \Pi_{SR}$) occurs at about $d \sim a$. $\Pi_0 \equiv k_B T\,(l_B/a^4) \times 10^{-3}$.

melting transition driven by dislocations[15]. Therefore, our formulation captures the essential physics of the attraction not only arising from the ground state "structural" correlations, but also from the high temperature charge-fluctuations.

5.4 Quantum Contribution to the Long-Ranged Attraction

According to the *classical* calculations above, correlation effects give rise to a "structural" short-ranged and a long-ranged attractive force. Recall that the long-ranged force vanishes as $T \to 0$, and that the short-ranged force is strongest at zero temperature but vanishes exponentially with distance. This observation suggests that for sufficiently large separations correlated attractions at finite temperatures are stronger than those arising from the zero temperature ground state. However, at low temperatures zero-point fluctuations of the plasmons should be incorporated and as demonstrated below they induce an attractive long-ranged interaction, which exhibits an unusual fractional-power-law decay ($\sim d^{-7/2}$), in contrast to the zero-temperature van der Waals interaction ($\sim d^{-4}$). Hence, in the $T \to 0$ limit, this long-ranged attraction from zero-point fluctuations dominates the short-ranged "structural" force at large separations. Furthermore, we expect that quantum fluctuations persist at finite temperature, and in this section, we also compute their temperature dependence.

To this end, it may be more convenient to employ a method with which fluctuation-induced forces are usually calculated[3]. The advantage of the elastic approach in Sec. 5.2 is that the short-ranged force is captured more transparently. However, for the long-ranged force, an equivalent formulation in terms of the plasmon excitations seems more natural in the low temperature regime where quantum effects are important. Below, we recall the phonon spectrum of the coupled Wigner crystals, identify the plasmon modes, which characterize the density fluctuations of the system, and compute the attractive force arising from fluctuations using explicitly the Bose-Einstein distribution, which appropriately captures quantum effects at very low temperature and thermal effects at higher temperature, for phonons in general and plasmons in this particular case.

Within the harmonic approximation to the effective Hamiltonian, the dynamical matrix can be diagonalized to yield four modes. Two of them are the shear modes of the system that do not contribute to the long-ranged force[4]. The dominate modes which lead to the long-ranged attraction are the two plasmon modes of two coupled 2D Wigner crytals, which have the following dispersion relations:

$$\omega_1^2(q) = \frac{8\pi e^2 n}{m\epsilon}\,\Delta_0(d) + \frac{2\pi e^2 n}{m\epsilon}\,q\,(\,1 - e^{-qd}\,); \tag{5.28}$$

$$\omega_2^2(q) = \frac{2\pi e^2 n}{m\epsilon}\,q\,(\,1 + e^{-qd}\,), \tag{5.29}$$

where m is the mass of the charges and $\Delta_0(d) \sim e^{-Gd}$ is proportional to the energy gap (the “mass” term) for the out-of-phase mode. The plasmon modes are related to the correlated charge-density fluctuations in the two layers. At any finite temperature, the free energy of the low-lying plasmon excitations is given by the Bose-Einstein distribution

$$\mathcal{F}(d)/A_0 = \frac{\hbar}{2}\sum_{i=1,2}\int\frac{d^2\mathbf{q}}{(2\pi)^2}\,\omega_i(\mathbf{q}) + k_BT\sum_{i=1,2}\int\frac{d^2\mathbf{q}}{(2\pi)^2}\,\ln\left[1 - e^{-\beta\hbar\omega_i(\mathbf{q})}\right], \tag{5.30}$$

where A_0 is the area of the plane. Since the energy gap Δ_0 is exponentially damped for large distances, its contribution to the free energy may be neglected in the large distance limit, where the long-ranged force is expected to be dominant.

The first term in Eq. (5.30) arising from the zero-point fluctuations leads to an attractive pressure

$$\Pi^0_{LR}(d) = -\frac{1}{A_0}\frac{\partial\,\mathcal{F}_0(d)}{\partial\,d} = -\sqrt{\frac{\hbar^2 e^2 n}{m\epsilon}}\,\frac{\alpha_1}{d^{7/2}}, \tag{5.31}$$

where α_1 is a positive numerical constant of order unity, explicitly given by

$$\alpha_1 = \frac{1}{4\sqrt{2\pi}}\int_0^\infty dx\,x^{5/2}\,e^{-x}\left\{\frac{1}{\sqrt{1-e^{-x}}} - \frac{1}{\sqrt{1+e^{-x}}}\right\}. \tag{5.32}$$

Thus, zero-point fluctuations induce a long-range attraction which decays with a novel power law $\sim d^{-7/2}$. This should be contrasted with the usual Casimir-like force $\sim d^{-4}$, which arises from, for example, the acoustic phonon zero-point fluctuations. We note that this power law stems from the 2 dimensional nature of charged systems: 2-D plasmons do not have a finite gap, as they do in 3D. For an order of magnitude estimate, assuming $m \sim 10^{-25}\, kg$, $n \sim 1/50\, \text{Å}^{-2}$, $d \sim 10\, \text{Å}$, and $\epsilon \sim 80$, we find $\Pi \sim 10^{-25}\, J/\text{Å}^3$. This is close to the magnitude of the short-ranged force in Eq. (5.24) at zero temperature: $\Pi_{SR}(d) \sim 10^{-24}\, J/\text{Å}^3$, and thus may be just as important under suitable conditions.

An additional contribution to the pressure at finite temperature can be derived from the second term in Eq. (5.30),

$$\beta\Pi_{LR}(d) = -\frac{\hbar\Lambda}{4\pi d^{7/2}} \int_0^\infty dx\, x^{5/2} \left\{ \frac{1}{\exp[\eta\sqrt{x(1-e^{-x})}]-1}\, \frac{e^{-x}}{\sqrt{1-e^{-x}}} \right.$$
$$\left. - \frac{1}{\exp[\eta\sqrt{x(1+e^{-x})}]-1}\, \frac{e^{-x}}{\sqrt{1+e^{-x}}} \right\}, \qquad (5.33)$$

where $\Lambda = \sqrt{\frac{2\pi e^2 n}{m\epsilon}}$ and $\eta = \beta\hbar\Lambda/\sqrt{d}$.

In the limit $\eta \gg 1$, Eq. (5.33) can be systematically expanded in powers of η^{-1}. The lowest order term is given by $\Pi_{LR}(d) = -\alpha_2 \frac{k_B T}{\lambda_L d^2}$, where $\lambda_L \equiv a_B \frac{l_B}{2\lambda_D}$, $a_B \equiv \epsilon\hbar^2/(me^2)$ is the effective Bohr radius, $\alpha_2 \equiv \frac{1}{4\pi}\int_0^\infty dx\, \frac{x^2}{e^x-1} = \zeta(3)/(2\pi)$, and ζ is the Riemann zeta function. We observe that the low temperature condition $\eta > 1$ is equivalent to the short distance limit $d < \lambda_L$. In the opposite limit $\eta \ll 1$ or the large distance limit $d > \lambda_L$, we expand the exponential in the denominator of Eq. (5.33) to obtain $\Pi_{LR}(d) = -\alpha \frac{k_B T}{d^3}$, where $\alpha = \zeta(3)/(8\pi)$. This result agrees with the classical calculation in Sec. 5.3.1 as it should. Therefore, we have the following regimes for correlated attraction from plasmon fluctuations at finite temperature

$$\Pi_{LR}(d) \sim \begin{cases} -k_B T/d^3, & \text{for } \lambda_L < d, \\ -k_B T/(\lambda_L d^2), & \text{for } \lambda_L > d. \end{cases} \qquad (5.34)$$

We note that λ_L, in contrast to λ_D, increases with decreasing temperature, indicating, as one might expect, that quantum fluctuations are important at low temperatures. Furthermore, since $\Pi_{LR}(d) \to 0$ as $T \to 0$, the attractive interaction as $T \to 0$ is governed by zero-point fluctuations as emphasized above. In the strong Coulomb coupling limit $l_B/\lambda_D \sim 100$, we get $\lambda_L \sim 3\,\text{Å}$ for $\epsilon \sim 100$ and $a_B \sim 1/20\,\text{Å}$.

It should be emphasized that the results in this section is independent of the nature of the ground state. Thus, any system where low temperature modes of plasmon are important may, in principle, exhibit the behavior predicted in this section. This means that quantum contributions to the long-ranged attraction are unlikely to be relevant for macroions. Our motivation here stems from the desire to understand the charge-fluctuation-induced attraction between coupled layers in a complete picture. However, our results may have real impact in a greater field of fluctuation-induced forces in general and for electrons in bilayer semiconductor systems in particular. Indeed, there exist recent theoretical efforts devoted to this subject[7].

5.5 Discussion and Conclusion

In this chapter, we have studied analytically the electrostatic attraction between two planar Wigner crystals in the strong Coulomb coupling limit. We show that the total attractive pressure can be separated into a long-ranged and short-ranged component. The long-ranged pressure arises from *correlated fluctuations* and the short-ranged pressure from the ground state *"structural" correlations.* We also compute the very low temperature behavior of the fluctuation-induced attraction, where long-wavelength plasmon excitation must be described by Bose-Einstein statistics. The results are summarized in Fig. 5.3, showing different regimes for the charge-fluctuation-induced long-ranged attraction, including the high temperature results in Ref. [1] and the characteristic decay length l_{SR} for the short-ranged force. For small d, the short-ranged force is always dominant, but the decay length shrinks with increasing temperature. The crossover from the short-ranged to long-ranged dominant regimes occurs about $d \sim a$. Thus, for large $d \gg a$ only the long-ranged

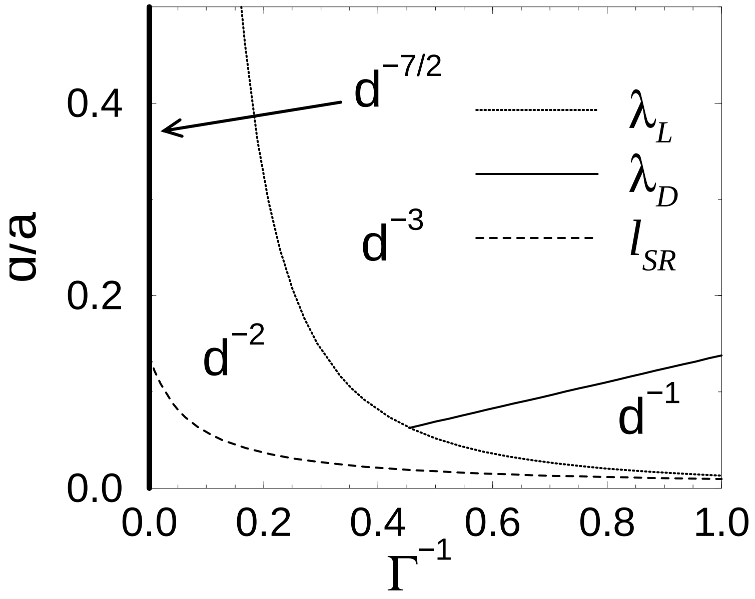

Figure 5.3: A schematic phase diagram summarizing different charge-fluctuation-induced attraction regimes. The characteristic decay length l_{SR} of the short-ranged force is also shown.

force is operative, which crosses over from $d^{-7/2}$ at zero temperature to the finite temperature distance dependence of d^{-2} if $d < \lambda_L$ and d^{-3} if $d > \lambda_L$. This provides a unified description to the electrostatic attraction between two coupled Wigner crystals.

In addition, our formulation may offer further insights into the nature of the counterion-mediated attraction at short distances. As discussed in Sec. 5.3.2, the reason that the short-ranged force in Eq. (5.22) does not vanish is because of the cosine term in $\mathcal{H}_{-}$, which represents the underlying lattice structures, and our results indicate that the strength of the short-ranged force decreases exponentially with temperature. However, at higher temperatures the expression for Π_{SR} in Eq. (5.24) is no longer valid, since the harmonic approximation breaks down. Indeed, the scaling argument leading to Eq. (5.27) suggests that if the full cosine term is retained, Π_{SR} may exhibit nonperturbative behaviors as $\xi \to 2^-$.

To discuss qualitatively what happens at higher temperatures, we assume that $\Delta_{\mathbf{G}}(d)$ is sufficiently small and the system of interacting Wigner crystals is below its melting temperature T_m. Then, the charges between the two layers may unlock via a Kosterlitz-Thouless (KT) type of transition, determined by the relevancy of the cosine term in $\mathcal{H}_-$, at $\xi = 2$ [16]. (An order of magnitude estimate for the coupling constant is $\Gamma \sim 13$.) In the locked phase, $\xi \ll 2$, the periodic symmetry in $\mathcal{H}_-$ is spontaneously broken, and the resulting state is well captured by the harmonic approximation. On the other hand, when $\xi > 2$ the fluctuations are so large that the ground state becomes nondegenerate (gapless), *i.e.* the layers are decoupled. To compute Π_{SR} in the unlocked phase, $\mathcal{H}^S_{int}$ given in Eq. (5.10) can be treated as a perturbation in evaluating the "Debye-Waller" factor in Eq. (5.22). To the lowest order, we obtain

$$\Pi_{SR}(d) \simeq -\frac{k_B T}{\lambda_D^2 a} \left(\frac{\xi - 1}{\xi - 2} \right) e^{-2G_0 d}. \tag{5.35}$$

We first note that this expression diverges as $\xi \to 2^+$, indicating the breakdown of the perturbation theory as the temperature is lowered. Furthermore, in contrast to Eq. (5.24), the range of Π_{SR} remains constant and the amplitude acquires a temperature dependence of $\sim 1/T$ (for large $\xi \gg 2$), reminiscent of a high temperature expansion.

However, the above picture may be modified if the charges have melted into a Coulomb fluid via a dislocation-mediated melting transition[15] before $\xi \to 2^-$. If this is the case, further analysis is necessary to obtain a more complete picture of the high temperature phase. Although the spatial correlations in a system of coupled 2D Coulomb fluids are expected to be somewhat different from 2D Wigner crystals, the solid phase results above suggest a qualitative *lower* limit of $\Gamma \sim 13$ at which Π_{SR} crosses over from low temperature in Eq. (5.24) to high temperature behavior in Eq. (5.35). It may be of interest to note that in Ref. [7], an estimate for the *upper* limit of Γ at which the Poisson-Boltzmann equation breaks down is of the order of $\Gamma \sim 3$. For divalent counterions "condensed" onto a highly charged (opposite) plate of surface charge density $\sigma \sim e/10\,\text{Å}^{-2}$, $\Gamma \sim 20$ at room temperature and the counterions are best described as a 2D correlated Coulomb fluid. However, as long as the characteristic lateral correlation length is much larger than the spacing between the two layers, our elastic approach should capture the qualitative behavior of the short-ranged attraction. A better theory should include melting of coupled 2D Wigner crystals by introducing excitations of dislocations into the effective Hamiltonian Eq. (5.11) similar to what is done in Ref. [17]. These considerations may help to establish an analytical theory of the attraction arising from counterion correlations, not captured by the Poisson-Boltzmann theory. The present formulation is a first step in that direction.

Bibliography

[1] Phil Attard, Roland Kjellander, and D. John Mitchell, Chem. Phys. Lett. **139**, 219 (1987); B.-Y. Ha and A. J. Liu, Phys. Rev. Lett. **79**, 1289 (1997); P. Pincus and S.A. Safran, Europhys. Lett. **42**, 103 (1998); D. B. Lukatsky and S. A. Safran, Phys. Rev. E **60**, 5848 (1999).

[2] I. Rouzina and V.A. Bloomfield, J. Phys. Chem. **100**, 9977 (1996); B.I. Shklovskii, Phys. Rev. Lett. **82**, 3268 (1999); J. Arenzon, J.F. Stilck, and Y. Levin, Eur. Phys. J. B. **12**, 79 (1999).

[3] Mehran Kardar and Ramin Golestanian, Rev. Mod. Phys. **71**, 1233 (1999).

[4] A.W.C. Lau, Dov Levine, and P. Pincus, Phys. Rev. Lett. **84**, 4116 (2000).

[5] Y. Levin, J.J. Arenzon, and J.F. Stilck, Phys. Rev. Lett. **83**, 2680 (1999); B.-Y Ha and A.J. Liu, Phys. Rev. Lett. **83**, 2681 (1999).

[6] It should be pointed out that we have assumed a uniform charge distribution on the surface of the charged plates in our model for electrostatic attraction, mediated by the "condensed" counterions. This assumption of a uniform neutralizing background may not be a good approximation to real experimental settings, since charges on macroion surfaces are discrete. For monovalent counterions, they tend to bind to the charges on the surface and form dipolar molecules. Therefore, the ground state for this system may not be a Wigner crystal, which

relies on mutual repulsion among charges for its stability, and short-ranged effects are likely to be important. However, for polyvalent counterions, a Wigner crystal is likely to form since each counterion does not bind to a particular charge on the surface, and a uniform background may be more appropriate. The detailed structure of the ground state as determined by short-ranged effects and valences will be the subject for another study.

[7] B.E. Sernelius and P. Björk, Phys. Rev. B **57**, 6592 (1998); J.F. Dobson and J. Wang, Phys. Rev. Lett. **82**, 2123 (1999); M. Boström and Bo E. Sernelius, Phys. Rev. B **61**, 2204 (2000).

[8] V.M. Mostepanenko and N.N. Trunov, *The Casimir Effect and its Applications* (Clarendon, Oxford, 1997).

[9] P.M. Chaikin and T.C. Lubensky, *Principles of Condensed Matter Physics* (Cambridge Univ. Press, NY, 1995).

[10] Y. Imry and L. Gunther, Phys. Rev. B **3**, 3939 (1971).

[11] L. Bonsall and A.A. Maradudin, Phys. Rev. B **15**, 1959 (1977).

[12] F.D.M. Haldane, Phys. Rev. Lett. **66**, 2270 (1991); Thierry Giamarchi and Pierre Le Doussal, Phys. Rev. Lett. **72**, 1530 (1994); Phys. Rev. B **52**, 1242 (1995).

[13] G. Goldoni and F.M. Peeters, Phys. Rev. B **53**, 4591 (1996); K. Esfarjani and Y. Kawazoe, J. Phys.: Condens. Matter **7**, 7217 (1995); V.I. Falko, Phys. Rev. B **49**, 7774 (1994).

[14] A.B. Zamolodchikov and S. Lukyanov, Nucl. Phys. B **493**, 571 (1997); V. Fateev, S. Lukyanov, A.B. Zamolodchikov, and Al.B. Zamolodchikov, Phys. Lett. B **406**, 83 (1997).

[15] For a review of dislocation-mediated melting transition for 2D solids, see D.R. Nelson, in *Phase Transitions and Critical Phenomena*, eds. C. Domb and J. L. Lebowitz (Academic Press, New York, 1983).

[16] H.A. Fertig, Phys. Rev. Lett. **82**, 3693 (1999).

[17] C.S. O'Hern, T.C. Lubensky, and J. Toner, Phys. Rev. Lett. **83**, 2745 (1999).

Chapter 6

Conclusion

In this thesis, we have discussed fluctuation and correlation effects in highly-charged surfaces. These effects are neglected in the mean-field Poisson-Boltzmann theory, which has been sucessful in explaining phenomena occuring in weakly-charged systems. However, in recent years, a different paradigm has started to emerge. Various experiments and computer simulations suggest that fluctuations and correlations cannot be neglected in many electrostatic phenomena in the context of colloidal and biophysical systems. The attraction between like-charged objects provides a striking example. This thesis has explored the physics of this attraction for a particular geometry of two plates in two limits: fluctuations about the high-temperature "saddle" point (mean-field) and correlations arising from the zero-temperature ground-state. Another interesting manifestation of correlation effects is the condensation of counterions. We have shown that there is a finite fraction of counterions "condensed" onto the charged plate if its surface charge density exceeds a certain threshold. Thus, mean-field treatment fails to capture the counterion distribution at high surface charge density. Of course, many conceptual questions still remain. For example, melting of coupled Wigner crystals and its implication for the short-ranged attraction are particular relevant, since in most biological systems, counterions are best described as a correlated fluid. However, we have demonstrated in this thesis that fluctuation and correlation effects are crucial to our understanding of physical phenonmena in which electrostatics plays an central role.

Appendix A

Membrane Curvature Elasticity

In this appendix, we review the essential elements of membrane curvature free energy. This provides the necessary background to understand electrostatic contribution to the bending rigidity.

Membranes are composed of self-assembling amphiphilic molecules. They contain a hydrophilic polar head and a hydrophobic tails. When dissolved in a aqueous solution like water, they spontaneously organize into different morphologies. Under suitable conditions, in particular, they form the lamellae phase, consisting of a stack of alternating amphiphilic bilayers and water regions. In addition, the polar head of these amphiphilic molecules acts as a surface agent which substantially lower the surface tension between water and their tails (oil) by adjusting their areal density. Hence, the elastic properties of these fluid membranes are characterized by three macroscopic parameters – a bending elastic modulus κ_b, a Gaussian modulus κ_G, and a spontaneous curvature H_0, which characterize their curvature deformation. The deformation free energy per unit area, expressed in terms of the mean curvature (see Fig. A.1)

$$H = \frac{1}{2}\left(\frac{1}{R_1} + \frac{1}{R_2}\right), \tag{A.1}$$

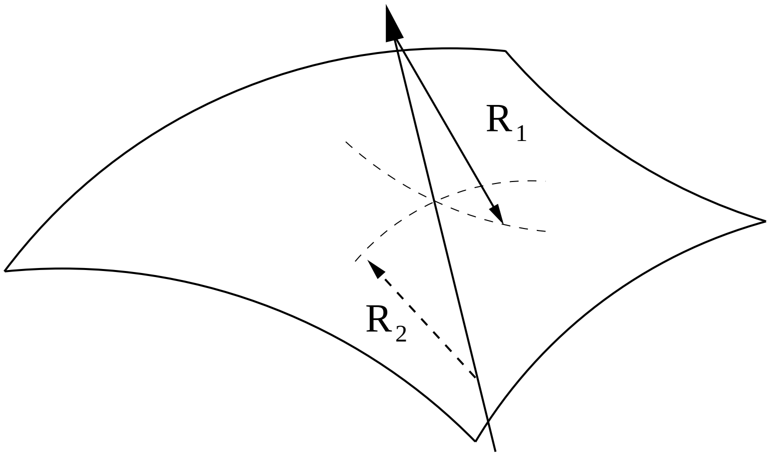

Figure A.1: Curvature on a 2D surface. The length scales R_1 and R_2 denote the radii of curvature.

and Gaussian curvature

$$K = \frac{1}{R_1 R_2}, \tag{A.2}$$

given by the Helfrich free energy may be written as:

$$f_{cur} = \frac{\kappa_b}{2}\,(H\, -\, H_0)^2 + \kappa_G\, K. \tag{A.3}$$

This form for the curvature free energy per unit area is the most general expansion in curvatures H and K up to quadratic order, consistent with the symmetry of the problem. Within an additive constant, the free energy of a sphere with radius R, a cylinder with radius R, and a sinusoidal undulating membrane $H_0 = 0$ with wavenumber q and a amplitude h are given by

$$\begin{aligned} f_{sp} &= \frac{2\kappa_b + \kappa_G}{R^2} - \frac{2\kappa_b H_0}{R}, && \text{(A.4)}\\ f_{cyl} &= \frac{\kappa_b}{2R^2} - \frac{\kappa_b\, H_0}{R}, && \text{(A.5)}\\ f_{un} &= \frac{1}{4}\kappa_b\, q^4\, h^2. && \text{(A.6)} \end{aligned}$$

Therefore, the parameters $\kappa_b H_0$ and $\kappa_b + \kappa_G$ may be extracted by expanding the electrostatic free energy up to second order in $1/R$ for spherical and cylindrical geometries and κ_b can be directly obtained by expanding terms up to $q^4\,h^2$ for an undulating membrane.